MALE-SPECIFIC DEVELOPMENT OF THE GERMLINE STEM CELL NICHE REGULATED BY DOUBLESEX AND FRUITLESS

By

Hong Zhou

A dissertation submitted to The Johns Hopkins University in conformity with the requirements for the degree of Doctor of Philosophy

Baltimore, Maryland
October, 2018

ABSTRACT

In *Drosophila melanogaster*, sexual development of the male and female gonads is controlled by the key sex-specific transcription factor Doublesex (Dsx). While homologs of Dsx are known to control gonad development in virtually all animals, the molecular mechanism remains largely unknown. Previously, we took genomic and bioinformatic approaches to identify Dsx targets genome-wide. *fruitless (fru)* was identified as a candidate target of Dsx involved in male gonad development. *fru*, like *dsx*, is regulated by sex-specific alternative splicing to promote male-specific mating behaviors. Surprisingly, we found that male-specific Fru expression in the gonad does not depend on sex-specific alternative splicing. Instead, *dsx* is necessary and sufficient to activate Fru expression in the gonad. Further, our Dsx occupancy data and enhancer-reporter analyses support that Dsx directly regulates transcription from the *fru* P4 promoter.

A key step in establishing gonadal sex is the formation of sexually-dimorphic germline stem cell (GSC) niche. Important components of the niche, named terminal filaments (TFs) in females and hubs in males, are different in morphology and molecular marks, yet originate from a shared pool of progenitor cells. Previously, we proposed that *dsx* regulates male-specific niche development by inhibiting hub-to-TFs trans-differentiation during the 3rd instar larval stage. Here we report that *fru* functions downstream of *dsx* in this process. Loss of *dsx* causes Fru expression to be reduced and variable in the gonad. Niche sex reversal occurs when the Fru level in *dsx* gonads is below a threshold. We further show that *fru* is sufficient to block TF formation and masculinize the niche when expressed in wildtype ovaries, but loss of *fru* is insufficient to induce gonad sex reversal.

The male GSC niche is maintained throughout adulthood for continuous spermatogenesis. We show that *fru* is not required to prevent sexual cell-fate reprogramming in the male niche and insufficient to masculinize the female niche in adults. Instead, *fru* functions in the cyst stem cells to anchor the hub at the testis apex and maintain CySC self-renewal. *fru* also is required to regulate proper spermatogenesis through promoting cyst cell survival and differentiation.

In summary, we discovered a previously unrecognized branch of the *Drosophila* sex determination pathway, where the master regulator of the behavior dimorphism functions downstream of *dsx* to regulate male-specific development of the gonad stem cell niche. This study highlights the interaction between sex-determining genes of the CNS and the gonad, and provide insight into the evolution of the sex determination pathway.

Advisor: Dr. Mark Van Doren

ACKNOWLEDGEMENTS

I acknowledge the many people who made this thesis work possible. Foremost, I would like to express the deepest appreciation to my thesis advisor Dr. Mark Van Doren, whose expertise, patience, generous guidance, and support made it possible for me to undertake this groundbreaking thesis work and complete my Ph.D. thesis. I appreciate his contributions of time and ideas to my research work and the thesis.

I would like to express my special appreciation and thanks to a former lab member, Dr. Cale Whitworth, for his pioneer work on characterizing Fru expression pattern in the gonad, discovering the regulation of Fru by *dsx,* and screening fru-GMR-Gal4 lines. I also want to thank him for allowing me to continue this project. I acknowledge past and present members of the Van Doren lab, especially Caitlin Pozmanter who assisted me in finding that Fru expression is activated by dsxD in the CNS.

I would like to thank my thesis committee members, Dr. Robert Johnston, Dr. Allan Spradling, and Dr. Daniella Drummond-Barbosa, for serving on my committee, giving me invaluable guidance and suggestions through the course of my thesis research and supporting me.

I am indebted to Dr. Steven Goodwin and Dr. Megan Neville for their generous sharing of Fru antibodies, stocks and ideas. I also acknowledge the little fly community on Mudd 3rd floor, including the Chen lab, the Johnston lab, and the Van Doren lab, for sharing inspiring ideas, reliable protocols, equipment, and reagents. I acknowledge the Drosophila community, especially the Bloomington Drosophila Stock Center, BacPac Resources Program, the Transgenic RNAi Project, and the FlyLight Project for sharing tools and reagents. The Johns Hopkins Integrated Imaging Center plays an integral part in

this work. I appreciate Michael McCaffery and Erin Pryce for their technical support. I acknowledge the faculty, staff, and other members of the Biology department who aided my growth as a scientist. I want to thank the CMDB program for offering me excellent graduate training.

Finally, I want to thank my family and friends, who have been supporting me physically and emotionally during my time at Johns Hopkins University. I especially thank my husband for understanding and believing in me in my pursuit to be a scientist. I dedicate this dissertation to my parents for their constant encouragement and unconditional support during my six years at Johns Hopkins University.

TABLE OF CONTENTS

LIST OF FIGURES

LIST OF TABLES

CHAPTER 1: INTRODUCTION

Summary

In this Chapter, I will discuss known genes and pathways that control sexual development of the *Drosophila* gonad. I will explain from the evolutionary perspective why I focus on studying *dsx* and its downstream genes. I will introduce the *fru* gene locus and explain our motivation to investigate the sex-specific expression and function of *fru* in the gonad.

Sexual reproduction is one of the most ancient and fundamental features of eukaryotes. Species have developed an amazing and diverse set of mechanisms to distinguish one sex from the other, to produce gametes and to bring gametes together. It has been long debated whether an evolutionarily conserved program exists to govern sex development in different species. Despite the diversity in sex-related traits, sexual dimorphism, which describes the intraspecies differences in anatomy, physiology, and behaviors between opposing sexes, remains as a universal feature in all sexually reproducing species. Through studying the genetic and developmental mechanisms of sexual dimorphism, we are starting to understand how sexual diversity and commonality are coordinated in the course of evolution.

The Sex Determination Pathway and the Conserved DMRTs

The mechanism that controls sexual dimorphism starts with a switch-like cue that determines if an individual initiates development in a male or female mode. The nature of this switch falls into two major categories: genetic sex determination and environmental sex determination. The molecular mechanisms vary widely in distant as well as closely related species, arguing against the existence of a conserved mechanism in the initial step of sex determination.

Sex determination in most species depends on chromosomal constitution. Several sex chromosome systems exist. In mammals, individuals with a Y chromosome develop into males. A single sex-determining gene *Sry* on the Y-chromosome is the switch that is necessary and sufficient to initiate the male development (Schafer and Goodfellow, 1996). Birds, some reptiles, amphibians, fish, and lepidopteran insects use the ZW/ZZ female heterogametic system, where individuals with a W chromosome develop into females. A higher Z chromosome dosage in males or the presence of a W chromosome in the female functions as the switch. X0 is yet another sex determination system where only one type of sex chromosome exists. Individuals with a single copy of X will develop as males. Some invertebrate species such as *C. elegans* utilizes this system to determine the sex.

Reptiles represent an extreme example where closely related species use diverse mechanisms to determine sex. Some reptile species such as lizards have X and Y sex chromosomes, while snake species all use Z and W sex chromosomes. Even more fascinating is that turtles and alligators have temperature-dependent sex determination. In many turtle species, eggs laid in cool nests hatch as males and eggs incubated at high temperatures hatch as females. The American alligator, however, develops into females in

both low and high temperatures and develops into male broods at temperatures in between. These pieces of evidence suggest that sex switches evolve rapidly and divergently.

Downstream of sex switches are the actuators that enact developmental programs along the male or female path. It has become increasingly clear that the sex determination pathway converges at this point upon a highly conserved gene family called the *doublesex* (*dsx*) and *male-abnormal-3* (*mab-3*) related transcription factors (DMRTs). DMRT homologs have been identified in species spanning the metazoan kingdom. In all examined species, *dsx* orthologs are essential for the normal sexual development of the gonad.

Human *DMRT1* is located in a region of chromosome 9 that is associated with XY sex reversal (Ottolenghi and McElreavey, 2000). Sertoli cells are the key somatic cell component of the seminiferous tubule and facilitate spermatogenesis. In mice and chicken, *DMRT1* is necessary to maintain the Sertoli cell fate after fetal gonadal sex is determined. Loss of *DMRT1* in Sertoli cells results sexual cell-fate reprogramming of Sertoli cells into the female counterparts called granulosa cells (Raymond et al., 1999), whereas ectopic expression of *DMRT1* in the ovary causes granulosa cells to trans-differentiation into Sertoli cells and masculinization of the ovary (Lambeth et al., 2014; Lindeman et al., 2015). In the primitive invertebrate planaria, *Smed-dmd-1* is required for *de novo* specification and maintenance of male germ cells, and the regeneration of male reproductive organs (Chong et al., 2013). This body of evidence strongly suggests DMRTs play an evolutionarily conserved role in the development and maintenance of male characteristics in the gonad.

However, the mechanisms that connect the sex switch to DMRTs are divergent. The male-specific expression of mammalian *DMRT1* is controlled at the transcriptional

level. Chromosomal sex determination leads to the female sex-determining gene Forkhead box L2 (FOXL2) to be expressed in female gonads, which repress *DMRT1* transcription (Lei et al., 2009). In the teleost fish medaka, a Y chromosome duplicate of *DMRT* (*Dmy*) functions as the Y-chromosome linked master switch of male development (Matsuda et al., 2002). In the African frog *X. laevis*, a W-linked determinant *dm-w* encodes a truncated DM domain protein and acts as a dominant-negative inhibitor to block autosomal DMRT1 function in female (Yoshimoto et al., 2010). Insects *DMRTs*, including the founding members *dsx* and *mab-3*, are regulated by sex-specific pre-mRNA splicing, resulting in the production of female- and male-specific protein isoforms that regulates female and male development, respectively (Burtis et al., 1991; Kiuchi et al., 2014; Shen and Hodgkin, 1988; Xu et al., 2017). Lastly, it was recently found that the Branchiopod Crustacean *Daphnia magna* uses a lncRNA to activate *dsx1* only in males (Kato et al., 2018). These data collectively demonstrate that conservation of the sex determination pathway only lies in DMRTs and potentially its downstream genes.

DMRTs all contain a novel zinc-finger related DNA binding domain, the DM domain. The vertebrates and invertebrate DM domains bind to similar DNA sequences (Murphy et al., 2007). However, DMRTs target genes remain largely unknown, and it is unclear whether DMRTs control sexual development through a set of conserved target genes. In this thesis work, I aim to shed light on this question through understanding how gonad sexual development is regulated by *dsx* and its target gene, *fruitless*, in *Drosophila melanogaster.*

The *Drosophila melanogaster* Somatic Sex Determination Hierarchy

The molecular mechanism of sex determination has been well characterized in *Drosophila melanogaster* (Figure 1.1). The sex chromosomes in *D. melanogaster* are designated as X and Y. Unlike the mammalian XY system, the Y chromosome is not involved in determining sex. Sex is determined by the number of X chromosomes in an individual. A fly with one X chromosome will develop as a male, whereas two or more XX chromosomes lead to the development of a female-like fly (Erickson and Quintero, 2007). The presence of two X chromosomes triggers a splicing cascade that leads to the production of Sex-lethal (Sxl) in females (Salz and Erickson, 2010). Sxl controls the sex-specific splicing of its downstream target gene *transformer* (*tra*) to produce functional Tra only in females (Cline and Meyer, 1996).

Figure 1.1: **The somatic sex determination hierarchy in *Drosophila melanogaster*.** Sex is determined by the X chromosome number. XX is female, and XY is male. The presence of two X activates an alternative splicing cascade leading to the female-specific expression of the RNA binding proteins Sex-lethal (Sxl) and Transformer (Tra). In combination with the general splicing cofactor Transformer-2 (Tra-2), Tra splices the two downstream genes, *doublesex* (*dsx*) and *fruitless* (*fru*) into female-specific transcripts that encode DsxF or no functional protein (labeled as {fruF}). In the absence of Tra, default splicing results in the production of DsxM and FruM proteins. DsxF and DsxM control sexual dimorphism of the soma as well as the nervous system/behavior. FruM controls the male-specific neuronal circuitry and courtship behaviors.

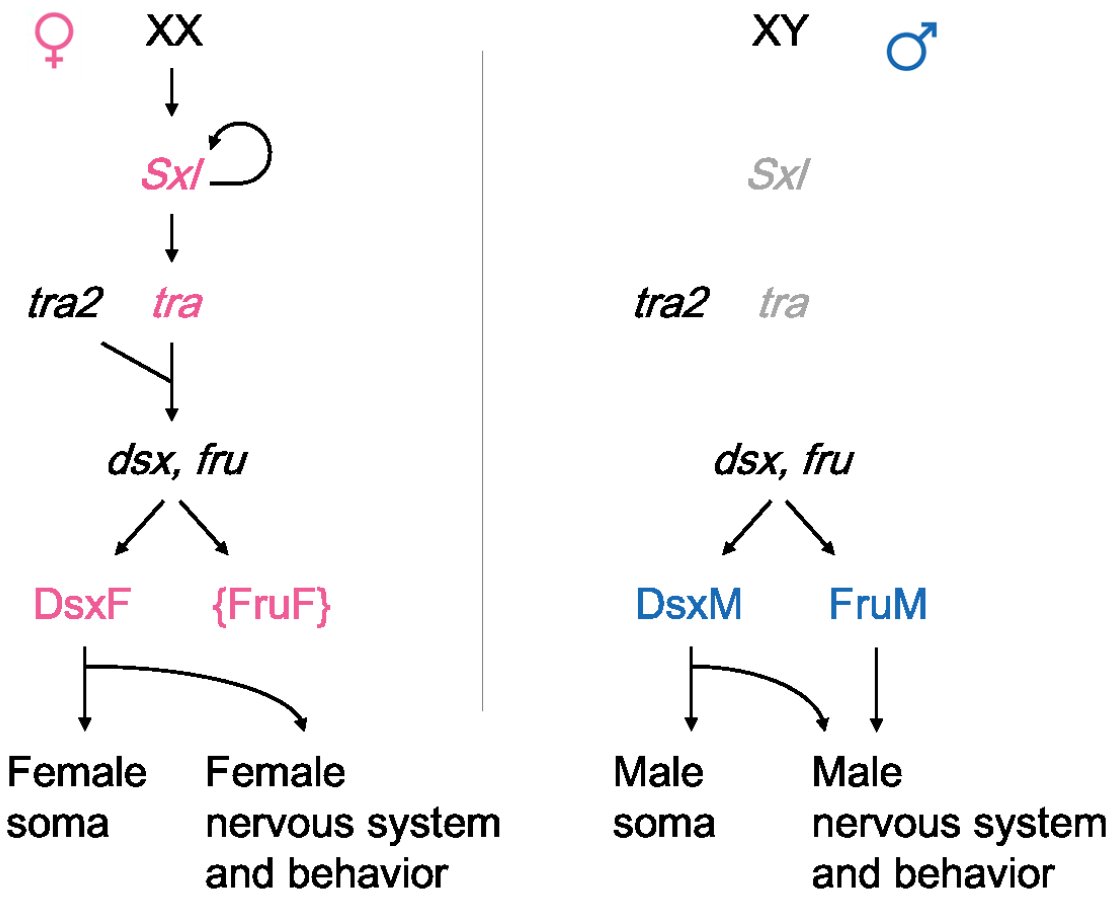
♀
XX
Sxl
tra2
tra
dsx, fru
DsxF
{FruF}
Female soma
Female nervous system and behavior
XY
♂
Sxl
tra2
tra
dsx, fru
DsxM
FruM
Male soma
Male nervous system and behavior

tra controls all known aspects of somatic sexual dimorphism (McKeown et al., 1987; McKeown et al., 1988). This is also accomplished through sex-specific alternative splicing. To date, only two Tra direct targets have been identified, *doublesex* (*dsx*) and *fruitless* (*fru*) (Burtis and Baker, 1989; Ito et al., 1996). *fru* is the master regulator of courtship behaviors, whereas *dsx* is responsible for the development of sex-specific morphological traits. Additionally, it has become increasingly clear that *dsx* also helps to sculpt sexual dimorphism in the nervous system. Recently, a *dsx*- and *fru*-independent pathway has been revealed that controls sex differences in intestinal physiology and body size (Hudry et al., 2016; Mathews et al., 2017; Rideout et al., 2015). The Tra target controlling this branch remains unknown.

Together with the sex-nonspecific cofactor Transformer-2 (Tra2), Tra splices *dsx* and *fru* into female-specific transcripts, *dsxF* and *fruF*. In the absence of Tra, default splicing results in the production of *dsxM* and *fruM* transcripts in males. While *dsxF* and *dsxM* both encode functional transcription factors, only FruM proteins are produced due to the presence of a premature stop codon in the *fruF* transcripts. DsxF, DsxM, and FruM are the terminal actuators of the *Drosophila* sex determination hierarchy. By regulating sex-specific gene expression, they control the development of sex-specific traits.

Dsx and the Regulation of Target Gene Expression

DsxM and DsxF share the same conserved DM DNA binding domain and the N-terminal dimerization domain but differ in the C-termini that include a sex-specific dimerization domain and a sex-specific tail domain that interacts with other proteins (Burtis et al., 1991; Erdman and Burtis, 1993). The C-terminal tail of DsxF interacts with Intersex (Ix) (Garrett-Engele et al., 2002). It was proposed that because DsxF lacks a transcriptional activation domain, Ix is required for DsxF function (Garrett-Engele et al., 2002; Siegal and Baker, 2005). Cofactors of DsxM have been identified, indicating that the male-specific C-terminal tail is long enough for transcriptional regulation (Siegal and Baker, 2005).

The DM domain contains a novel zinc finger that binds the DNA minor groove (Zhu et al., 2000). A preferred Dsx-binding sequence was first determined biochemically as a 13-basepair palindromic sequence, (G/A)nnAC(A/T)A(T/A)GTnn(C/T), composed of two half-sites around a central (A/T) base pair (Erdman et al., 1996). Mutations blocking Dsx dimerization resulted in intersexual individuals, suggesting that each DM domain recognizes a half site and dimerization is required for Dsx to bind DNA and regulate transcription. From genome-wide analyses of Dsx occupancy, consensus binding motifs were further identified with the same 7-nucleotide core sequence ACAATGT (Clough et al., 2014; Luo et al., 2011). Through comparing Dsx occupancy in different tissues of both sexes, Clough et al. proposed that DsxF and DsxM bind to the same target genes regardless of tissues and that additional gene-specific factors are required for Dsx regulation (Clough et al., 2014).

Although Dsx has been under intense scrutiny, only few direct target genes of Dsx have been reported: *Yolk protein* (*Yp*) genes, *bric à brac 1* (*bab1*), *Fad2*, *Fmo-2* and

lozenge (Burtis et al., 1991; Luo and Baker, 2015; Shirangi et al., 2009; Wagamitsu et al., 2017; Williams et al., 2008). A model of DsxF and DsxM regulating gene expression has been proposed based on the understanding of these targets: 1) DsxF and DsxM bind to the same target; 2) DsxF activates target gene transcription in females whereas DsxM represses gene transcription in males; 3) In the absence of Dsx activity, target genes are expressed at an intermediate level in both sexes.

With the limited case studies of Dsx targets, it remains unclear if DsxF acts only as an activator and DsxM only as a repressor. So far, the identified Dsx direct targets exhibit female-biased gene expression, supporting DsxF as an activator. However, some sexually dimorphic tissues have male-biased genes. These genes are upregulated by DsxM, downregulated by DsxF and expressed at an intermediate level in the absence of *dsx*, which indicates that DsxM may also positively regulate gene expression (Ahmad and Baker, 2002; DeFalco et al., 2008; Foronda et al., 2012). Another possible model is that while both DsxM and DsxF bind to the same target, only one isoform regulates gene expression. This model is supported by the case of *Fad2*, where DsxM does not repress *Fad2* expression in males (Shirangi et al., 2009). It is necessary to identify additional Dsx target genes in order to address these questions.

Dsx and Sex-specific Gonad Development

Sexual dimorphism in the embryonic gonad

The earliest manifestations of sexual dimorphism in the gonad are observed at the time of gonad formation, when somatic gonad precursors show sex-specific gene expression, female and male germ cells proliferate at different rates, and the male-specific SGPs (msSGPs) are eliminated in females (Casper and Van Doren, 2009; DeFalco et al., 2003; Wawersik et al., 2005). At this time, *dsx* is expressed in the SGPs and is responsible for all the aspects of sexual dimorphism established in the embryonic gonad (Hempel and Oliver 2007). Notably, through controlling the sexual identity of SGPs, *dsx* non-autonomously determines the sex of the primordial germ cells (PGCs) via JAK/STAT signaling and recruits the male-specific pigment cell precursors from the surrounding fat body via Wnt2 signaling (DeFalco et al., 2008; Wawersik et al., 2005).

Sexual dimorphism of the adult germline stem cell niche

The germline stem cell (GSC) niche is a specialized microenvironment located at the tip of ovaries and testes that nourishes and maintains the GSCs for the continuous production of gametes throughout adulthood. Important components of the niche are hub cells and cyst stem cells (CySCs) in males and terminal filament (TF) cells and cap cells (CpCs) in females (Figure 1.2) (Fuller and Spradling, 2007; Voog et al., 2008; Xie and Spradling, 2000).

The male and female niche share a lot of common features. The female and male niche cells originate from the same pool of anterior SGPs (Asaoka and Lin, 2004; Le Bras and Van Doren, 2006). After their specification, hub cells and TF/Cp cells no longer

proliferate. The female and male niches anchor GSCs via adherens junction molecules, such as DE-cadherin, DN-cadherin and Armadillo (β-catenin) (Le Bras and Van Doren, 2006; Song et al., 2002b). The short-range BMP signaling provided by the female and male niche is required for GSC self-renewal (Kawase et al., 2004; Morris and Spradling, 2011). When male and female GSC daughters, which are known as the gonialblast and cystoblast respectively, move beyond the range of local niche signals, they undergo 4 rounds of synchronous incomplete divisions to generate analogous 16-cell germline cysts. The differentiation of GSCs requires Bag of marble (Bam) and its partner Benign gonial cell neoplasm (Bgcn).

Drastic differences also exist between the male and female niches. A single hub, which consists of a tight cluster of approximately 10-15 hub cells, is formed at the apex of the testis and accommodates 6-9 GSCs. The ovary, however, is comprised of 16-18 parallel repetitive structures called ovarioles (Sarikaya et al., 2012). Each ovariole has a GSC niche with 8-9 disc-shaped cells stacking into the terminal filament and 5-7 cap cells located at the base of the terminal filament and housing only 2-3 GSCs (Panchal et al., 2017; Sahut-Barnola et al., 1995). Besides the morphological differences, male and female niches also have distinct molecular markers (Camara and Van Doren, submitted; Le Bras and Van Doren, 2006; Nanda et al., 2009).

Additional somatic cell types that are analogous but different in the male and female adult GSC niches are CySCs and cyst cells in the testis and escort cells, follicle stem cells (FSCs) and follicle cells in the ovary. Interaction with somatic cells is crucial for proper spermatogenesis and oogenesis (Gilboa and Lehmann, 2004; Kiger et al., 2001). Therefore, a somatic stem cell population is needed in both sexes to continuously support the germline.

In the testis, CySCs are juxtaposed with GSCs around the hub, but their nuclei are located farther from the hub than those of the GSCs and they make limited contact with the hub via thin cytoplasmic extensions. Each GSC is encapsulated by two CySCs. When the GSC divides, the two flanking CySCs also divide to produce two cyst cells that encapsulate the gonialblast. These two non-proliferative cyst cells are the only somatic cells with which the germline interact during spermatogenesis. An additional role of the CySC is to occasionally replenish hub cells (Voog et al., 2008).

In females, a radially symmetric ring of follicle stem cells (FSCs) locate at the region 2a/2b border of the germarium (Reilein et al., 2017; Sahai-Hernandez and Nystul, 2013). The FSCs give rise to follicle cells that envelope the 16-cell germline cyst and contribute to the anterior somatic cell population, the escort cells (Reilein et al., 2017). While escort cells interact with the pre-meiotic germ cells analogously to cyst cells, they do not envelop and migrate along with the GSC daughters. Instead, they pass germline cysts down the germarium with dynamic cytoplasmic extensions until the cysts reach the region 2a/2b boundary (Morris and Spradling, 2011). Escort cells remain quiescent most of the time, but they do occasionally divide to maintain the germ cell/escort cell ratio. Follicle cells undergo multiple rounds of divisions during early oogenesis to form the follicular epithelium.

Figure 1.2: **Sexual dimorphism of the adult male and female germline stem cell niches.** Adult female GSC niche (A) and male GSC niche (B) are illustrated. Terminal filament cells and hub cells are labeled in orange. Cap cells are colored in red. Light pink and blue cells represent female and male germline stem cells. The escort cell and cyst cell are colored in green. Follicle stem cells are colored in brown and their progeny, follicle cells, are colored in yellow. Branched fusome structures connect germ cells of the same cyst. Confocal images of the female (C) and male (B) niche are shown. N-cadherin (green) indicates terminal filaments and the hub. Germ cells are labeled by Vasa in red. The female and male niche are marked with brackets and a circle.

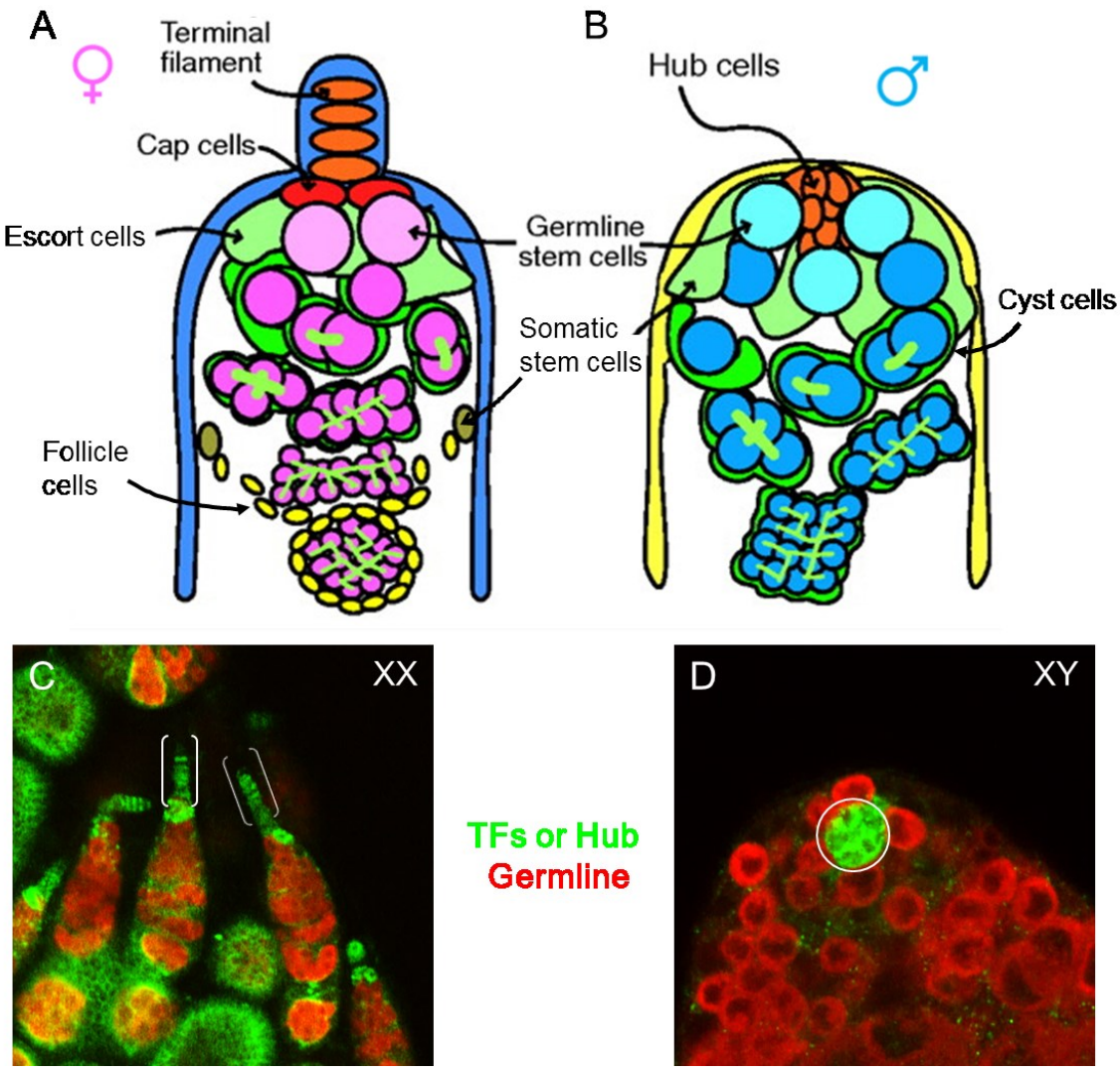
A
Terminal filament
Cap cells
Escort cells
Follicle cells
B
Hub cells
Germline stem cells
Somatic stem cells
Cyst cells
C
XX
TFs or Hub
Germline
D
XY

Temporal difference in the formation of the male and female niche

Apart from structural differences, the male and female gonad stem cell niches are specified at different developmental stages (Figure 1.3). The hub forms during the last stage of embryogenesis from a subset of anterior SGPs that express *esg* and *upd* (Gonczy et al., 1992; Le Bras and Van Doren, 2006; Wawersik et al., 2005). Following hub formation, JAK/STAT response in the primordial germ cells is restricted to those adjacent to the hub to establish the GSC identity (Wawersik et al., 2005). Similarly, SGPs that anchor to the hub take on the CySC identity. By the time of embryonic-larval transition, a fully functional male GSC niche has formed, and spermatogenesis has begun. The male gonad continues to grow in size in larval stages to accommodate the increasing number of spermatogonial cysts produced by the dividing GSCs. During metamorphosis, the male gonad attaches to the genital imaginal disc derivatives, which will develop into the reproductive tract. Pigment cell precursors further recruit muscle cells from the genital disc to form the muscle sheath and reshape the oval-shaped larval gonad into elongated and coiled testis tube seen in adults (Nanda et al., 2009).

While much is known about the structure and function of the adult female GSC niche, the development of the female niche is less clear. After gonad coalescence, female gonad morphogenesis is temporarily arrested. Within the first two larval stages, ovary development is limited to the proliferation of SGPs and PGCs. SGP division results in the formation of an apical cap consisting of anterior SGPs that do not intermingle with the PGCs and express *hedgehog* (*hh*) in early L2 stage (King, 1970; Lai et al., 2017), and the intermingle cells that interact with PGCs in the posterior gonad and expresse Traffic jam (Tj). The first noticeable sign of niche development is the specification of TFs from anterior

SGPs in the 3rd larval instar beginning approximately 12 hours after the second molt (Godt and Laski, 1995). After TF formation, cap cells are recruited from the intermingle cells to the base of TFs during larval to pupal transition. Spatial restriction of the BMP ligand Decapentaplegic (Dpp) to cap cells specifies PGCs adjacent to the niche as GSCs and allows other PGCs to differentiate (Gilboa and Lehmann, 2004; Zhu and Xie, 2003). Escort cells and follicle stem cells are specified from intermingle cells during pupal stages (Lai et al., 2017). However, the mechanism remains elusive.

Figure 1.3: **A schematic representation of sex-specific gonad morphogenesis in Drosophila.** In stage 12, the coalescing gonad is still bipotential. The posterior SGPs, termed as msSGPs, join the male gonad in stage 15 but are lost in female gonad. At this stage, some of the anterior SGPs start to accumulate hub-specific markers and adhesion molecules. By stage 17, a functional hub is formed in the male gonad. While GSC proliferation and differentiation continues in the male gonad leading to increased organ size, the L1 female gonad remains quiescent. The sexual dimorphism in organ size continues till L3 stage. Terminal filaments are formed by late third larval instar. Development of the ovary continues in pupal stages to form the adult female GSC niche. Germ cells: yellow and bipotential in stage 12, then light pink (female) or blue (male) for GSC, pink and blue for differentiating germ cells. Somatic cells: green and bipotential in stage 12; msSGPs in brown; hub cells and terminal filaments in orange; cap cells in red; cyst stem cells in light green; escort cells and cyst cells, green; follicle stem cells, grey; follicle cells, yellow.

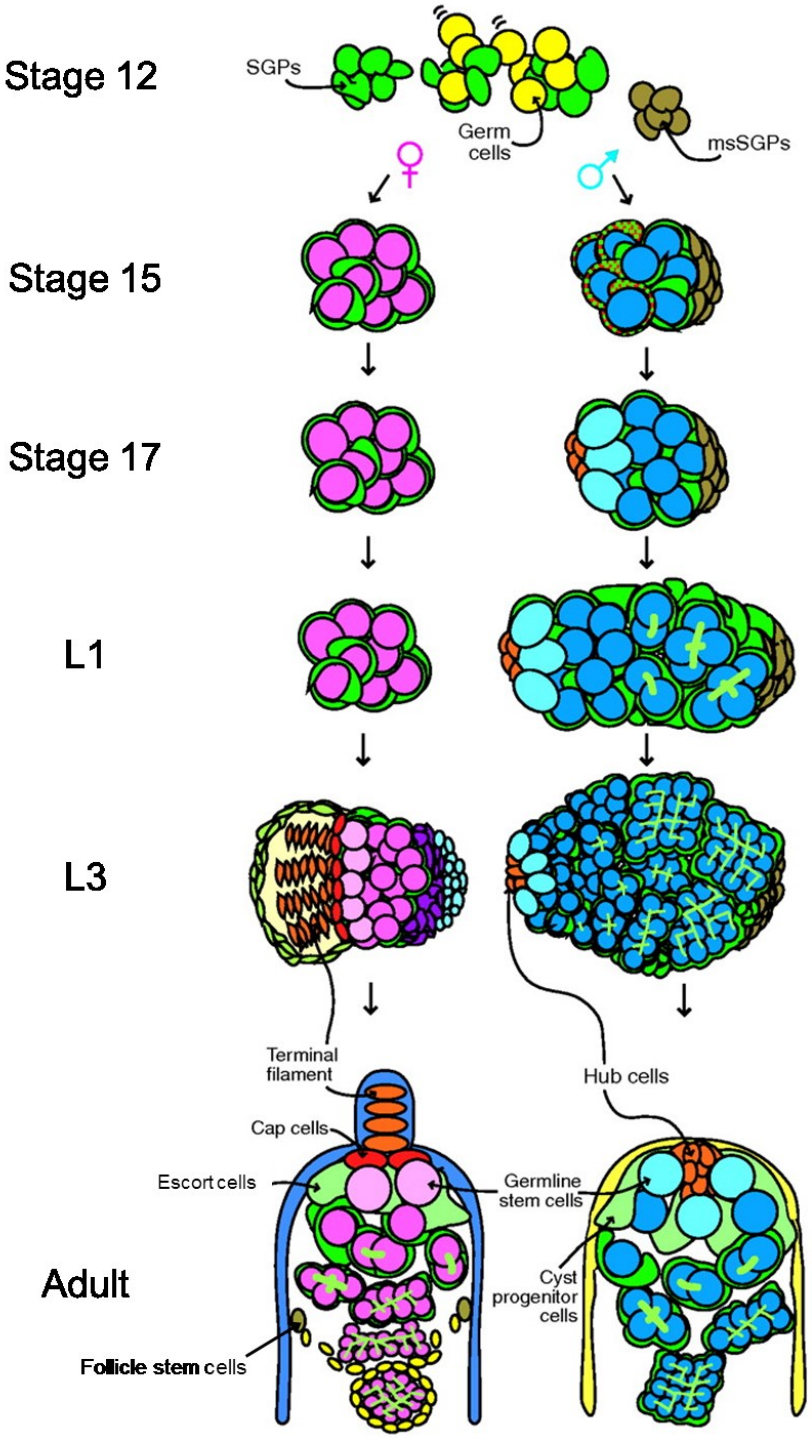
Stage 12
SGPs
Germ cells
msSGPs
Stage 15
Stage 17
L1
L3
Terminal filament
Hub cells
Cap cells
Escort cells
Germline stem cells
Adult
Cyst progenitor cells
Follicle stem cells

Signaling pathways required for male stem cell niche formation

While no mutant has been found to affect the timing of male niche specification, a few signaling pathways are known to regulate the hub and CySC fate. The Notch signaling is necessary and sufficient for differentiation of hub cells from the SGPs (Dinardo et al., 2011; Kitadate and Kobayashi, 2010). When PGCs travel through the gut to coalesce with the SGPs, anterior SGPs are briefly exposed to endodermally-derived Delta ligand, leading to the activation of Notch (Dinardo et al., 2011). Notch activation downregulates Tj expression in some SGPs, thus relieving the repression of *unpaired* and allowing Fas-3 accumulation in hub cells (Wingert and DiNardo, 2015). The other branched pathway downstream of Notch is mediated by *lines*, which represses hub cell fate and promotes CySC fate in the shared pool of anterior SGPs through antagonizing *bowl* (Dinardo et al., 2011).

The Receptor Tyrosine Kinase signaling from primordial germ cells negatively regulates hub formation. The receptor Sevenless and Epidermal Growth Factor Receptor (EGFR) are expressed in the posterior SGPs to prevent ectopic hub formation in the posterior gonad (Kitadate and Kobayashi, 2010; Kitadate et al., 2007).

Signaling pathways required for female niche formation

The onset of TF specification is under the control of ecdysone signaling (Hodin and Riddiford, 1998). Repression of the ecdysone signaling target gene *broad* is required to repress precocious niche formation (Gancz et al., 2011). While the mechanism that determines the TF fate remain unclear, a small number of genes, including *bric-à-brac* (*bab*), *engrailed* (*en*) and *twinstar*, have been shown to affect TF development and overall

organization of the adult female GSC niche (Bolivar et al., 2006; Chen et al., 2001; Godt and Laski, 1995; Sahut-Barnola et al., 1995). The ovariole number is determined by the total number of TF cells and the sorting of TF cells into stacks (Sarikaya et al., 2012). *Wnt4* is required for the migration of the apical cells in between TFs, thus affecting the number of TFs incorporated per ovariole (Cohen et al., 2002).

Following the specification of the TFs, Delta ligand produced by the posterior TF cells activates Notch in intermingle cells adjacent to the TFs, resulting in the formation of cap cells (Zhu and Xie, 2003). Insulin signals maintain cap cells via modulating Notch signaling (Hsu and Drummond-Barbosa, 2011). The attachment of GSCs to cap cells is also mediated by insulin peptides (Hsu and Drummond-Barbosa, 2009, 2011).

A few signal pathways, including Wnt, Hedgehog, and JAK/STAT signaling, have been shown to involve in the maintenance of adult follicle stem cells (Chang et al., 2013; Sahai-Hernandez and Nystul, 2013; Vied et al., 2012; Zhang and Kalderon, 2001). However, the microenvironment that defines the location and the fate of follicle stem cells remains elusive.

Dsx and sex-specific niche formation

In the Van Doren lab, we have investigated the roles of *dsx* in sexually dimorphic niche development and identified many interesting aspects on how sexual identity influences the SGPs to produce distinct stem cell niches (Camara and Van Doren, submitted). In the absence of *dsx*, most tissues develop into intersexual characteristics. However, we found a strikingly different result for the gonad stem cell niches. At stage 17 embryos, both XX and XY *dsx* mutant gonads form the hub, which signals to the GSCs

through JAK/STAT signaling. However, when examined later in adult, 50% of animals lost the hub and formed TFs in their place. This occurred in 50% of both XX and XY animals (Figure 1.4 A-E). These modes of development seemed to be mutually exclusive– we did not observe the presence of both a hub and TFs in a gonad. However, for gonads in the same animal, one could have a hub and the other TFs. We further found that the TFs were transdifferentiated from hub cells, which started to proliferate in the late L2 stage and continued in the L3 stage. By the late L3 stage, we observed 50% of examined *dsx* mutant gonads having a hub and the other 50% having TFs.

We further identified sex differences in niche plasticity. When a hub was allowed to form in the presence of DsxM, and then switched at the 2nd larval instar to DsxF using a *tra2^{ts}* allele, the hub failed to transdifferentiate into TFs. Conversely, when the somatic gonad switched from the female to male identity at the same developmental stage, hub formation occurred. The niche plasticity of female gonads was lost in the pupal stage.

From these observations, we make the following conclusions and build our model for how DsxF and DsxM regulate sexual dimorphism in the gonad stem cell niche (Figure 1.4 G). First, pathways controlling hub and TF development exist that can be modulated by *dsx*, but do not require *dsx* for their function. *dsx* acts to ensure that the hub and TF formation pathways are activated in animals with the matching sexual genotype (XY vs. XX). Second, *dsx* acts at critical time windows to ensure hub and TF formation. Since hub formation occurs in both XX and XY *dsx* gonads, DsxF acts during female embryogenesis to block hub formation. Given that hub-to-TF conversion in the *dsx* mutant gonad occurs at the time when TFs form in the wildtype ovary and that prior exposure to DsxM prevents hub-to-TF conversion in the presence of DsxF, we conclude that DsxM acts in the L3 stage

to “lock in” the hub fate and prevent hub-to-TF trans-differentiation. Since not all hubs converted into TFs, DsxF acts in L3 stage female gonads to ensure a robust response to the TF formation pathway so that all female gonads form TFs. Lastly, our finding suggests the existence of a non-autonomous signal through which niche cells “agree” with each other about which pathway to activate.

Figure 1.4: ***dsx* is required for correct niche specification.** TFs and the hub are consistently specified in wildtype female (A) and male (B) adult gonads, respectively. XY (C-D) and XX (E-F) *dsx* mutant gonads can have either TFs or a hub. Arrows indicate TFs; a circle indicates the hub. (G) A model illustrates when and how DsxF and DsxM regulate niche development.

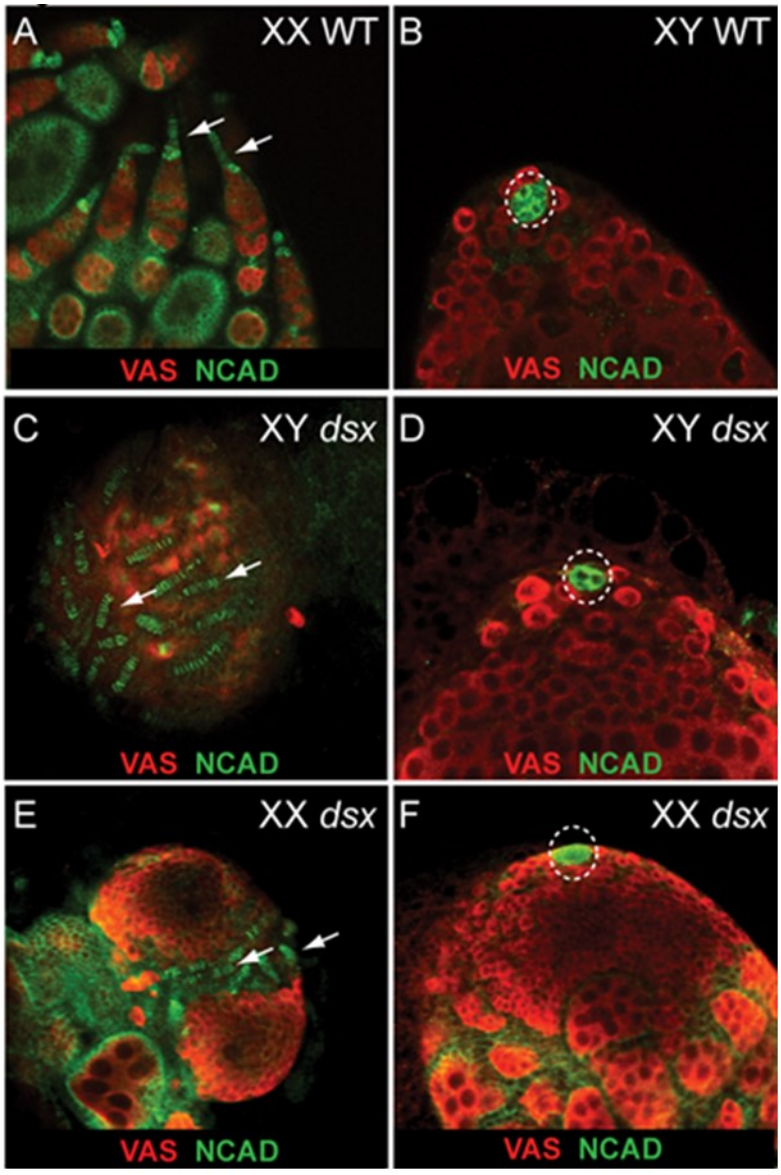
A
XX WT
VAS NCAD
B
XY WT
VAS NCAD
C
XY dsx
VAS NCAD
D
XY dsx
VAS NCAD
E
XX dsx
VAS NCAD
F
XX dsx
VAS NCAD

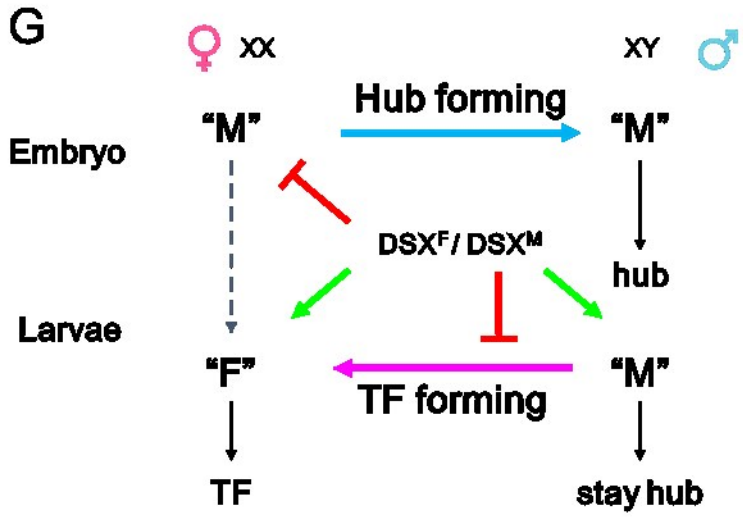
G
XX
XY
Hub forming
"M"
"M"
Embryo
DSX^F / DSX^M
hub
Larvae
"F"
TF forming
"M"
TF
stay hub

Fru and Dsx in Sexual Dimorphism of the Nervous System

There has been a longstanding distinction between morphological dimorphism and the sexual dimorphism required for fly courtship behaviors. The existence of a *dsx*-independent sex determination branch was first proposed when the development of the muscle of Lawrence (MOL), a male-specific muscle needed for copulation, was found to be regulated by *fru* rather than *dsx* (Gailey et al., 1991; Taylor, 1992). The strongest evidence supporting that *fru* is the master regulator of courtship behaviors comes from analyses of courtship defects in flies mutant for *fru* and *dsx*. While males lacking DsxM showed some courtship defects, females expressing DsxM failed to initiate courtship behaviors (Taylor et al., 1994; Villella and Hall, 1996). On the other hand, strong *fruM* mutant males completely lack courtship behaviors, and weaker *fru* mutants significantly reduce courtship towards females and form male-male courting chains (Gailey and Hall, 1989; Ito et al., 1996; Ryner et al., 1996). FruM is also sufficient to enable female flies to perform male-specific courtship behaviors (Demir and Dickson, 2005). Based on these findings, it has been proposed that the sex determination pathway bifurcates into the morphological and the behavior branches that are controlled independently by *dsx* and *fru* through Tra-mediated sex-specific alternative splicing.

Over the last decade, with new tools and techniques that enabled closer examination of the neuronal architecture required for courtship behaviors, it has become increasingly clear that *dsx* also plays important roles in sexual dimorphism of the nervous system and courtship behaviors. Dsx is expressed in approximately 700 neurons, much less than the number (~2,000) of FruM-expressing neurons estimated in the central nervous system (Pan et al., 2012). However, Dsx-expressing neuron clusters exhibit more pronounced sexual-

dimorphism in cell number and neural circuitry than FruM-expressing neuron clusters (Rideout et al., 2010; Robinett et al., 2010). Interestingly, DsxM and FruM colocalize and functionally cooperate in sexually-dimorphic neural clusters (Lee et al., 2002; Rideout et al., 2010; Robinett et al., 2010; Sanders and Arbeitman, 2008). DsxM and FruM are both required to prevent programmed cell death and establish the full number of male-specific neurons (Kimura et al., 2005; Rideout et al., 2010; Sanders and Arbeitman, 2008). A *dsx* positive neural cluster, pC1, is subdivided into two groups based on *fru* expression. The DsxM+/FruM+ subcluster acts as the courtship-triggering center, whereas the DsxM+/FruM- subcluster acts as the aggression-triggering center (Koganezawa et al., 2016). Most strikingly, two recent studies showed that *fruM* mutant female and male flies have latent courtship circuitry that is dependent on DsxM and group-raising experiences (Pan and Baker, 2014; Rezaval et al., 2016).

Potential Fru Function in Morphological Dimorphism

The fru gene locus

The *fru* gene locus is a complex transcription unit with multiple promoters and multiple alternative splicing events (Figure 1.5). Due to the existence of at least four promoters (P1-P4), sex-specific alternative splicing of P1-derived transcripts and four different 3' alternatively spliced exons, 15 protein isoforms can be generated. Transcripts produced by the most distal P1 promoter are alternatively spliced by Tra/Tra-2 to produce the male-specific FruM proteins. Transcripts produced by the downstream promoters showed no sex difference in splicing isoforms (Ryner et al., 1996). Therefore, it is assumed

that Fru isoforms (collectively named as FruCom) produced by downstream promoters (P2-P4) are expressed in both sexes, and are not components of the sex determination pathway.

The *fru* gene encodes a set of putative transcription factors belonging to the *tramtrak* family of BTB (Broad-Ccomplex, Tramtrak and Bric a brac) Zinc Finger transcription factors. While all Fru isoforms contain a BTB oligomerization domain, each Fru isoform can have one of four potential C-terminal ZnF DNA binding domain encoded by the A, B, C and D exons (Figure 1.5). Each of the A-, B-, and C-type of ZnF domains has a distinct optimal binding motif and plays distinct functions in the nervous system (Dalton et al., 2013; Neville et al., 2014; Nojima et al., 2014; von Philipsborn et al., 2014).

Figure 1.5: **Diagram of the *fru* gene locus.** *fru* transcripts are produced from P1-P4 promoters. The male-specific P1 promoter is colored in blue, and other sex-nonspecific promoters are in grey. Sex-specific splicing of P1 transcripts is shown, blue indicates male and pink indicates female. Tra/Tra-2 bind to the second exon of P1. An early stop codon (UAA) is present in the female-specific transcripts. Sex-nonspecific splicing of the 3' isoforms (A, B, C, and D) is shown in grey.

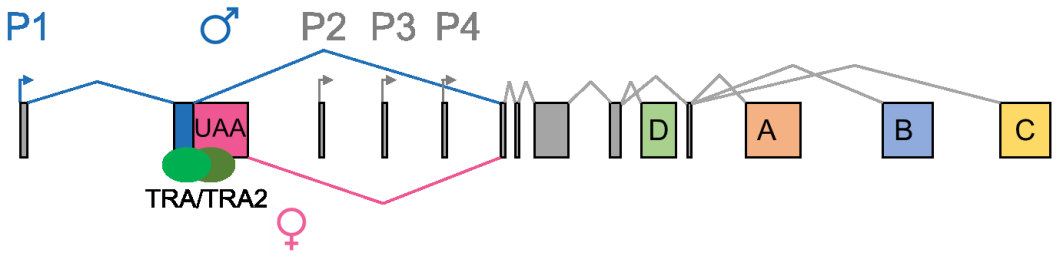

Sex-specific expression of fru isoforms in and outside the nervous system

Sex-specific alternative splicing of the P1-derived transcripts only occurs in the CNS, whereas expression of FruCom isoforms has been observed in the CNS as well as several non-neural tissues (Dornan et al., 2005; Lee et al., 2000; Ryner et al., 1996). Interestingly, in the larval CNS of both sexes, an antibody that recognizes all Fru isoforms detected Fru expression in a similar pattern in both sexes. However, Fru expression was no longer detected in pupal and adult female CNS (Dornan et al., 2005; Lee et al., 2000). These observations suggest that FruCom may also be expressed in a sex-specific pattern. Furthermore, FruCom is expressed in a few sex-specific cell types of the reproductive systems, including the follicle cells of the ovary and the secondary cells of the accessory gland (Dornan et al., 2005). These data raise the possibility that *fru* is involved in the morphological branch of the sex determination pathway.

Preliminary data generated in the Van Doren lab further indicate that *fru* may have sex-specific functions in the gonad. In a previous comprehensive genome-wide analysis of Dsx putative targets, we identified *fru* as a candidate gene that is directly regulated by Dsx (see Chapter 3 Introduction for details) (Clough et al., 2014). Using the antibody that recognizes all Fru isoforms, we detected sex-specific Fru expression in the gonad, especially in the GSC niche (Whitworth. C, unpublished). Furthermore, Fru expression in the testis is independent of *fru* P1 and sex-specific alternative splicing (see Chapter 2 Results). These preliminary data led us to hypothesize that Dsx regulates sex-specific FruCom expression and that *fruCom* functions downstream of *dsx* to control the sexual development of the gonad.

Conclusions

In this thesis work, we sought to characterize the Fru expression pattern in the gonad, to understand the molecular mechanisms that control the sex-specific expression of Fru, and to study the functions of *fru* in the gonad. This work provides an excellent system where interactions between the two terminal actuators of the sex determination pathway can be studied, and the potential roles of *fru* in the morphological branch of the *Drosophila* sex determination pathway can be assessed.

Results from Chapter 2, 3 and 4 are included in the following manuscript:

fruitless functions downstream of *doublesex* to promote sexual dimorphism of the gonad stem cell niche.

Hong Zhou, Cale Whitworth, Caitlin Pozmanter and Mark Van Doren.

Abstract

doublesex (*dsx*) and *fruitless* (*fru*) are the two actuators of the *Drosophila* sex determination hierarchy. While *dsx* assists *fru* to regulate behavioral dimorphism, whether *fru* collaborates with *dsx* in regulating morphological dimorphism remains unknown. The germline stem cell (GSC) niche is an important component of the gonad that displays sexual dimorphism. Little is known about how *dsx* regulates sexual development of the niche. Here we report that *fru* is expressed male-specifically in the GSC niche and plays important roles in the development and maintenance of the male GSC niche. We show that *dsx* rather than *tra* is responsible for male-specific Fru expression in the gonad. *fru* genetically interacts with *dsx* to prevent sex-reversal of the male niche. Ectopic expression of Fru inhibited female niche formation and partially masculinized the ovary. While Fru appears to be dispensable for the maintenance of male niche identity, it is required autonomously for cyst stem cell maintenance and cyst cell survival, and non-autonomously for the survival of trans-amplifying germ cells. Finally, we show that *fru* is likely a direct target of Dsx. We identified a conserved Dsx binding site upstream of *fru* P4 that is required for normal P4 expression in the hub. These findings reveal a non-canonical pathway where *fru* functions downstream of *dsx* to promote the maleness of the gonad and demonstrate

that sex-specific expression of Fru in neural and in non-neural tissues is controlled through two molecular mechanisms by the sex determination hierarchy.

Author contribution

H.Z., C.W., and M.V.D. designed the experiments. C.W. performed gonad Fru expression and *fru* GMR screen experiments. C.P. performed CNS Fru expression experiments. H.Z. performed gonad and CNS Fru expression, *fru* P4 enhancer-reporter analysis, and gonad Fru function experiments, analyzed data and wrote the paper. M.V.D. supervised the project.

CHAPTER 2: FRUITLESS IS TRANSCRIPTIONALLY ACTIVATED IN A MALE-SPECIFIC MANNER IN THE SOMATIC GONAD

Summary

Sex-specific expression of Fru in the gonad has been implicated but not carefully examined. In this Chapter, we characterized the male-specific expression pattern of Fru in the gonad stem cell niche. We showed that Fru expression in the male gonad does not require sex-specific alternative splicing, which is the only known mechanism that generates male-specific Fru expression patterns.

Introduction

The *fru* gene locus produces a set of BTB-zinc finger (BTB-ZnF) protein isoforms from the four known alternative promoters (P1-P4). The sex-specific P1 promoter generates *fruM* and *fruF* transcripts through Tra-dependent alternative splicing (Ryner et al., 1996). Since the *fruF* transcripts are not translatable, male-specific FruM proteins are produced from P1in the CNS and function as the master regulator of courtship behaviors in the *Drosophila* sex determination pathway. On the other hand, transcripts produced from nonP1 promoters (P2-P4) shows no sex difference in the splicing isoform and are present in both sexes (Ryner et al., 1996). Therefore, it is assumed that Fru isoforms encoded by these *fru* transcripts (collectively named as FruCom) are expressed in both sexes and do not play a role in the sex determination pathway.

However, a few pieces of evidence indicate that FruCom isoforms exhibit sex-specific expression patterns. It has been shown that FruCom is initially expressed in the third instar larval CNS in both sexes, but is turned off female-specifically in pupal and adult CNS (Gyunghee Lee et al. 2000). Sex-biased expression of FruCom isoforms was also observed in several non-neuronal tissues. Notably, FruCom was detected in a few sex-specific tissues of the reproductive system, including the female-specific follicle cells and the male-specific accessory gland (Dornan et al., 2005). The modENCODE tissue expression dataset also shows that *fru* expression is higher in adult testes and accessory glands than the ovary (flybase.org). Lastly, our recent comprehensive genome-wide analyses of Dsx putative targets (see Chapter 3 for details) suggests that *fru* expression may be regulated by Dsx in the gonad.

In this Chapter, we examined the spatial and temporal expression patterns of Fru in the female and male gonad. We sought to determine the cell types that express *fru*, the *fru* isoform that is used in the gonad, and whether *fru* expression in the gonad is controlled by the known sex-specific alternative splicing mechanism.

Materials and Methods

Fly stocks

The following stocks were used: fru^{W24}(S. Goodwin), fru^{Sat15} (S. Goodwin), fru^{Gal4} (B. Dickson), fru^{F} (B. Dickson), $fru^{\Delta B}$ (S. Goodwin), $fru^{\Delta C}$ (S. Goodwin), bam^{1}, bam^{114}, *P{w*$^{+mc}$*=UAS-mCD8:GFP}LL6* (L. Luo), and w^{1118} as a control.

Immunohistochemistry

Testes were dissected from adult male flies aged 5 days in PBS followed by fixation at room temperature for 15 minutes in 4.5% formaldehyde in PBS containing 0.1% Triton X-100 (PBTx). Ovaries and larval gonads were dissected from adult female flies aged 5 days or larvae of desired developmental stages in PBS followed by a 10-minute fixation at room temperature in 5.14% formaldehyde in PBS containing 0.1% Triton X-100 (PBTx). Staining was performed as described in (Gonczy et al., 1997), and samples were mounted on slides containing 2.5% DABCO.

The following primary antibodies were used: rat anti-FruCOM at 1:300 (S. Goodwin); guinea pig anti-Traffic-jam (D. Godt) at 1:10,000; mouse anti-Arm N2 7A1 (DSHB, E. Wieschaus) at 1:100; chicken anti-Vasa (K. Howard) at 1:10,000; mouse anti-Fas3 7G10 (DHSB, C. Goodman) at 1:30; mouse anti-Eya 10H6 (DSHB, S. Benzer/N.M. Bonini) at 1:25; rabbit anti-Sox100B at 1:1,000 (S. Russell); rabbit anti-GFP (abcam) at

1:2000. The following secondary antibodies were used: Alexa 488 goat anti-rat at 1:500; Alexa 488 goat anti-rabbit at 1:500; Alexa 546 goat anti-mouse at 1:500; Alexa 546 goat anti-guinea pig at 1:500; Alexa 546 goat anti-rabbit at 1:500; Alexa 633 goat anti-chicken at 1:500; Alexa 633 goat anti-mouse at 1:500. All Alexa probes were from Molecular Probes (Invitrogen, Carlsbad, CA).

All immunohistochemistry samples were imaged on a Zeiss LSM 700 confocal microscope with 20x, 40x or 63x objectives and processed with Zen software (Zeiss).

Developmental staging

Flies were transferred to a cage to allow egg-laying on an apple juice plate for 4 hours and were then removed. Apple juice plates were kept at 25°C and larvae of desired developmental stages were collected (36 h for mid first instar, 72 h for late second instar). Immobile third instar larvae were collected from vials as late L3 stage larvae.

Larval Mutant Genotyping

GFP-expressing balancer chromosomes were used to distinguish heterozygous siblings from trans-heterozygous *fru* mutant larvae.

RT-PCR

50 pairs of late 3rd instar larval gonads were dissected into ice cold PBS and cDNA was prepared following manufacturers' protocols (Zymo Research Quick-RNA Miniprep Kit and Invitrongen Superscript III Kit). PCR was performed on cDNA using the following intron-spanning primer pairs (given in the 5'-3' orientation):

RP48-F - CCGCTTCAAGGGACAGTATCTG

RP48-R - ATCTCGCCGCAGTAAACGC

Tj-F- ACCAGTGGCACATGGACGAA

Tj-R - CGCTCCCGAAGATGTGTTCA

Actin5C-F - TAATCCAGAGACACCAAACC

Actin5C-F – CAGCAACTTCTTCGTCACAC

Fru-P1-F - CGGAAAAGGGCGTATGGATTG

Fru-P1-R - TGTGCCAGTCAGCCTCTG

Fru-P2-F - AGCACGCCGGTCAAATTTG

Fru-P2-R - TCGCTCGGTTTTAGTTTCCCA

Fru-P3-F - GCACGTTCTCAGTTTGGAATTC

Fru-P3-R - CAACGAAAACCGTGAACTGTG

Fru-P4-F - GAATTGCTGGTCCATCGCTC

Fru-P4-R - GCAACTGAACCCAACTGTACC

Fru-Com-F - ATTACTCGGCCCACGTCC

Fru-Com-R - CTGCCCATGTTTCTCAAGACG

Fru-A-F - GCTGGACCAGACGGACAATA

Fru-A-R - GTCGTGCTCCCGATGATTT

Fru-B-F - same as Fru-A-F

Fru-B-R - CAACGGTGCAGGTTGCAG

Fru-C-F - same as Fru-A-F

Fru-C-R - GACAGGTGCATCCCGAAAG

Fru-D-F - CCAGATTACTTGCCGGTGAA

Fru-D-R - GCTCTTCAACTGAGCCTCCA

Each primer pair was validated for efficacy using whole fly cDNA from adult male flies.

Results

Fruitless is expressed in the somatic gonad in a sexually-dimorphic manner

To verify Fru expression in the gonad, we used the same anti-Fru^{COM} antibody that recognizes all Fru isoforms to more closely analyze Fru expression in female and male gonads (Lee et al., 2000). We used Vasa to indicate the germline and Armadillo (Arm) to distinguish the hub from TFs. Traffic jam (Tj) is expressed in all somatic cells interacting with the germline, which include cyst stem cells (CySCs) and undifferentiated cyst cells of the male gonad and intermingle cells, cap cells, escort cells, follicle stem cell and follicle cells of the ovary. Interestingly, we found that Fru has a dynamic and sex-specific pattern of expression within the developing gonad.

While the gonad forms during embryogenesis and the hub and cyst stem cells are specified in the late embryo and early (L1) larval stage (Le Bras and Van Doren, 2006; Sheng et al., 2009), Fru expression was first observed in some late L2 stage testes (Figure 2.1 A-D), but was only consistently observed in L3 stage testes (Figure 2.1 F).

In the 3rd instar larval (L3) stage, we observed Fru immunoreactivity at the apex of the testis in the region of the GSC niche, while we did not observe any expression in the developing female GSC niche of the L3 ovary (Figure 2.1 E and F). Coimmunostaining in the testis revealed that Fru expression overlapped with the hub marker Armadillo (Arm) and the early CySC lineage marker Tj (Figure 2.1 F). Within the ovary, we did not observe

Fru expression in the TFs, the apical cap from which TFs form, or the Tj-expressing intermingle cells (Figure 2.1 E). Occasionally we observed weak Fru expression in the basal epithelial cells (Figure 2.1 E).

Figure 2.1: Fru expression is expressed male-specifically in the larval gonads. (A-B) Female (A) and male (B) L1 gonads do no express Fru. (C-D) In L2 larval gonads, male-specific Fru expression in the GSC niche was first observed. (E-F) Fru is expressed robustly in the male GSC niche in the 3rd instar larval testis, whereas the ovary only expresses Fru at a very low level in the basal epithelial cells. Circles: the hub; brackets: TFs; Arrows: CySCs; arrowheads: basal epithelial cells with weak Fru expression. The scale bar represents 10 μm.

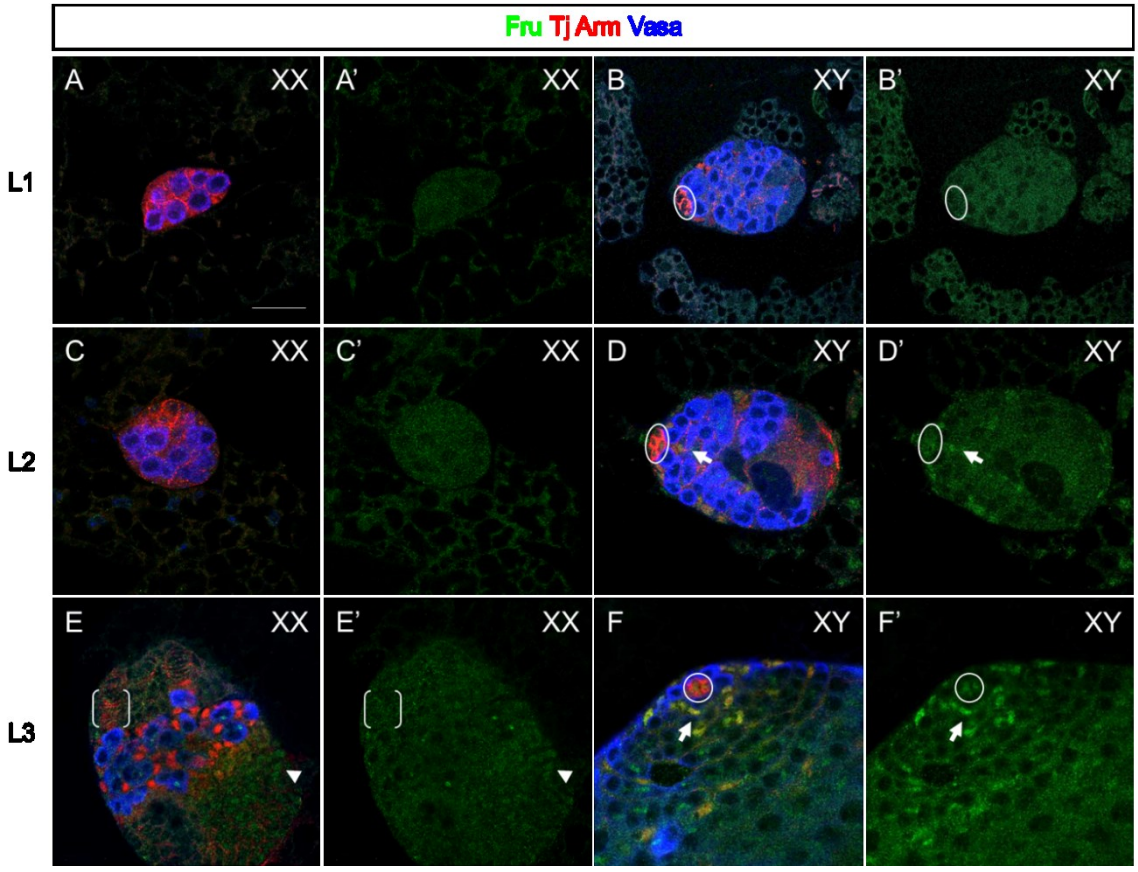

We observed a similar male-specific pattern of expression in the stem cell niche region of the adult testis and ovary. In the testis, Fru immunoreactivity was observed within the hub, CySCs and undifferentiated cyst cells that expressed Tj, but not in the germline that expressed Vasa (Figure 2.2 D). In the adult ovary, no Fru expression was observed in the TFs, cap cells, escort cells, follicle stem cells and follicle cells of the germarium (Figure 2.2 B). However, we did notice weak Fru expression in the follicle cells of later stage egg chambers and stronger Fru expression in migrating border cell and the forming dorsal appendage (Figure 2.2 A, B', and data not shown), which is consistent with earlier observations (Borensztejn et al., 2013; Lee et al., 2000). Additionally, we observed Fru expression in differentiated cyst cells

We conclude from the above observations that Fru exhibits sex-specific expression in the gonad stem cell niches and that this expression does not coincide with niche formation and only begins at the end of the L2 stage.

Figure 2.2: Fruitless expression is maintained in the adult male GSC niche. (A and B) Low magnification images of adult ovaries and testes showing sex-specific Fru expression. Arrowheads indicate the female and male GSC niche. Arrows indicate cells outside the female and male GSC niches expressing Fru. (B and D) Adult female (B) and male (D) GSC niches. (B' and D') Fru expression is shown separately in insets of the GSC niches. Arrow denotes weak Fru expression in follicle cells. Brackets: the TF; circle: the hub. Scale bar represents 100 µm (A and C), and 20 µm (B and D).

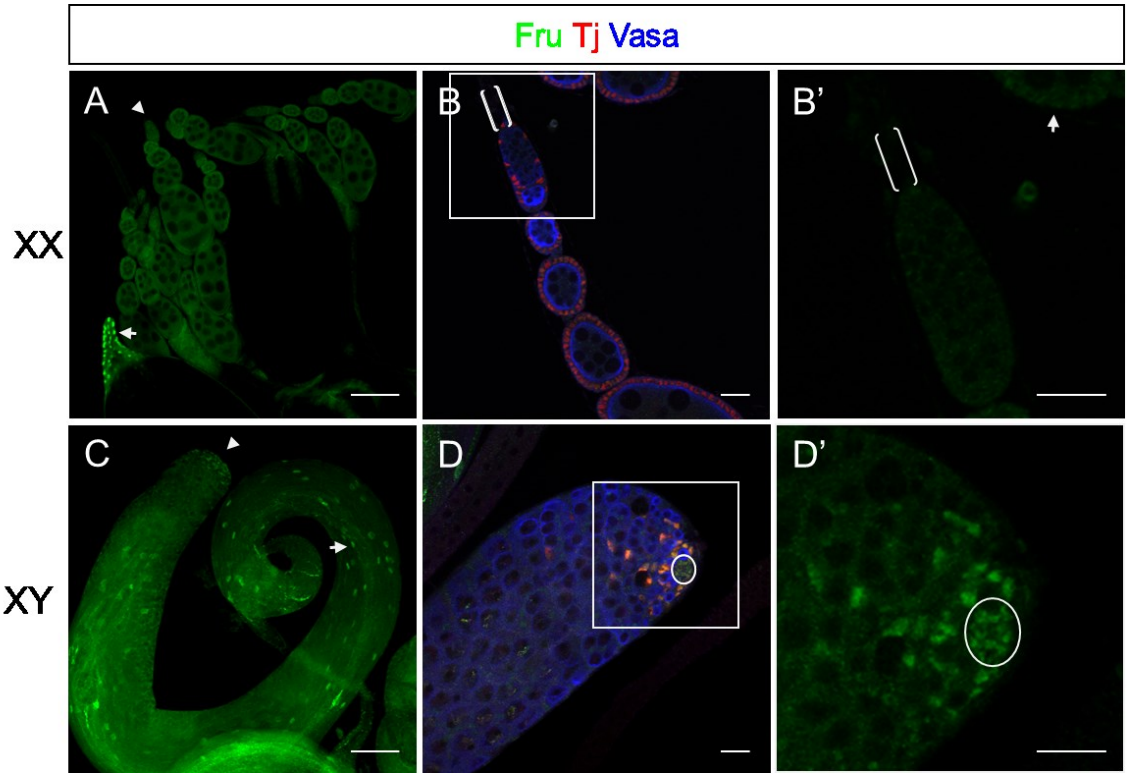

Next, we tried to determine when Fru expression is turned off in the cyst lineage during spermatogenesis. We used two cyst-cell specific transcription factors, Tj and Eyes absent (Eya), to indicate different stages of cyst cell differentiation (Figure 2.3 A''). While undifferentiated cyst cells express only Tj, differentiating cyst cells downregulate Tj expression and upregulate Eya expression. After cyst cells complete differentiation, they express only the differentiation marker Eya. We found that while Fru was expressed in Tj-positive cyst cells, it was not expressed in cells expressing Eya (Figure 2.3 B and B'). When we examined *bam* mutant testes where cyst cell differentiation was blocked, we observed an extended Fru expression pattern that correlated with the extended Tj expression pattern (Figure 2.3 B). We conclude from these data that Fru is expressed in undifferentiated cyst cells.

Figure 2.3: Fru is expressed in the undifferentiated cyst cells that expresse Tj but not Eya. (A) Fru expression in the late L3 larval testis is characterized with undifferentiated cyst cell marker Tj and differentiated cyst cell marker Eya. Arrowhead: Fru expression in a cyst cell that expresses only Tj; arrow: Fru is off in a cyst cell that expresses both Tj and Eya. Circles denote the hub. (B-C) Wildtype (B) and bam^{1}/bam^{114} (C) adult testes showing the extended Fru expression pattern correlates with the extended Tj expression pattern. Arrowhead: a Fru positive cyst cell; arrow: A differentiating cyst cell with reduced TJ and no Fru expression. Asterisk denotes the hub.

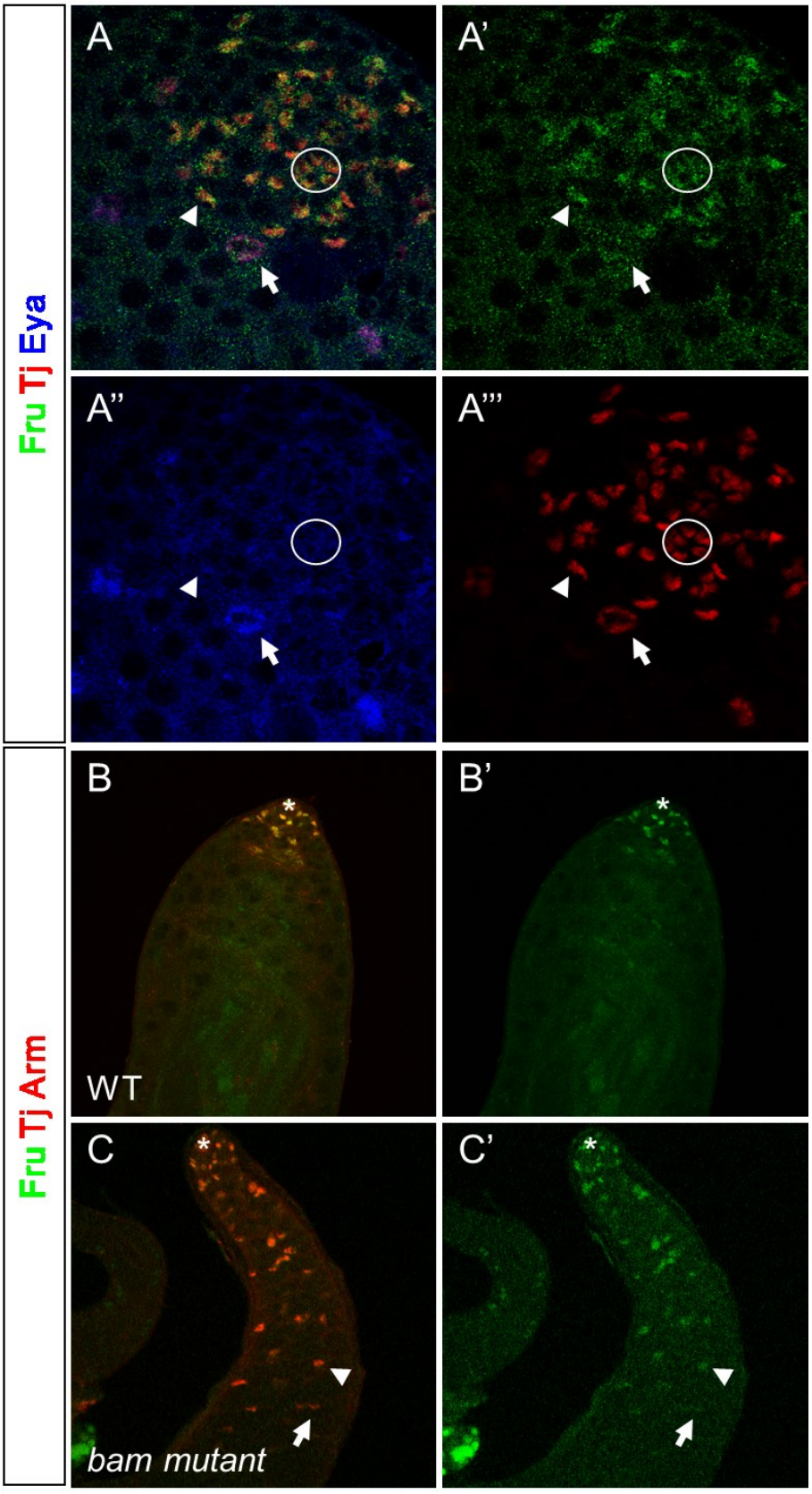
Fru Tj Eya
A
A'
A''
A'''
Fru Tj Arm
B
B'
WT
C
C'
bam mutant

It is worth noting that we also observed Fru expression in other sex-specific cell types of the larval testis. In the L3 stage, Fru was detected in the male-specific pigment cell precursors and the terminal epithelial cells of the male gonad (Figure 2.4 A and B). These male-specific cell types are also formed in the embryonic gonad. The onset of Fru expression in these cell types agrees with the onset of Fru expression in the GSC niche in late L2 stage testes (data not shown). The Fru expression level in pigment cell precursors and the terminal epithelium is comparable with its expression level in the GSC niche. However, while Fru expression in the GSC niche is maintained in adulthood, pigment cells of the adult testes do not express Fru (Figure 2.4 C). Instead, we observed Fru expression in differentiated cyst cells that were labeled by Eya.

Figure 2.4: Fru expression in other male-specific cell types of the gonad. L3 stage testes showing Fru expression in the pigment cell precursors (A) and terminal epithelium (B). Arrow: pigment cell precursor; arrowhead: Tj-positive cyst cells. (C) An adult testis showing Fru expression in the differentiated cyst cells which are marked with Eya rather than the pigment cell that expresses Sox100B. Arrow: a pigment cell.

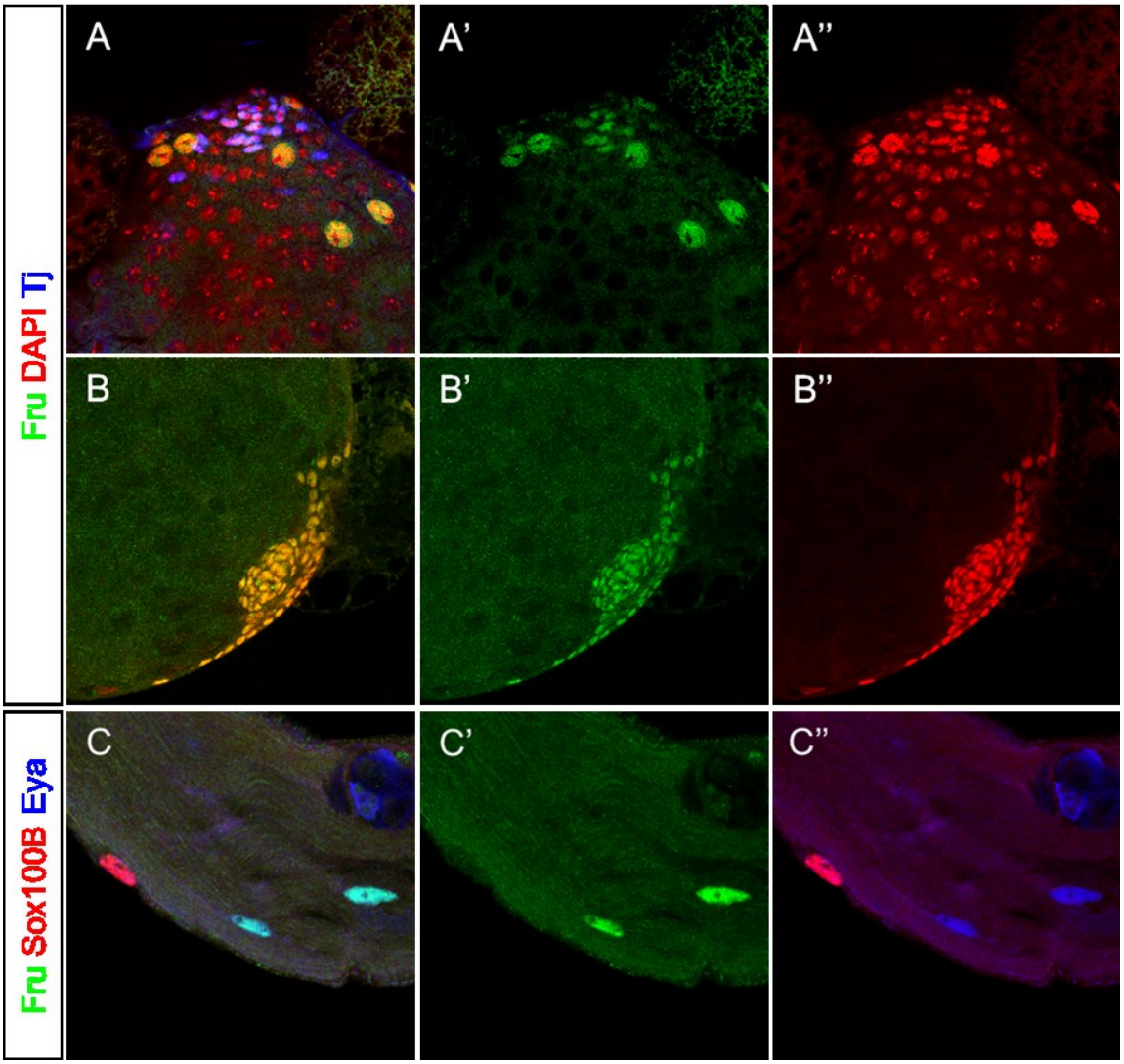

Male-specific FRU expression does not require sex-specific splicing of fru P1

Next, we wanted to understand the mechanism that regulates male-specific Fru expression in the gonad. As mentioned in the introduction, Tra/Tra-2 mediated alternative splicing of *fruP1* is the only mechanism that is known to generate male-specific FruM expression (Figure 2.5 A). Thus, we tested whether the male-specific Fru expression in the gonad was generated from P1 transcripts. We utilized an engineered *fru* allele, *fruF*, that only generates female-spliced transcripts from P1, which do not encode functional Fru protein and lack the anti-Fru^{Com} antibody epitope (Demir and Dickson, 2005). However, *fruF* mutant adult testes exhibited a normal Fru expression level (Figure 2.5 C). Consistent with this, flies containing a modified *fru* locus (fru^{Gal4}) expressing *Gal4* in place of P1 transcripts (Stockinger et al., 2005) exhibited no Gal4 activity in the testis tip (Figure 2.5 D and E). These results suggest that FruM is not responsible for male-specific Fru expression in the testis. To determine which promoter drives *fru* expression in the male GSC niche, we generated cDNA from L3 stage male gonads that were not innervated by the *fruM*-expressing neurons (Billeter and Goodwin, 2004). RT-PCR conducted with promoter-specific primers confirmed that P1 transcripts were absent in the male gonad. Instead, transcripts generated from the downstream P3 and P4 but not P2 promoters were detected (Figure 2.5 B).

We conclude from the above results that male-specific Fru expression in the gonad is regulated by a novel mechanism that does not require sex-specific splicing of the *fruP1* transcripts. Instead, Fru isoforms encoded by P3 and P4 transcripts, which were considered to be sex-nonspecific, are responsible for Fru expression in the testis.

Figure 2.5: Male-specific Fru expression does not require the sex-specific P1 promoter. (A) Schematic diagram of the *fru* promoter region. P1 is spliced sex-specifically by Tra/Tra-2 into the male (blue) and female (pink) isoforms. Sex-specific splicing does not regulate P2-P4. Therefore, P2-P4 are considered to be sex-nonspecific (grey) promoters. Intron-spanning primer sets used to detect specific promoters are as indicated. (B) RT-PCR of late L3 stage testes. *tj* and *RP49* were used as control genes to indicate the RNA abundance of cyst cells and the whole sample. (C) *fruP1* mutant (fru^{F}/fru^{W24}) adult testis showing Fru expression at the wildtype level. (D and E) fru^{Gal4} >mCD8:GFP adult testis showing no expression in the GSC niche. The hub and the tip of the testis are outlined. Arrow: the hub. Scar bars represent 20 μm.

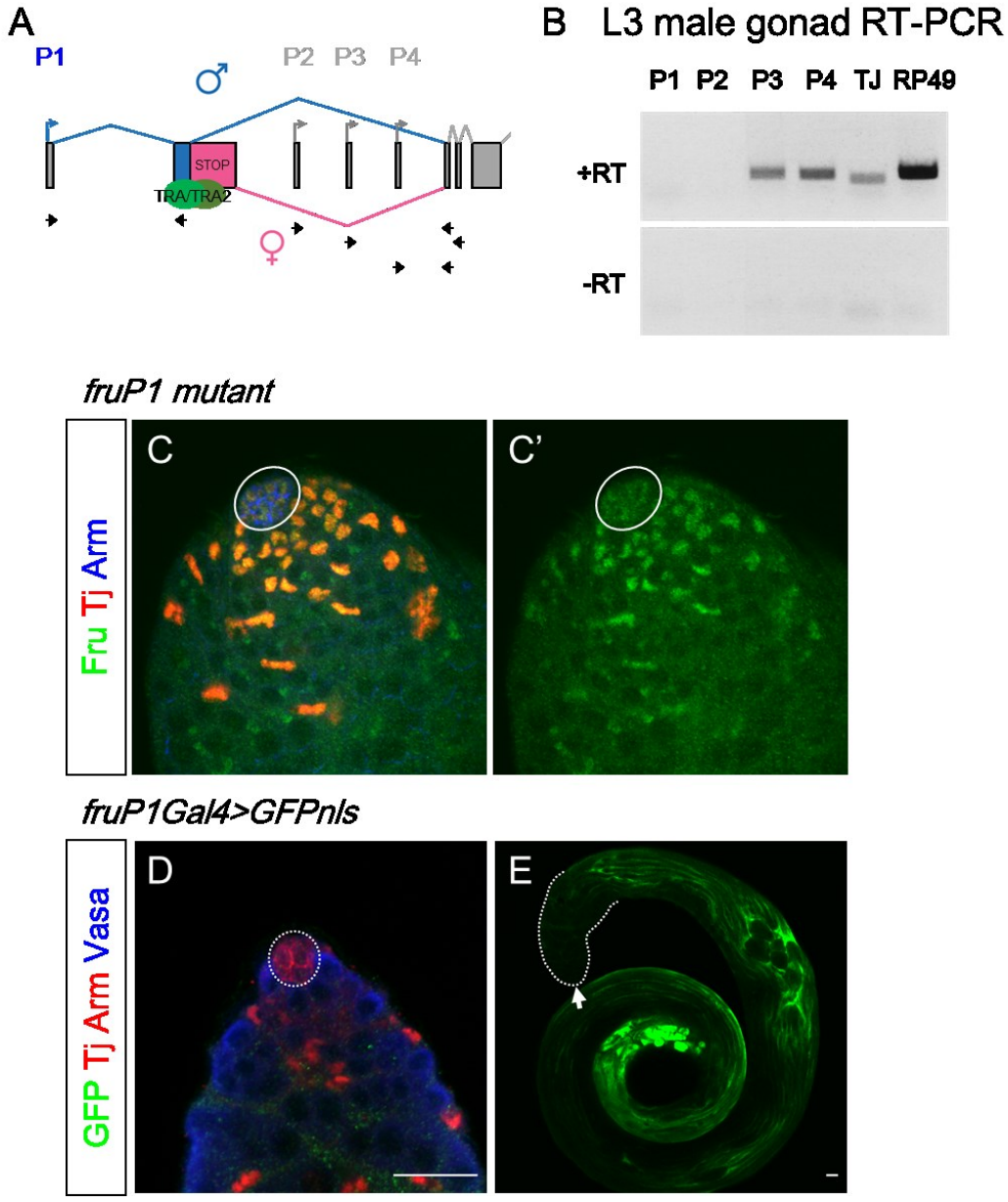
A
P1
P2 P3 P4
STOP
TRA/TRA2
B L3 male gonad RT-PCR
P1 P2 P3 P4 TJ RP49
+RT
-RT
fruP1 mutant
Fru Tj Arm
C
C'
fruP1Gal4>GFPnls
GFP Tj Arm Vasa
D
E

C-terminal isoform-specific Fru expression in the gonad

Next, we wanted to determine the C-terminal isoforms used in the male gonad. *fru* transcripts undergo Tra/Tra-2 independent alternatively splicing to include one of four C-terminal exons (A-D) (Figure 2.6 A). It has been shown that FruMA, FruMB, and FruMC have highly overlapping expression patterns in the CNS, except for a few neural clusters showing isoform-specific expression (Neville et al., 2014; von Philipsborn et al., 2014). We profiled *fru* C-terminal isoform usage in the L3 stage testis via RT-PCR. We detected all four isoforms at the mRNA level (Figure 2.6 B). Since different primer sets have varied amplification efficiency, we were unable to determine if one isoform was dominantly expressed. However, when we examined *fru* mutants that lack isoform-specific C-terminal domains, we found that $fru^{\Delta B}$ gonads significantly reduced the Fru immunoreactivity whereas the Fru expression level in $fru^{\Delta C}$ gonads was comparable to that in control testes (Figure 2.6 C and D, data not shown).

Figure 2.6: B-isoform mutant L3 testes lose most of Fru at the protein level, but transcripts containing A, B, C and D isoforms are all detected at the mRNA level. (A) Diagram showing sex-nonspecific splicing of the C-terminal isoforms. A, B, C, and D isoform each contains a distinct zinc-finger domain. Intron-spanning primer sets used to probe the isoforms are as indicated. (B) RT-PCR result using *actin*, *fruCOM*, or isoform-specific *fru* primers. (C and D) Wildtype (C) and $fru^{\Delta B}$ mutant (D) L3 male gonads. Circle: the hub; arrow: residual Fru expression in the cyst cell.

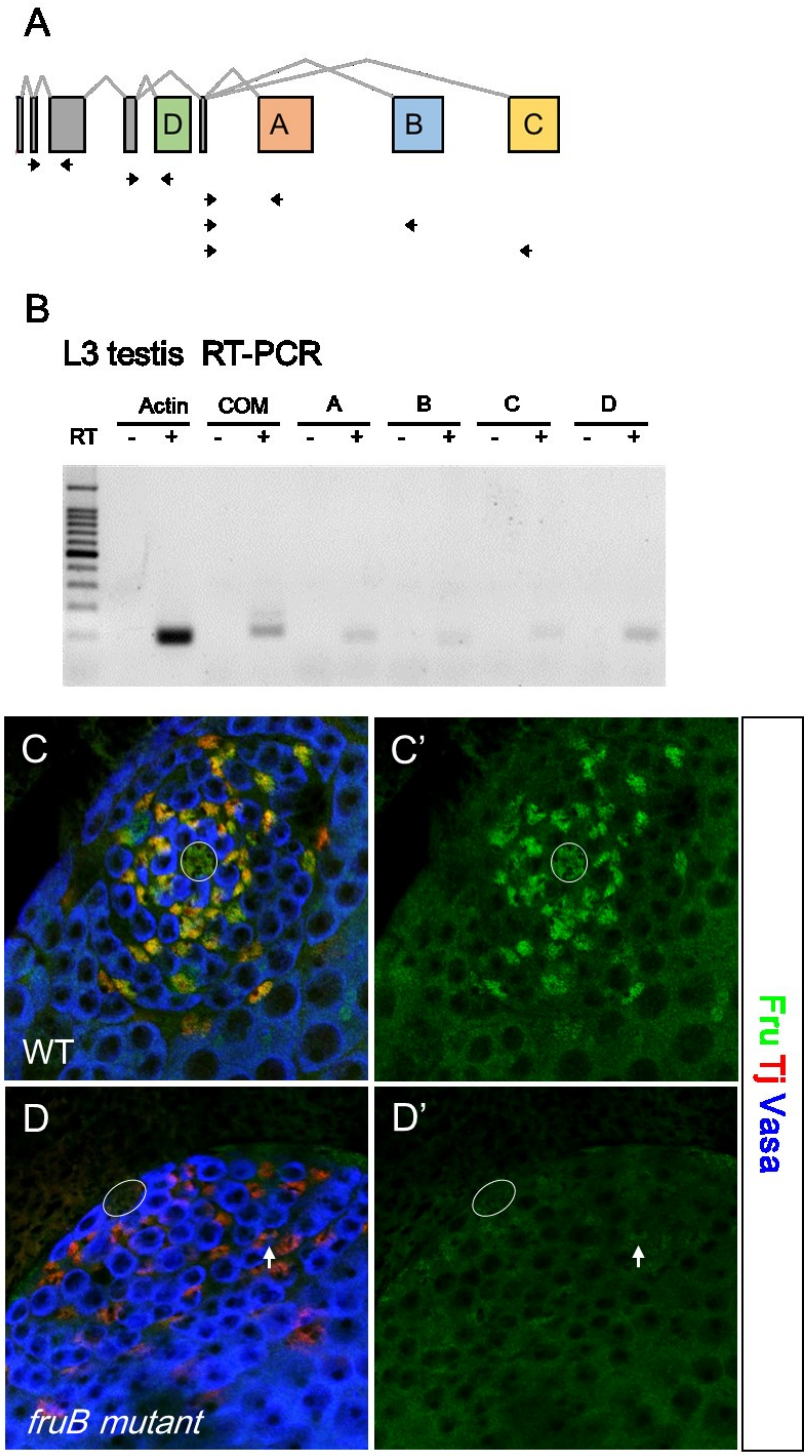
A
D
A
B
C
B
L3 testis RT-PCR
Actin
COM
A
B
C
D
RT
- + - + - + - + - + - +
C
C'
WT
D
D'
fruB mutant
Fru Tj Vasa

Conclusions and Discussion

We identified and characterized the sex-specific Fru expression pattern in the developing and adult gonad. Although male-specific cell types, including the hub cell, CySC, cyst cell, pigment cell precursor and the msSGPs, are specified in the embryonic stage, Fru is not expressed in the testis until late L2 stage. The onset of Fru expression in the gonad stem cell niche and the continued expression in adulthood are consistent with previously reported temporal expression pattern of *fru* in the CNS and non-neural tissues (Dornan et al., 2005; Lee et al., 2000; Ryner et al., 1996).

Because Tra/Tra2 only regulates P1 pre-mRNA splicing, it has always been assumed that expression from the nonP1 promoters has no sex-bias. Our finding that *fru* P3 and P4 promoters, rather than P1, are used for sex-specific expression in the gonad is the first piece of evidence that argues against this assumption. Functional studies of FruCom were neglected because FruCom was not considered part of the sex determination pathway. Our finding urges the field to re-examine *fru* expression and consider the possibility that nonP1 Fru isoforms play sex-specific roles in the CNS as well as in non-neural tissues.

Our finding that *fru* transcripts with all four C-terminal exons are expressed in the gonad is consistent with previous observations in the CNS. However, the significant reduction of Fru level in *fru* ^{B} mutant is quite surprising. The isoform-specific *fru* alleles were generated through the introduction of a premature stop codon near the 5' end of the C-terminal exons (Billeter et al., 2006; Neville et al., 2014). Theoretically, isoform-specific *fru* mutants will produce truncated proteins that lack the C-terminal ZnF domain but can still be detected by the anti-FruCom antibody. This may explain why we observed a normal

level of Fru expression in $fru^{\Delta C}$ mutant testes. However, this logic cannot explain the reduction of total Fru proteins in $fru^{\Delta B}$ mutant. There are two possibilities. First, the C-terminal ZnF domain of FruB is required to prevent Fru proteins from degradation. It is possible that FruB is the dominant protein isoform in the testis and is unstable when the ZnF domain is removed. If this is the case, FruC should be expressed in the gonad at such a low level that its removal cannot be noticed. It is also possible that FruB forms heterocomplexes with other Fru isoforms through the BTB domain and the B-type ZnF domain is required for stability of all Fru isoforms.

The alternative hypothesis is that FruB is required to maintain *fru* transcription in the gonad. This hypothesis is supported by FruM occupancy analyses in the CNS (Neville et al., 2014). Neville et al. found that FruMB binds to itself around P3 and P4 promoter regions and suggested that FruB might autoregulate *fru* gene expression from P3 and P4. This is consistent with P3 and P4 being expressed in the testis. Furthermore, we noticed potential Fru autoregulation in the testis. When we ectopically expressed Tra in the adult testis to masculinize the somatic gonad, Fru level was not reduced (Whitworth, C, unpublished data).

In summary, we have identified and characterized a male-specific expression pattern of Fru in the gonad. We showed that Tra/Tra-2 dependent sex-specific alternative splicing of P1 is not required for male-specific Fru expression in the. Instead, Fru isoforms generated from P3 and P4, which were thought to be sex-nonspecific, are accounted for the sex-specific Fru expression. Our findings in this Chapter demonstrate that sex-specific expression patterns of Fru exist outside the nervous system and raises the possibility that *fru* plays male-specific roles in the morphological branch of the sex determination pathway.

CHAPTER 3: FRU IS A DIRECT TRANSCRIPTIONAL TARGET FOR DSX

Summary

In this Chapter, we tested the hypothesis that male-specific Fru expression in the gonad stem cell niche is regulated by *dsx* at the transcriptional level. We showed that DsxM is necessary and sufficient for Fru expression. Our Dsx occupancy data and enhancer expression analyses further support that Dsx directly binds to *fru* and regulate sex-specific transcription from the P4 promoter.

Introduction

dsx and *fru* are the two terminal actuators of the *Drosophila* sex determination pathway. It is currently thought that the master sex switch gene *tra* independently controls the sex-specific alternative splicing of *dsx* and *fru* to generate DsxF, DsxM and FruM isoforms. DsxF and DsxM control sexual dimorphism of the soma and the nervous system, whereas FruM only controls sexual dimorphism of the nervous system and the male-specific courtship behaviors. The *fru* gene locus is a complex transcriptional unit with multiple promoters (P1-P4). Only pre-mRNA transcribed from the most distal *fru* P1 promoter is alternatively spliced to generate male-specific FruM isoforms in the CNS. Transcripts produced from nonP1 promoters are assumed to be not controlled by the sex-determining genes.

In Chapter 2, we found that the somatic gonad exhibits male-specific Fru expression pattern. However, this is not due to Tra-dependent sex-specific splicing of P1. We showed that *fru* transcripts in the testis are generated from P3 and P4 promoters. These findings suggest that a previously unrecognized mechanism is responsible for the male-specific Fru expression in the gonad. In *Drosophila*, sex-biased gene expression is regulated either by sex-specific alternative splicing or by transcriptional control of Dsx and Fru. Since Fru expression in the testis stem cell niche does not require *fruP1*, we considered the possibility that Dsx-dependent transcriptional regulation is responsible for the male-specific Fru expression in the gonad.

Previously, we performed a comprehensive genome-wide analysis that allowed us to predict Dsx direct target genes (Clough et al., 2014). From these data, we found several pieces of evidence suggesting that Fru expression in the gonad is regulated directly by Dsx

at the transcriptional level. The Dsx DNA binding specificity has been biochemically-define (Erdman et al., 1996; Yi and Zarkower, 1999). When the *fru* gene locus was analyzed, we found significant enrichment for sequences scored as top Dsx binding motifs by position weight matrix (PWM) (Figure 3.1 B). When comparative genomics was used to analyze the conservation of Dsx binding motifs among 20 Drosophila species, some Dsx motifs located around the P3 promoter region appeared to be conserved (Figure 3.1 B). Dsx occupancy datasets, including ChIP-seq of S2 cells expressing tagged DsxF or DsxM (Figure 3.1 C) and DamID-seq of adult female and male fat body expressing Dam-Dsx (Figure 3.1 D), suggest that P3 and P4 promoters are bound by DsxF and DsxM. This is consistent with our finding that *fru* is transcribed from P3 and P4 in the testis.

The sex-specific colocalization between Dsx and Fru also supports that Fru is a Dsx target. Fru expression in the male gonad overlaps with known DsxM expression in the hub and the Tj-expressing CySCs and undifferentiated cyst cells (Hempel and Oliver, 2007). Using a Dsx-GFP BAC transgene, we also observed colocalization between Dsx and Fru in the male GSC niche (Figure 3.2 A). In the late L3 stage ovary, Dsx is expressed in the corresponding cell types, which include the apical cap, intermingle cells and basal epithelium, whereas Fru is absent (Figure 3.2 B). If Dsx activates gene expression in one sex and represses expression in the opposing sex, the absence of Fru in the ovary can be explained by the transcriptional repression of DsxF.

In this Chapter, we tested the hypothesis that Dsx regulates male-specific Fru expression in the gonad. Using multiple genetic approaches, we addressed the necessity and sufficiency of Dsx for Fru expression in the gonad. To determine if Fru is directly regulated by Dsx, we performed enhancer-promoter analyses and site-directed mutagenesis

to identify the *cis*-regulatory element and the Dsx binding site that control male-specific Fru expression in the niche.

Figure 3.1: Dsx binding motif analyses and Dsx occupancy datasets suggest *fru* P3 and P4 are directly regulated by Dsx at the transcriptional level. (A) The promoter region of *fru* gene locus (reversely oriented) is shown to scale. Promoter P1 - P4 are as indicated. The FlyBase track shows transcripts made from each promoter. (B) Putative Dsx binding sites in the *fru* promoter region are shown as top1% and 10% sites scored by position weight matrix and evolutionarily conserved sites across 21 fly species (Clough et al., 2014) (Clough, Jimenez, Kim, Whitworth, Neville, Hempel, Pavlou, Chen, Sturgill, and Dale 2014). Three sites (red bar) that are highly conserved across 21 Drosophila species were missed by the comparative genomics analysis. (C) Male and female fat body Dsx-DamID peaks are shown. (D) ChIP-Seq was conducted in S2 cells expressing tagged DsxM and DsxF.

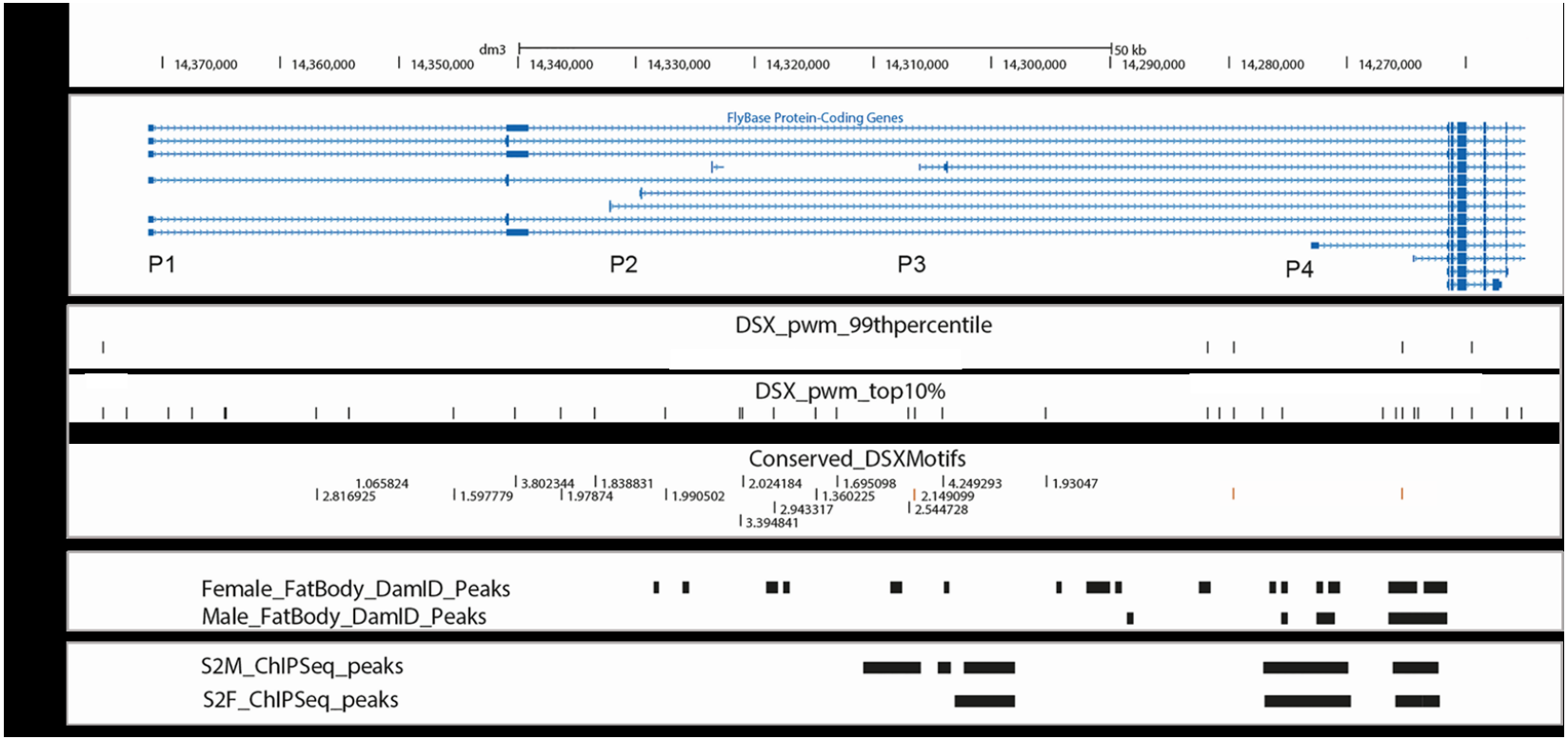
dm3
50 kb
14,370,000
14,360,000
14,350,000
14,340,000
14,330,000
14,320,000
14,310,000
14,300,000
14,290,000
14,280,000
14,270,000
FlyBase Protein-Coding Genes
P1
P2
P3
P4
DSX_pwm_99thpercentile
DSX_pwm_top10%
Conserved_DSXMotifs
1.065824
2.816925
1.597779
3.802344
1.838831
1.97874
1.990502
2.024184
2.943317
3.394841
1.695098
1.360225
4.249293
2.149099
2.544728
1.93047
Female_FatBody_DamID_Peaks
Male_FatBody_DamID_Peaks
S2M_ChIPSeq_peaks
S2F_ChIPSeq_peaks

Figure 3.2: FRU and DSX colocalize in the male gonad. Male (A) and female (B) late L3 stage gonads carrying a Dsx-GFP BAC were shown. Fru and Dsx expression overlap in the hub and early cyst lineage of the male GSC niche. Dsx is expressed in the intermingle cells and basal epithelial cells of the female larval gonad, and at a very low level in the apical cap excluding the TFs. Fru is not expressed in the female gonad.

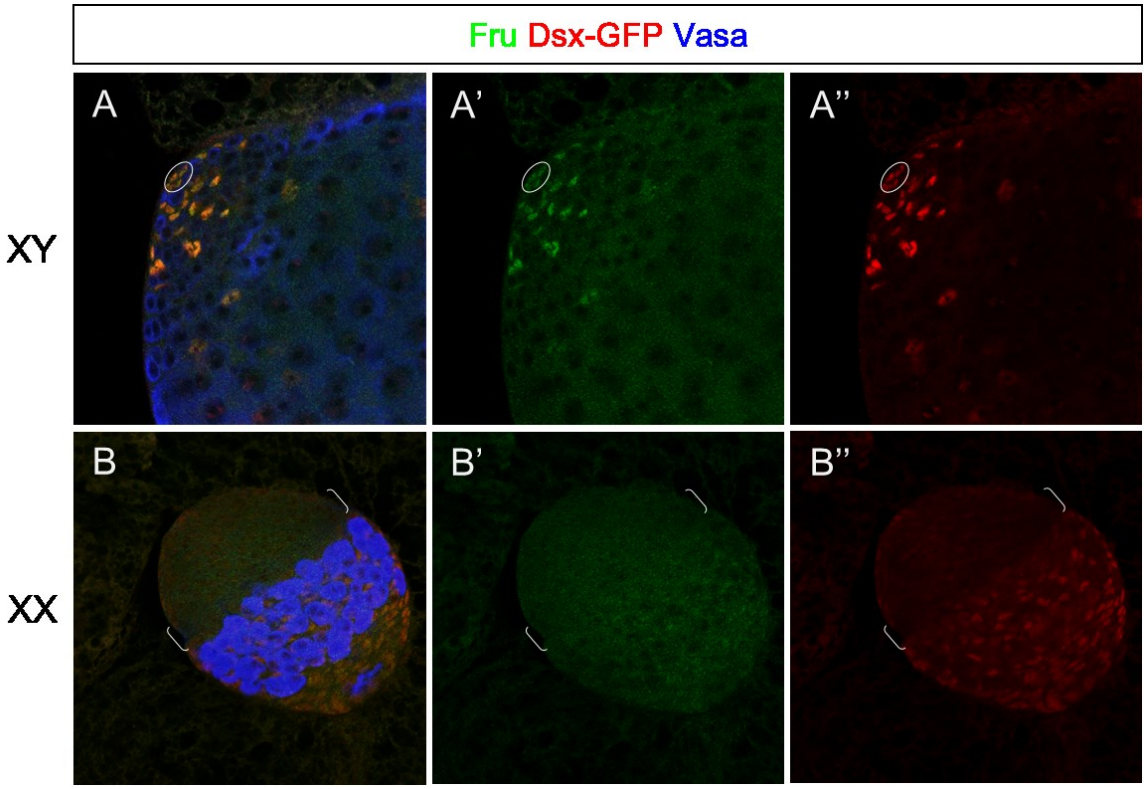

Materials and Methods

Fly stocks

The following stocks were used: PBac{y[+mDint2] w[+mC]=dsx-GFP.FPTB}VK00037 (BDSC #51966), dsx^{D}, $Df(3R)dsx^{3}$, dsx^{1}, $dsx^{Gal4\Delta 2}$ (B. Baker), w^{1118}; $P\{w^{+mc}=UAS\text{-}GFP.nls\}14$, *upd-Gal4* (T. Xie), *w[*]; P{w[+mC]=UAS-RedStinger}4, P{w[+mC]=UAS-FLP.D}JD1, P[w{+mC]=Ubi-p63E(FRT.STOP)Stinger}9F6/CyO* (BDSC #28280), and w^{1118} as a control.

Developmental staging

Flies were raised at 25°C. Immobile third instar larvae were collected from the vials as late third instar larvae.

Genotyping and sex identification of dsx mutants

Balancer chromosomes containing a *P{Kr-GFP}* transgene were used to distinguish transheterozygous *dsx* mutant larvae from heterozygous siblings. Sex chromosome genotype of *dsx* null mutants was identified using a male-specific *P{msl-3-GFP}* (J. Sedat) transgene, or Y chromosome marked with *Bs* ($Dp(1;Y)B^{S}$). XX $dsx^{D}/+$ and dsx^{D}/dsx^{-} mutants were distinguished from XY siblings by abnormal testis morphology.

Immunohistochemistry

L3 testes and ovaries were dissected in PBS and fixed at room temperature for 10 minutes in 6% formaldehyde in PBS containing 0.1% Triton X-100 (PBTx). Immunostained was performed as previously described (Gonczy et al., 1997), and samples

were mounted in 2.5% DABCO. Adult brains were dissected from 2-day-old flies in PBS, and processed as previously described (Lee et al., 2000).

The following primary antibodies were used: rat anti-FRU^{COM} at 1:300 (S. Goodwin); guinea pig anti-Traffic-jam (D. Godt) at 1:10,000; mouse anti-Arm N2 7A1 (DSHB, E. Wieschaus) at 1:100; mouse anti-Fas3 7G10 (DHSB, C. Goodman) at 1:30; chicken anti-Vasa (K. Howard) at 1:10,000; rabbit anti-GFP (abcam) at 1:2000; mouse anti-Piwi 4K5 (H. Lin) at 1:100; mouse anti-nc82 at 1:30 (DHSB, E. Buchner) . The following secondary antibodies were used: Alexa 488 goat anti-rat at 1:500; Alexa 488 goat anti-rabbit at 1:500; Alexa 546 goat anti-mouse at 1:500; Alexa 546 goat anti-guinea pig at 1:500; Alexa 546 goat anti-rabbit at 1:500; Alexa 633 goat anti-chicken at 1:500; Alexa 633 goat anti-mouse at 1:500; Alexa 633 goat anti-rabbit at 1:500. All Alexa probes are from Molecular Probes (Invitrogen, Carlsbad, CA).

All immunohistochemistry samples were imaged on a Zeiss LSM 700 confocal microscope with 20x, 40x or 63x objectives and processed with Zen software (Zeiss).

Identification of conserved Dsx binding sites in related Drosophila species

30 *D. mel* Dsx binding motifs with top 10% score in the PWM analyses were used. A 32-nt sequence with the DSX binding site in the center was blated in the USCS genome browser, and the comparative genomics data sets were used to indicate conservation across 27 insect species.

Fru reporter constructs and transgenes

To generate the WT *fru* P4 enhancer promoter reporter construct, a 7.5 kb genomic sequence from *fru* genomic clone BACRP98-2G21(BACPAC Resources Center) was amplified with the following primers (given in the 5' to 3' orientation), and cloned into pJR16 vector (R. Johnston) between the BamHI and PstI site.

Fru-P4-8K-WT-F - CGGGATCCGCAACCCGTCCGTATC

Fru-P4-8K-WT-R - CAACTGCAGTGTGGGTATGGGCAAATTGA

To generate *fruP4* reporter constructs with mutated DSX sites, DNA fragments carrying individual DSX binding sites were obtained through restriction digest of the WT constructs (DSX1: SrfI/PstI; DSX2: HindIII/NdeI, DSX3: BamHI/HindIII), and subcloned into the TA vector (Invitrogen TA Cloning Kit). Site-directed mutagenesis of DSX sites was performed according to the manufacture's protocol (New England Biolabs Q5 Site-Directed Mutagenesis Kit). The following primer sets were used:

DSX1mut-F - GGGTGTGTTAATTTGCCAGG

DSX1mut-R - CCCCTGGCTCATTAACAGACCAAT

DSX2mut-F - GGGATTTATTGCACAGGTTG

DSX2mut-R - CCCCAAATGTTAGAAAACCAAGCATTTTT

DSX3mut-F - GGGTTCTGTAATAGATAATTCAGTTC

DSX3mut-R - CCCCATGAGTAACTTCTGTGC

DNA fragments with mutated DSX sites were then digested from the TA plasmids to swap the wildtype sites in the pJR16-P4-8K-WT construct, resulting in the P4-8K-DSXmut1 and P4-8K-DSXmut123 constructs.

Transgenic flies were generated via PhiC31 integrase-mediated transgenesis. The constructs were integrated into the same genomic location (attP40 on Chromosome II).

Imaging and quantification of fru reporter GFP expression in the hub

Z-stack images of the hub were taken under the same setting on a Zeiss LSM 700 confocal microscope with a 63x objective. Quantification of GFP fluorescent intensity was performed in Fiji software (ImageJ, NIH). For each gonad, five random hub cells were sampled and a 16-cell-stage germ cell was sampled as background. A circle of the same size was drawn as the sample area. Average fluorescence intensity of GFP and Piwi was acquired. The relative fluorescent intensity was measured as GFP[hub-background]/Piwi[hub-background].

Results

Dsx is sufficient for Fru expression in the gonad and the central nervous system

To test if male-specific Fru gonad expression is dependent on *dsx* and independent of *tra*, we utilized a genetic background (*XX; dsx^{D}/dsx^{-}*) that is otherwise female but expresses DsxM instead of DsxF (Figure 3.3 A) (Nagoshi and Baker, 1990). If Fru expression is regulated by Dsx, we would expect Fru to be expressed in the stem cell niche, similar to its expression pattern in wild-type testes. If sex-specific Fru expression is dependent on alternative splicing by Tra, or on any other component of the sex determination cascade, we would expect Fru to be not expressed in the gonad, similar to the expression pattern in the wildtype ovary. DsxM caused the XX somatic gonad to be fully masculinized and develop a male niche. We observed robust and consistent Fru expression in the *XX; dsx^{D}/dsx^{-}* gonad in late L3 stage (n=14) (Figure 3.3 C). Fru expression overlapped with FasIII and Tj in the hub cells and the early CySC lineage and was

indistinguishable from the XY siblings (Figure 3.3 B and C). This expression pattern was maintained in adulthood (data not shown).

We next sought to test if Dsx also regulates sex-specific *fru* transcription in the CNS. In adult males, Fru is expressed in a subset of sexually-dimorphic neurons in the posterior brain and partially colocalizes with Dsx, which is indicated by $dsx^{Gal4\Delta 2}$>GFP (Rideout et al., 2010) (Figure 3.3 D). In contrast, no Fru isoform is expressed in the adult female CNS (Figure 3.2 E) (Lee et al., 2000). Using the same genetic approach, we observed Fru expression in the CNS of *XX;* dsx^{D}/dsx^{-} flies (n=4). Fru was expressed in the posterior brain of XX pseudo-males in a similar pattern as its expression in XY siblings and wildtype males (Figure 3.3 D, F, and G). Since Tra spliced P1 transcripts into *fruF*, the Fru proteins detected by the anti-Fru^{Com} antibody were encoded by *fru* transcripts generated by nonP1 promoters. We conclude that FruCom expression in the CNS is dependent on Dsx in addition to the previously reported FruM expression that is regulated by Tra-mediated sex-specific alternative splicing.

Figure 3.3 Sex-specific Fru expression in the niche is controlled by Dsx-mediated transcriptional regulation rather than Tra-mediated splicing. (A) Schematic diagram of the experiment setup. In *XX; $dsx^{D/}dsx^{-}$* gonads, the sex determination pathway up to the point of *tra* remains unchanged. Female-specific splicing of *fruP1* transcripts still occurs. DsxM rather than DsxF is produced from the dsx^{D} allele. (B-C) FRU is expressed in XX dsx^{D}/dsx^{3} late L3 stage gonads at a comparable level to XY siblings. Circles: the hub. (D-G) Genotype as indicated. 2-day-old posterior brains.

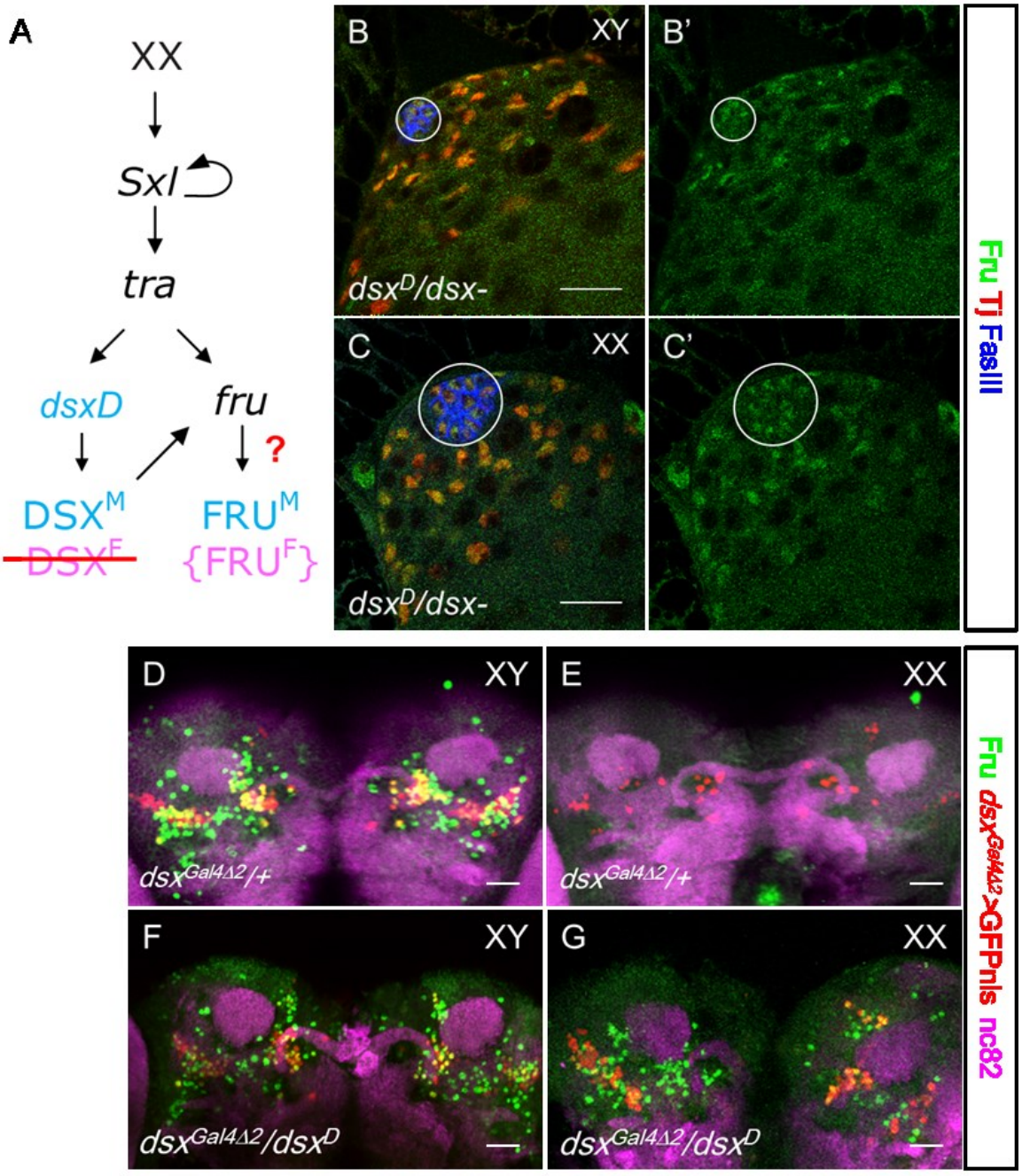
A
XX
Sxl
tra
dsxD
fru
?
DSXM
DSXF
FRUM
{FRUF}
B
XY
B'
dsxD/dsx-
C
XX
C'
dsxD/dsx-
Fru Tj FasIII
D
XY
E
XX
dsxGal4Δ2/+
dsxGal4Δ2/+
F
XY
G
XX
dsxGal4Δ2/dsxD
dsxGal4Δ2/dsxD
Fru dsxGal4Δ2>GFPnls nc82

Dsx is required for normal Fru expression in the gonad

We then wanted to determine the expression pattern of Fru in the absence of *dsx*. Based on studies of known Dsx targets (Burtis et al., 1991; Kopp et al., 2000; Luo and Baker, 2015; Wagamitsu et al., 2017), it is thought that DsxF and DsxM bind to the same target gene and regulate gene expression in the opposite directions. Therefore, we predicted that DsxM activates Fru expression in the testis and DsxF represses Fru expression in the ovary and that loss of *dsx* would cause Fru to be expressed at an intermediate level in both XX and XY gonads (Figure 3.4 A). What makes this experiment complicated is that, in the absence of *dsx*, both XX and XY initiate along the male path to form a hub at the embryonic stage, and then stochastically transdifferentiate from the hub into TFs during the 3rd larval instar (Camara and Van Doren, submitted).

We examined *dsx* null gonads at the late L3 stage and categorized the results by chromosomal sex and niche fate (Figure 3.4 B). Indeed, we found that XX gonads started to express Fru and XY gonads expressed Fru at a reduced level when *dsx* gonads with hubs were examined (Figure 3.5 A-D). However, we also observed stochasticity in Fru expression levels. While 50% of XX and 57.1% of XY gonads expressed Fru at a reduced level, 25% of XX and 28.6% of XY gonads expressed Fru at the wild-type level and 25% of XX and 14.3% of XY gonads did not express Fru (XX, n=12; XY, n=7; Figure 3.4 B).

Further, we noticed that gonads with TFs were less likely to express Fru in the apical cap and TFs. When *dsx* mutant gonads with TFs were socred, 100% of the XX gonads (n=4) and 75% of the XY gonads (n=8) had no Fru expression (Figure 3.4 B and 3.5 E-G). When Fru was observed in the apical cap of XY gonads, the level was reduced compared to that of control testes (Figure 3.5 H).

Taking the above findings together, we conclude that male-specific Fru expression in the gonad is dependent on *dsx*. DsxM is sufficient to activate Fru expression in XX flies both in the gonad and in the CNS. DsxF is also required to repress Fru expression in female gonads. In the absence of *dsx*, Fru expression was overall reduced but variable, with a lower level correlating with the female niche fate and a higher level correlating with the male niche fate (Figure 3.4 C). While we do not know what regulates the variable level of Fru expression in the absence of *dsx*, the correlation between a higher Fru expression level and the male niche fate suggests that *fru* influences male niche identity (see Chapter 4).

Figure 3.4: *dsx* is required for Fru expression in the gonad. (A) Proposed models of Fru expression in wild-type gonads and *dsx* null gonads. In wild-type gonads, DsxM activates Fru expression, and DsxF represses Fru. In *dsx* null gonads, Fru is expressed at a reduced level in both XX and XY individuals. (B) Distribution of Fru expression level in *dsx* null gonads categorized by sex chromosomes and niche fate. n=4,8, 12, and 7. (C) Schematic of Fru expression in *dsx* mutant gonads. In the absence of Dsx, Fru expression level becomes reduced but variable. Gonads with hubs tend to have higher Fru levels and gonads with TFs tend not to express Fru.

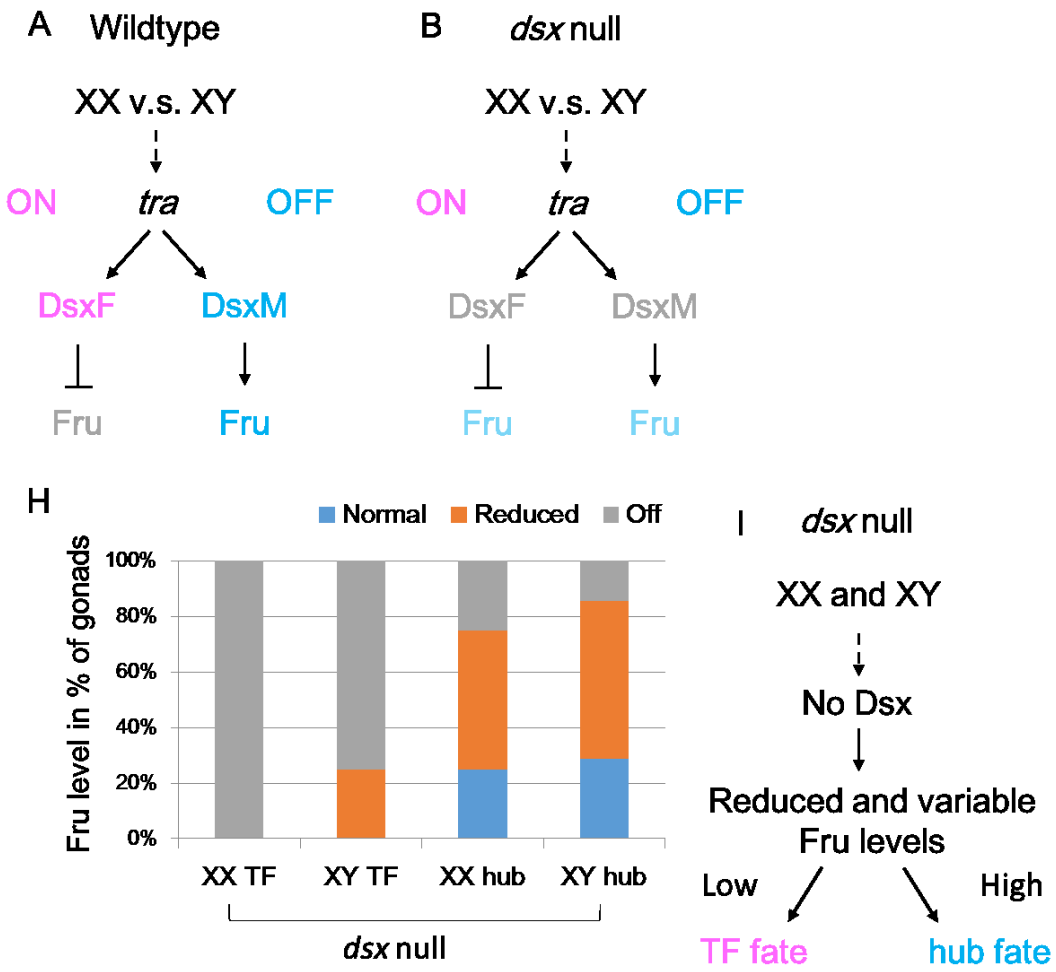

Figure 3.5 Loss of *dsx* causes Fru expression to be reduced and correlate with the niche fate rather than chromosomal sex. Late L3 stage larval gonads. Genotype as indicated. Control XY (A) and XX (E) gonads show male-specific Fru expression in the niche. XX (B) and XY (C-D) *dsx* null (dsx^{1}/dsx^{3}) gonads that committed to the hub fate have reduced Fru levels. XX (F) and XY (G-H) *dsx* null gonads that committed to the TF fate exhibit no Fru expression or very weak Fru expression (H) in the apical cap. Circles: hub. Arrows: CySCs. (A-H) Circles: Hub; brackets: TF; arrows: CySC.

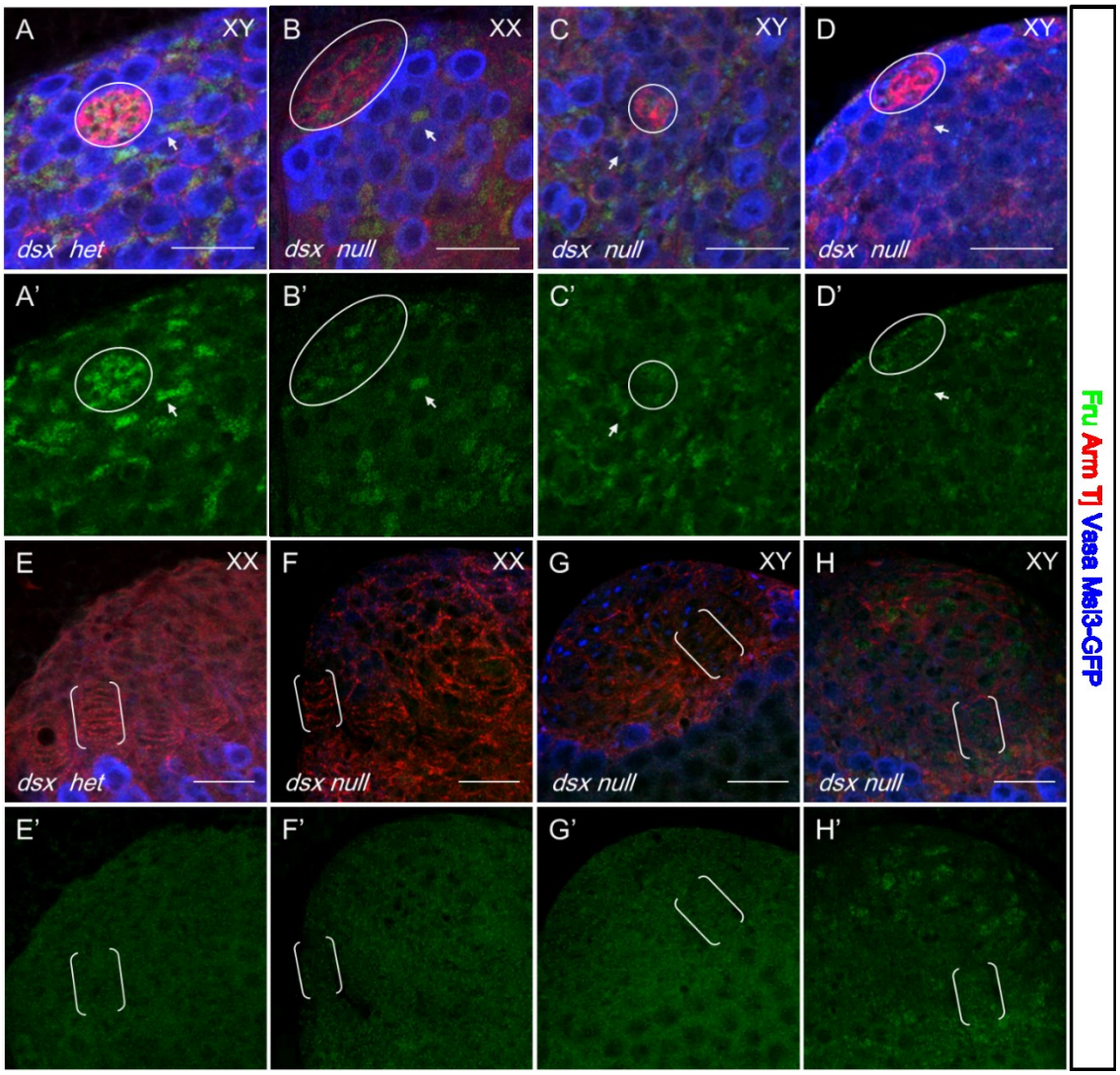

A conserved Dsx binding site upstream is required for fru P4 expression

We next wanted to determine if Dsx acts as a direct transcriptional activator of *fru*. *fru* promoter usage and Dsx occupancy both suggest that P3 and P4 promoters are potentially regulated by Dsx. Additionally, among 52 putative brain enhancers (Pfeiffer et al., 2008) that cover the whole *fru* gene locus, we only identified two enhancers (GMR22B06 and GMR23C08) that are located between P3 and P4 and drive GFP expression in the adult testis tip (Figure 3.6 A-C). However, these *GMR-Gal4* failed to drive expression in hub cells of the larval testis. Additionally, they drove expression in the apical cap and TFs of the larval ovary (Figure 3.6 D-G). These results indicate that either the two *GMR-Gal4* lines lacked sex-specific *cis*-elements or the synthetic core promoter used in the *GMR-Gal4* drove ectopic expression in the female niche.

Figure 3.6: Two *fru* GMR-Gal4 drives expression in the GSC niche. (A) Schematic of the *fru* GMR-Gal4 screen. Enhancer sequences used in GMR-Gal4 lines are mapped to the *fru* locus. (B-C) Expression of P3-proximal (B) and P4-proximal (C) GMR-Gal4 in the adult testes are shown. Magnified images of the testis tip are shown in the lower right corner. (D-G) Late L3 larval gonads. GMR expression in the male and female niche are shown. Circle: hubs; Brackets: TFs.

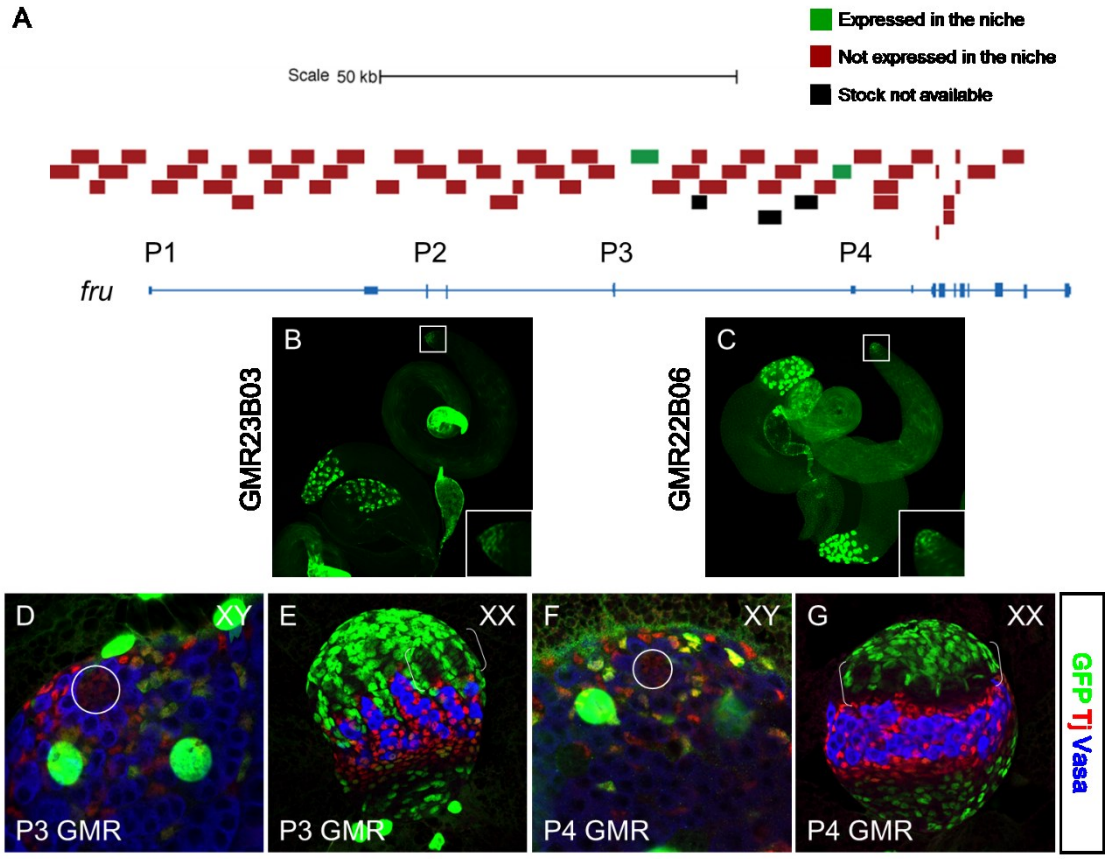

Through analyzing putative Dsx binding sites in the *fru* locus, we identified a Dsx motif (DSX1) 6.3 kb upstream of P4 which is completely conserved across 21 *Drosophila* species and matches 11 core nucleotides of the 13-nucleotide consensus motif (Luo, Shi, and Baker 2011) (Figure 3.7 A and 3.8 A). Two additional Dsx motifs (DSX2 and DSX3) were identified between DSX1 and P4, but their sequences are neither palindromic nor conserved (Figure 3.7 B, 3.7 C, and 3.8 A). To test if DSX1 is a Dsx-responsive element, an enhancer reporter construct was created in which a 7.5 kb genomic sequence including DSX1 and the tissue-specific enhancer sequence was fused to the GFPnls cDNA sequence (Figure 3.8 A). Transgenic flies carrying this wildtype construct (WT) expressed GFP in the hub at a comparable level as wildtype Fru expression level and did not express in the apical cap and TFs of L3 stage ovaries (Figure 3.8 B and 3.9 A-B).

To test if DSX1 is required for transcription from P4, we created the Mut1 reporter construct with the 7 core nucleotides of DSX1 replaced by G nucleotides. When GFP expression level in the hub was compared between transgenic flies containing WT and Mut1 constructs, we found that loss of the putative Dsx binding site significantly reduced the relative fluorescent intensity of GFP in hub cells ($p<0.0001$, student t-test) (Figure 3.8 B-D).

We further tested whether DSX2 and DSX3 were also required for normal P4 expression level in the hub. We created the Mut123 reporter construct with all three Dsx sites mutated (Figure 3.8 A). This mutated construct still drove GFP expression in hub cells (Figure 3.9 C). When the relative GFP fluorescent intensity in hub cells was compared among WT, Mut1, and Mut123 constructs, we did not observe a further reduction of expression in Mut 123 compared to Mut1, whereas both mutant constructs expressed GFP

at lower levels than the WT (Figure 3.9 A-D). Collectively, these results suggest that the conserved DSX1 motif, but not DSX2 or DSX3, is necessary for normal P4 expression in hub cells.

It is worth noting that mutating DSX1 or all three sites failed to turn on GFP expression in the apical cap, TFs or intermingle cells in late L3 stage ovary (Figure 3.9 E-G). This result indicates that additional Dsx binding sites may be required to regulate sexually-dimorphic Fru expression in the gonad.

Figure 3.7 Evolutionary conservation analysis of DSX1, DSX2, and DSX3. DSX1 (A), DSX2 (B), and DSX3 (C) with upstream and downstream sequences are shown in the UCSC Genome Browser. The comparative genomics tracks show sequence conservation in 27 insect species. Sequence alignment among *Drosophila* species is shown with matching nucleotides abbreviated as dots and missing nucleotides denoted by – or =.

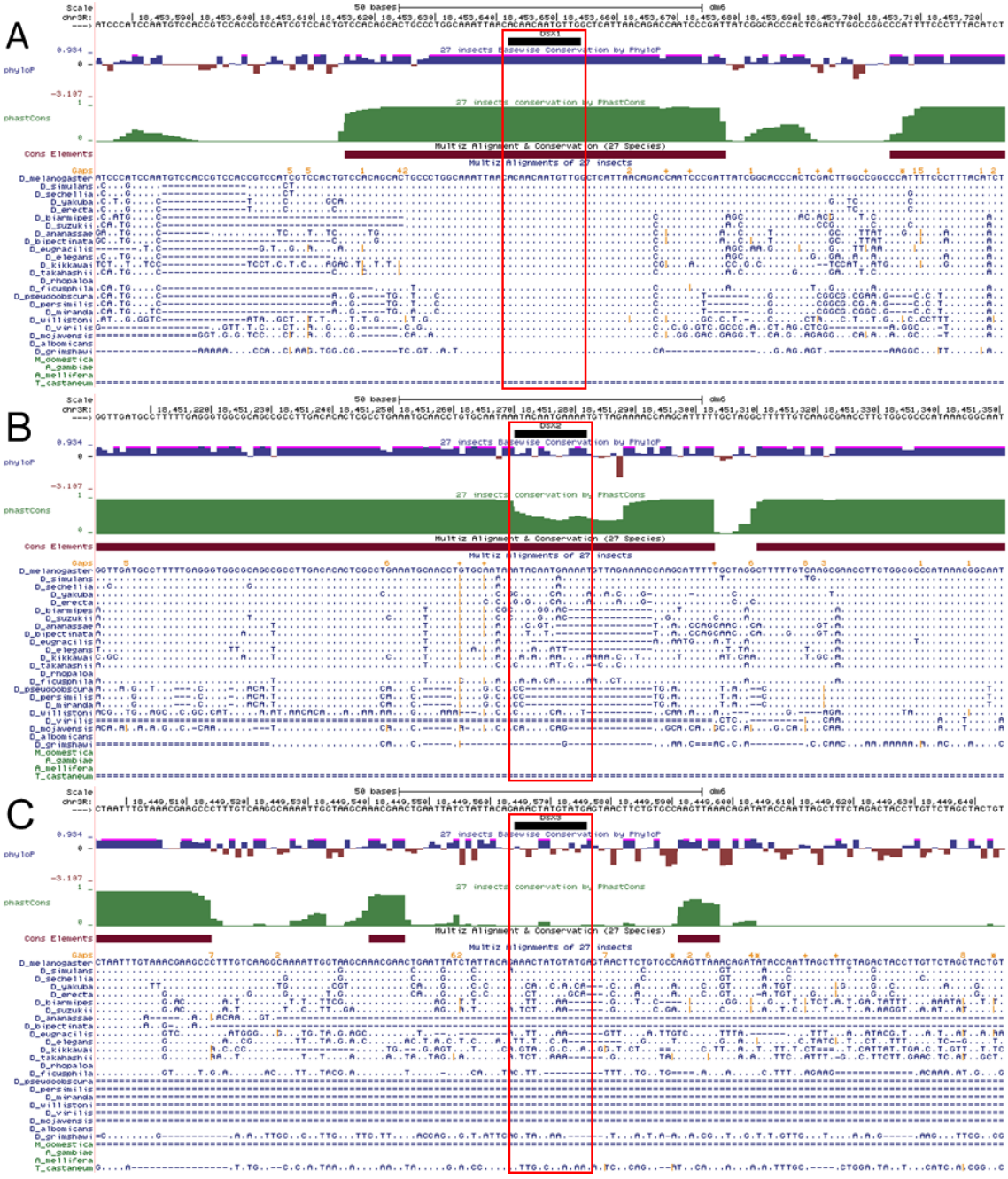
A
B
C
phyloP
phastCons
Cons Elements
Multiz Alignment & Conservation (27 Species)
Multiz Alignments of 27 insects
27 insects conservation by PhastCons
D_melanogaster
D_simulans
D_sechellia
D_yakuba
D_erecta
D_biarmipes
D_suzukii
D_ananassae
D_bipectinata
D_eugracilis
D_elegans
D_kikkawai
D_takahashii
D_rhopaloa
D_ficusphila
D_pseudoobscura
D_persimilis
D_miranda
D_willistoni
D_virilis
D_mojavensis
D_albomicans
D_grimshawi
M_domestica
A_gambiae
A_mellifera
T_castaneum

Figure 3.8: A conserved DSX binding site upstream of P4 is required for Fru expression in the hub cells. (A) Schematic diagram of the genomic sequence containing DSX1, 2, and 3 used to perform P4 enhancer-promoter analyses. Red vertical bars represent top 10% DSX motif determined by Dsx position weight matrix. The green vertical bar represents the conserved DSX1 site. Grey vertical bars indicate mutated DSX sites. Schematics of the P4 enhancer-reporter constructs are as indicated. (B-C) GFP expression levels in the hub in transgenic flies with WT (B) and Mut1 (C) constructs. (D) Quantification of the GFP fluorescent intensity per hub cell in WT and Mut1 testes. Data are presented as Mean ± SEM. WT, n=125; Mut1, n=115. Student's t-test.

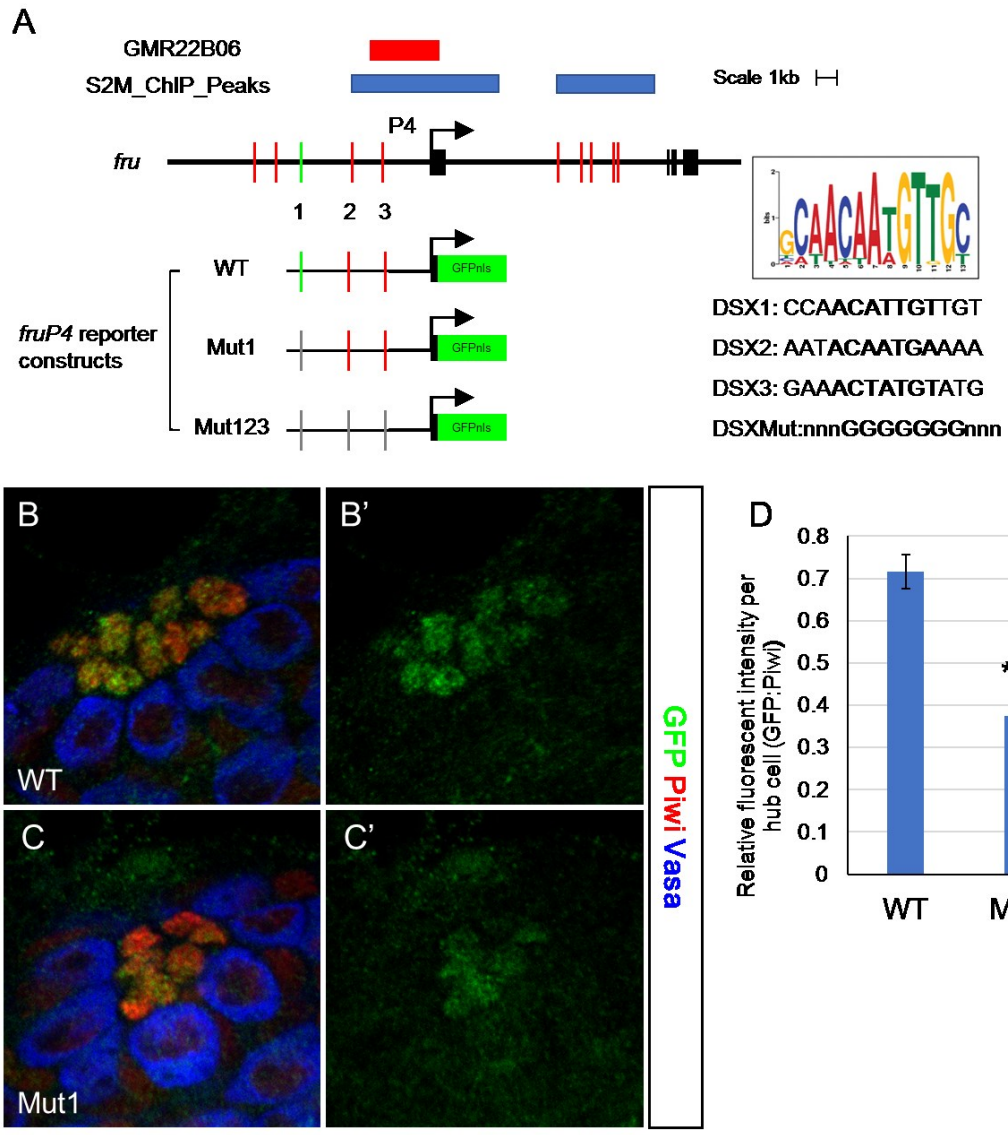
A
GMR22B06
S2M_ChIP_Peaks
Scale 1kb
P4
fru
1 2 3
WT
Mut1
Mut123
GFPnls
fruP4 reporter constructs
DSX1: CCAACATTGTTGT
DSX2: AATACAATGAAAA
DSX3: GAAACTATGTATG
DSXMut:nnnGGGGGGGnnn
B
B'
C
C'
WT
Mut1
GFP Piwi Vasa
D
Relative fluorescent intensity per hub cell (GFP:Piwi)
0.8
0.7
0.6
0.5
0.4
0.3
0.2
0.1
0
****
WT
Mut1

Figure 3.9: Mutating DSX1 did not derepress GFP expression in the apical cap, and mutating DSX2 and DSX3 did not further reduce GFP expression in the hub. (A-C) Expression of WT (A), Mut1 (B), and Mut123 (C) constructs in late L3 stage hub cells. (D) Comparison of relative GFP fluorescent intensity per hub cells (standardized by Piwi expression) in WT, Mut1 and Mut 123 constructs. Bars represent Mean±SEM. Sample size: WT, n=50; Mut1, n=35; Mut123, n=40. (E-G) Late L3 stage ovaries with WT (E), Mut1 (F) and Mut123 (G) constructs. Brackets: TFs.

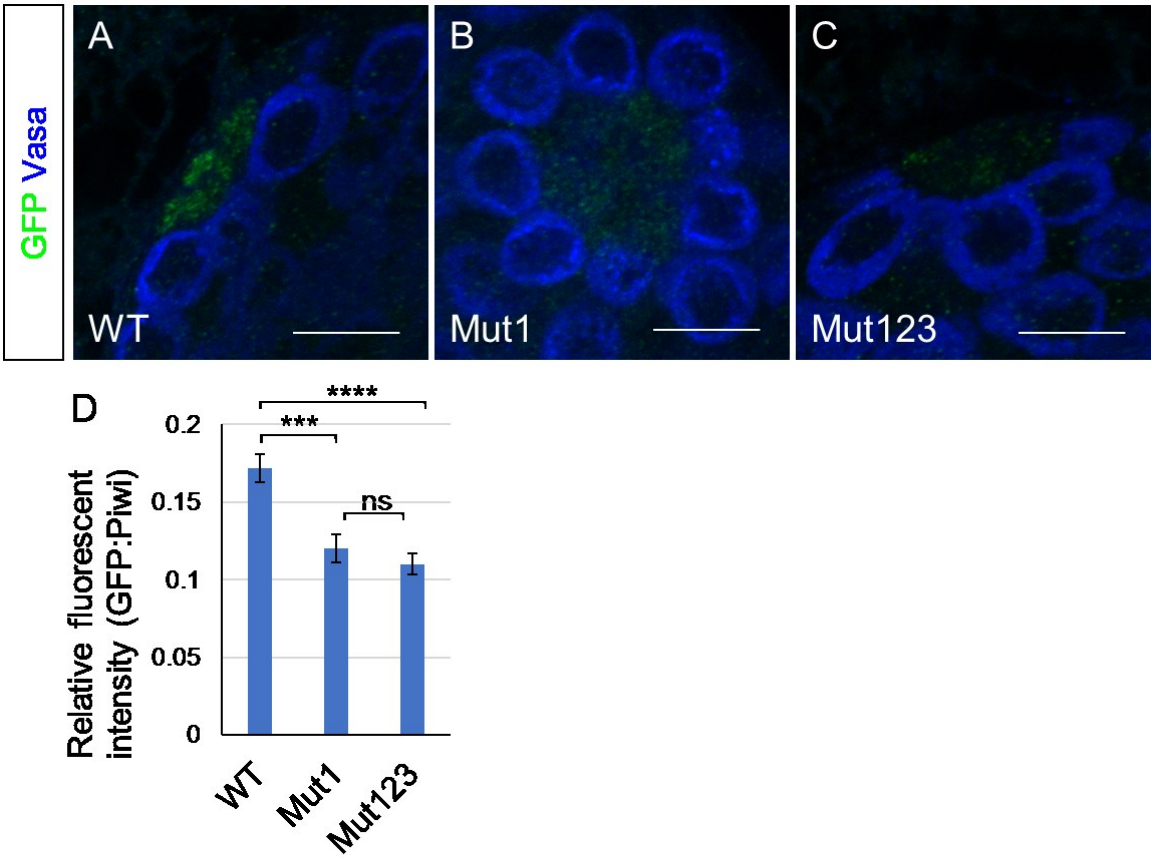
GFP Vasa
A
WT
B
Mut1
C
Mut123
D
Relative fluorescent intensity (GFP:Piwi)
0.2
0.15
0.1
0.05
0
****
***
ns
WT
Mut1
Mut123

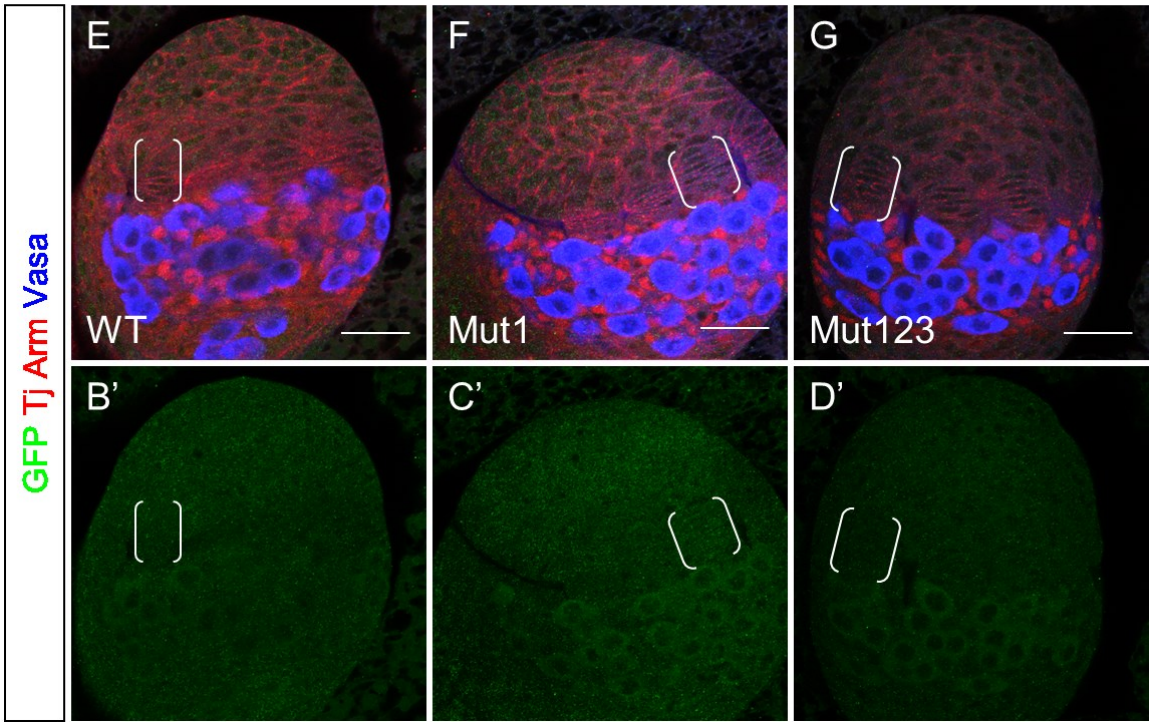
GFP Tj Arm Vasa
E
WT
F
Mut1
G
Mut123
B'
C'
D'

Conclusions and Discussion

In this Chapter, we demonstrated that male-specific Fru expression in the GSC niche is regulated by Dsx at the transcriptional level. We showed that *dsx* is both necessary and sufficient for Fru expression from the nonP1 promoters. The presence of DsxM in XX flies resulted in robust Fru expression in the GSC niche as well as the sexually-dimorphic neurons of the CNS. The absence of *dsx*, on the other hand, caused both XX and XY gonads with the hub fate to express Fru at an intermediate level. Interestingly, Fru expression in *dsx* mutant gonads became variable. While most gonads expressed Fru at a reduced level, some gonads expressed Fru at the wildtype level and others had no Fru expression at all. We also found that Fru expression in *dsx* mutants is correlated with the sexual identity of the niche rather than the chromosomal sex of the gonad. *dsx* mutant gonads committed to the TF fate were less likely to express Fru than those maintained the hub fate. Lastly, through expression analyses of *cis*-regulatory sequences, we found that the 7.5 kb genomic sequence immediately upstream of *fru* P4 contains both the niche-specific enhancer and the sex-specific enhancer and is sufficient to drive P4 expression in the same pattern as Fru in the niche. We further identified a Dsx binding site within this genomic sequence that is required for the normal expression level of P4 in the hub. This Dsx binding site matches 11 core nucleotides of the 13-nucleotide consensus DSX motif and is completely conserved in 21 *Drosophila* species that span 40 million years of evolution.

One unexpected observation is that while Fru was expressed in the *XX; dsx^{D}/dsx^{-}* CNS, its expression pattern did not completely overlap with the Dsx expression pattern indicated by $dsx^{Gal4\Delta 2}$. Lineage tracing of $dsx^{Ga4l\Delta 2}$expressing neurons with the G-TRACE system (Evans et al., 2009) showed complete overlap between historical Dsx-expressing

neurons and real-time Dsx-expressing neurons (data not shown). Therefore, it is unlikely that DsxM turned on Fru expression during pupal stages and those neurons no longer express DsxM in adult CNS. Considering that Fru is expressed in both sexes in the L3 CNS, a potential explanation is that while DsxM activated Fru expression in some neurons, other Fru-positive neurons failed to turn off Fru expression in pupal CNS due to a non-cell-autonomous signal that depends on Dsx. A more thorough analysis of Fru expression in wildtype and *XX; dsx^{D}/dsx^{-}* pupal CNS is needed to test this hypothesis.

While Fru expression was overall reduced in *dsx* mutant gonads of both sexes, the expression of Fru differs from known Dsx targets in that the distribution of Fru levels is bimodal with a higher level correlated with the male niche fate and a lower level correlated with the female niche fate. This is likely a reflection of the distinct all-or-none manner of niche sexual-fate specification. In most tissues, loss of *dsx* causes tissue development in an intersexual mode, either expressing sex-specific genes at an intermediate level or forming a mixture of cells comprising both male- and female-specific cell types. However, the *dsx* mutant niche cells initially all specify as hub cells in embryonic gonads, and during the 3rd larval instar stochastically trans-differentiate into TFs. It is likely that *fru* expression is activated in the male niche of all early L3 *dsx* mutant gonads, but only some gonads can maintain the *fru* expression level whereas other gonads gradually downregulate *fru* expression. When the Fru expression level decrease below a threshold, the hub will switch to TFs. This threshold effect is possibly due to autoregulation of *fru* expression, which was discussed in Chapter 2.

In our previous efforts to understand the origin of TFs in *dsx* mutant gonads, we observed re-initiation of the cell division in hub cells in the L2 stage, suggesting that the

apical cap that gives rise to TF cells originates from the initial hub cells. However, due to the lack of lineage tracing techniques and proper tissue-specific enhancer reporters, we were not able to directly address this hypothesis. Our observation that Fru, being a male-specific niche marker, was activated in the apical cap cells and terminal filament cells provides supporting evidence that the apical cap and terminal filament cells originate from the hub.

Lastly, while the conserved Dsx binding site (DSX1) upstream of *fru* P4 is required for P4 expression at a normal level, we do not think it accounts for all the Dsx regulation in the *fru* locus. Using CRISPR/Cas9, we specifically mutated DSX1 in the genome. Flies containing this mutated site did not exhibit a significant change in the total amount of *fru* transcripts in the gonad (data not shown). Additionally, we failed to observe activation of GFP expression in the apical cap and terminal filaments in ovaries with the Mut1 construct. This result indicates that DsxF may bind to additional Dsx binding sites in this construct to repress GFP expression. Interestingly, besides DSX1 we also identified a conserved DSX motif downstream of P4, which overlaps with a strong Dsx ChIP-Seq peak. Because the *fru* gene structure is very complicated and these elements span tens of kb, we did not generate reporter constructs containing this site and the tissue-specific enhancer and test if this DSX site is required for hub expression. A future direction would be to verify Dsx binding via ChIP-qPCR or ChIP-Seq of the testis. We have tested two tagged Dsx BAC transgenes. Unfortunately, neither of them was expressed in the testis at a level that is high enough for ChIP. Recently, we utilized the CRISPR technique to tag the endogenous *dsx* gene with GFP at the N-terminus. This new reagent may help us address this question.

In summary, we identified *fru* as a new direct target of Dsx. We revealed that in addition to the sex-specific alternative splicing mechanism, transcriptional control by DsxF and DsxM could also generate male-specific Fru expression in the gonad as well as the CNS. Our findings suggest a non-canonical sex determination pathway exists where *fru* is downstream of *dsx*. It further indicates that *fru* may function downstream of *dsx* to regulate sex-specific gonad development.

CHAPTER 4 FRU PROMOTES MALENESS DURING GONAD DEVELOPMENT AND MAINTAINS CYST STEM CELL HOMEOSTASIS IN ADULT TESTES

Summary

fru function in the developing and adult gonad stem cell niche remains unknown. In this Chapter, we took multiple experimental approaches to investigate the functions of *fru* during the sexual development of the niche, in the maintenance of the adult stem cell niche, and in regulating spermatogenesis. We found that *fru* acts in concert with *dsx* to ensure the faithful specification of the male niche. While *fru* does not play a role in maintaining the adult niche sexual identity, it is required in the CySC lineage for hub positioning, CySC maintenance, and cyst cell differentiation. It also non-autonomously regulates spermatogenesis.

Introduction

In the current paradigm of the *Drosophila* sex determination pathway, *fru* only controls the neuronal and behavioral aspects of sexual dimorphism via the FruM isoforms that are generated through sex-specific alternative splicing of P1 transcripts. Fru isoforms encoded by transcripts produced from nonP1 promoters (termed as FruCom) are considered to be common in both sexes and not involved in the sex determination pathway.

Our findings in Chapter 2 and Chapter 3, however, suggest that FruCom may also play sex-specific roles outside the nervous system. We revealed a non-canonical sex determination pathway in which the transcription of *fru* from nonP1 promoters is controlled by Dsx to generate male-specific Fru expression patterns in the gonad and the CNS. We also showed that *fru* might function downstream of *dsx* to regulate niche fate specification. First, the onset of Fru expression in the male GSC niche overlaps with the critical time window when DsxM need to promote the hub fate and antagonize the TF forming signal. Second, in the absence of *dsx,* gonads committed to the TF fate tend to express Fru at a lower level.

So far, only limited understanding of the potential function of FruCom isoforms has been achieved. From analyses of *fru* mutant alleles that affect transcription from the 3 "common" promoters, it was suggested that P2 is dispensable for fertility whereas P3 and P4 are essential for vitality (Anand et al., 2001; Billeter et al., 2006). Functions of FruCom in non-neural tissues have also been implicated from studies of C-terminal isoform-specific *fru* mutants (Nojima et al., 2014; von Philipsborn et al., 2014). While flies mutant for FruA have normal morphology and fertility, flies lacking functional ZnF domains encoded by exon B and exon C die in late pupal stages, and exhibit defects in leg and wing

development. Although sex-specific mutant phenotypes have not yet been reported, these results indicate that FruCom isoforms have essential roles during development.

How could FruCom function in the male gonad? We formulated a few hypotheses based on the mechanisms of *fruM* regulating sexual dimorphism in the nervous system. First, FruCom may establish the sexual identity of niche cells through chromatin remodeling. In the CNS, Fru forms a complex with the transcription cofactor Bonus, which further recruits either Histone deacetylase 1 or Heterochromatin protein 1a, respectively, to masculinize or demasculinize individual sexually-dimorphic neurons (Ito et al., 2012). Interestingly, *fruM* determines the sexual identity of mAL neurons in an all-or-none manner that is similar to the mutually-exclusive decision between the male and the female niche fate in *dsx* mutant gonads. It is possible that FruCom isoforms utilize a similar mechanism to regulate sets of male- versus female-promoting genes in the gonad stem cell niche.

Second, FruCom may mediate sex-specific programmed cell death. Sex-specific apoptosis is a commonly used mechanism to generate sexual dimorphism in cell numbers by *dsx* and *fruM*. Kimura et al. showed that FruM prevents *reaper*-mediated programmed cell death in a cluster of sexually dimorphic interneurons (Kimura et al., 2005). FruM can also promote apoptosis to eliminate the Ilp7 motoneurons specifically in males (Garner et al., 2018). Programmed cell death is a naturally occurring phenomenon in the gonad from flies to mammals. FruCom may modulate the apoptosis pathway to regulate cyst cell and germ cell numbers.

Lastly, FruCom may regulate cell adhesion molecules in the gonad. Genome-wide analysis of putative FruM target genes revealed enrichment of cell adhesion molecules,

including N-cad, Arm, FasII and FasIII, and signaling-pathway components (Wnt and Notch signaling) that modulate adherens juctions (Neville et al., 2014). While these putative FruM targets play essential roles in neurogenesis, they are also the key regulators in the development and maintenance of GSC niches. Loss of *fruCom* causes abnormal FasII expression in the embryonic CNS (Song et al., 2002a), suggesting that FruCom and FruM have shared targets. Therefore, FruCom may modulate cell adhesion molecules in the gonad to regulate sex-specific niche development and maintain the male GSC niche in adulthood.

In this Chapter, we undertook multiple experimental approaches to understand the functions of Fru in the hub, the CySCs, and the undifferentiated cyst cells. We sought to determine if *fru* plays a sex-specific role in the development and maintenance of the male GSC niche. Ultimately, we wanted to know whether *fru* contributes to the morphological branch of sexual dimorphism.

Materials and Methods

Fly stocks

The following stocks were used: fru^{W24} (S. Goodwin), fru^{Sat15} (S. Goodwin), $fru^{\Delta A}$ (S. Goodwin), $fru^{\Delta B}$ (S. Goodwin), $fru^{\Delta C}$ (S. Goodwin), dsx^{D}, $Df(3R)dsx^{3}$, dsx^{1}, $dsx^{Gal4\Delta 2}$ (B. Baker), *dsx-Gal4* (S. Goodwin), *UAS-fruMA* (S. Goodwin), *UAS-fruMB* (S. Goodwin), *UAS-fruMC* (S. Goodwin), *UAS-fruB* (S. Goodwin), *c587-Gal4* (T Xie), *tj-Gal4* (D. Godt), $tub\text{-}Gal80^{ts}$, $esg^{M5\text{-}4}$ (S. DiNardo), $y^{1}\ v^{1};\ P\{TRiP.JF01182\}attP2$ (*UAS-fruCom-RNAi 1*), *UAS-Valium20-fru-RNAi* (*UAS-fruCom-RNAi 2*), *yw, hs-FLP,UAS-mCD8:GFP;tub-*

Gal4,neoFRT82B,tub-Gal80, *hs-FLP, tub-Gal4, UAS-GFP.Myc.nls, yw; neoFRT82B, tub-Gal80*, *FRT82B*, *FRT82B, fru^{Sat15}*, *FRT82B, fru$^{\Delta B}$*, *FRT82B, fru$^{\Delta C}$* and *w^{1118}* as a control.

Antibody staining

Adult testes were dissected in PBS and fixed at room temperature for 15 minutes in 4.5% formaldehyde in PBS containing 0.1% Triton X-100 (PBTx). Adult ovaries, *dsx* mutant adult gonads and larval gonads were dissected in PBS followed by a 10-minute fixation at room temperature in 6% formaldehyde in PBTx. Immunostaining was performed as previously described (Gonczy *et al*., 1997), and samples were mounted in 2.5% DABCO.

The following primary antibodies were used: rat anti-Fru^{Com} at 1:300 (S. Goodwin); guinea pig anti-Traffic-jam (D. Godt) at 1:10,000; mouse anti-Eya 10H6 (DSHB, S. Benzer/N.M. Bonini) at 1:25; mouse anti-Arm N2 7A1 (DSHB, E. Wieschaus) at 1:100; chicken anti-Vasa (K. Howard) at 1:10,000; mouse anti-Fas3 7G10 (DHSB, C. Goodman) at 1:30; mouse anti-Engrailed 4D9 (DSHB, C. Goodman) at 1:2; rat anti-DN-Cad DN-EX#8 (DHSB, T. Uemura) at 1:20; rabbit anti-GFP (abcam) at 1:2000; rabbit anti-Vasa (R. Lehmann) at 1:10,000; rabbit anti-Sox100B (S. Russell) at 1:1,000; rabbit anti-β-Gal (Cappel) at 1:10,000; rabbit anti-Zfh1 (R. Lehman) at 1:5,000; rabbit anti-phospho histone H3 (Cell Signaling) at 1:5,000. The following secondary antibodies were used at 1:500: Alexa 488 goat anti-rat; Alexa 488, 546 and 633 goat anti-mouse; Alexa 488, 546 and 633 goat anti-rabbit; Alexa 546 and 633 goat anti-guinea pig at 1:500; Alexa 546 goat anti-rabbit; Alexa 633 goat anti-chicken. All Alexa probes were from Molecular Probes (Invitrogen, Carlsbad, CA).

All immunohistochemistry samples were imaged on a Zeiss LSM 700 confocal microscope with 20x, 40x or 63x objectives and processed with Zen software (Zeiss) or Fiji software.

Developmental staging

Larval and pupal staging were performed according to (Bainbridge *et al.* 1981). Immobile third instar larvae were collected as late L3 stage larvae. Larvae with everted spiracles and white puparium were collected as white prepupal (WPP) stage larvae.

Larval and pupal mutant genotyping

GFP-expressing balancer chromosomes were used to distinguish heterozygous control from trans-heterozygous *fru* mutants at larval and pupal stages.

Quantification of cell number

Z-stack images were taken with a Zeiss LSM 700 confocal microscope and subsequently analyzed with Fiji software. GSCs were counted as Vasa-positive germ cells contacting hub cells. CySCs were counted as Zfh-1-or Tj-positive cells within one cell diameter from the hub. Hub cell number was determined by DAPI stained nuclei surrounded by cell membrane bound Arm staining.

Cell death assays and quantification of Vasa-negative cysts

Z-stack images were taken with a Zeiss LSM 700 confocal microscope and analyzed with Zen software (Zeiss). Vasa-negative and DAPI positive clusters of germ

cells were counted as a dying cyst. For detection of germ cell death with Lysotracker, testes were stained with Lysotracker Red DND-99 in PBS (1:1,000) for 30 mins prior to formaldehyde fixation. Immunostaining was followed as normal. For TUNEL-dependent detection of cell death, testes were fixed as normal and label with Click-iT TUNEL Alex Fluor 594 Imaging Kit (ThermoFisher) according to manufacturer's instructions.

Quantification of hub elongation and displacement

Z-stack images were taken with a Zeiss LSM 700 confocal microscope and analyzed with Zen (Zeiss) software. Hubs that were less than 3-cell-wide and more than 3-cell-long along the A-P axis were considered as elongated hub. Hubs that were not touching the tip of the testis were measured from the center of the hub to the tip of the testis. Hubs with over 20 m from the testis tip were scored as displaced.

Clonal analysis

Flies of the following genotype were used for MARCM: *hs-FLP, UAS-mCD8:GFP/Y; tub-Gal4, FRT82B, tub-Gal80/FRT82B* (control 1); *hs-FLP, UAS-mCD8:GFP/Y; tub-Gal4, FRT82B, tub-Gal80/FRT82B, ry* (control 2); *hs-FLP, UAS-mCD8:GFP/Y; tub-Gal4, FRT82B, tub-Gal80/FRT82B,* fru^{Sat15} ; *hs-FLP, UAS-mCD8:GFP/Y; tub-Gal4, FRT82B, tub-Gal80/FRT82B,* $fru^{\Delta B}$; *hs-FLP, UAS-mCD8:GFP/Y; tub-Gal4, FRT82B, tub-Gal80/FRT82B,* $fru^{\Delta C}$. Newly eclosed adult males (0-2 day old) were collected at 25 ºC prior to heat shock. Flies were heat-shocked at 37 ºC for 1 hr and returned to 25 ºC and raised in fresh vials with yeast paste. Control and mutant clones were analyzed at the indicated time points post clonal induction (pci).

CySC clones were counted as GFP-marked Zfh-1- or Tj-positive cells within one cell diameter to the hub and directly contacting the hub with cytoplasmic extension as indicated by mCD8:GFP. Rest of the GFP marked Zfh-1- or Tj-positive cells were considered as cyst cell clones.

Quantification of niche identity in dsx mutant adults and tj>fruB adults

Adult flies less than 2 day old were dissected and stained with antibodies against DN-Cad, FasIII and Vasa, and cell nuclei were visualized via DAPI staining. Z-stack images were taken with a Zeiss LSM 700 confocal microscope with 20x or 40x objectives. Hub was defined as a compact cluster of DAPI bright somatic cells that coexpressed N-Cad and FasIII and were surrounded by a rosette of Vasa-positive germ cells. TFs were determined by ladder-shaped N-Cad staining around stacks of disc-shaped somatic nuclei indicated by DAPI staining. No niche was defined as neither TFs nor a hub was identified in the gonad.

Results

Loss of fru causes hub phenotypes, but the hub fate is not altered

In order to investigate *fru* function in the male gonad, we first examined testis development in *fru* null mutants, which die during early pupal stages. Up to white prepupal stage, no significant morphological defect was observed in the hub of *fru* mutant testes in comparison to heterozygous control testes (Figure 4.1 A and B). Quantification of niche components showed a slight decrease in GSC number from 7.9±0.2 (n=14) per control

testis to 6.9±0.2 (n=20) per *fru* null testis ($p<0.0001$), and no change in CySC number (*fru* het: 8.8±0.3, n=14; *fru* null: 8.3±0.3, n=20; $p=0.24$) (Figure 4.1 C).

We next examined *fruB* mutants, which survive to later pupal stages and has been implied in Chapter 2 to be the key isoform in the gonad. At 3 days after puparium formation (AFP), defects in hub morphology were first observed in *fruB* mutant gonads. In control gonads, the hub was a round plug of cells with a diameter of 3-4 cells (Figure 4.1 D). In contrast, 18.2% of *fruB* mutant gonads had a slender hub that elongated along the A-P axis and was of 1-2 cell wide and 3-4 cell long (Figure 4.1 E). Consistent with the change in hub shape, the number of GSCs harbored by the hub decreased from 9.0±0.0 to 7.5±0.3 (Mean±SEM, $p=0.0007$, Student's t-test), and the hub cell number also decreased from 12.0±0.2 to 10.2±0.7 (Mean±SEM, $p=0.03$; *fruB* het, n=9; *fruB* null, n=12; Figure 4.1 F). Examining *fruB* mutant testes in earlier stages (late L3 stage, WPP stage, 1 day AFP, and 2 days AFP) did not reveal any hub defect (data not shown).

Figure 4.1: *fru* mutants display minor defects in the male GSC niche. (A-B) Representative images of the male GSC niche from *fru* heterozygous (A) and *fru* null (B, fru^{Sat15}/fru^{W24}) male gonads of the white prepupal stage. Outlined regions: Vasa-negative cysts. (C) Quantification of GSC number and CySC number in *fru* het and *fru* null gonads. Mean±SEM; *fru* het, n= 14; *fru* null, n=20; student's t-test. (D-E) Male GSC niches at 3 days after puparium formation. (D) Normal hub morphology in a *fruB* heterozygous gonad. (E) Elongated hub in a *fruB* mutant (E, $fru^{\Delta B}/fru^{Sat15}$) gonad. (F) Quantification of GSC number and hub cell number in the niche in control (n=9) and *fruB* mutant (n=12) gonads 4 days APF. Mean±SEM, Student's t-test.

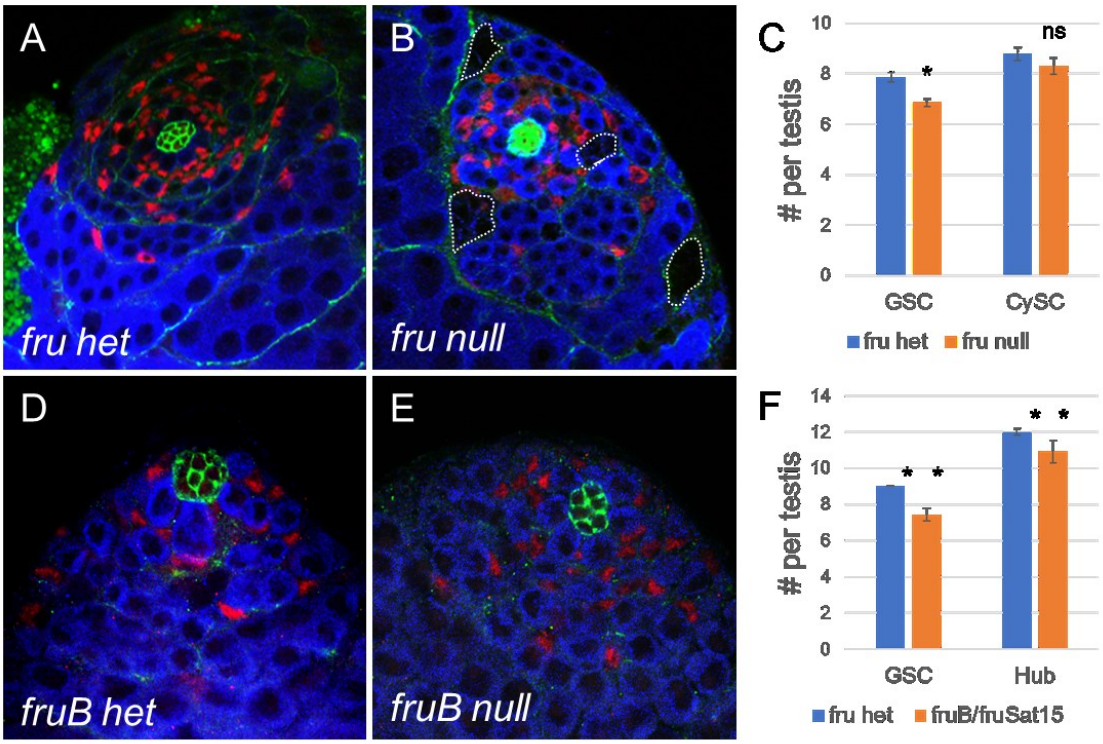

Owing to the size of the *fru* locus and the complexity of *fru* transcription, we could not rescue the lethality phenotype and examine *fru* mutant gonads in adulthood. To further investigate *fru* function in the hub, we performed RNA interference (RNAi)-mediated knockdown of *fru* in the testis with two independent *fru-RNAi* lines (Com1 and Com2) that target the common coding region of all *fru* transcripts. Both *fruCom-RNAi* lines efficiently and specifically removed FruCom immunoreactivity when combined with cell-type specific *Gal4* lines (Figure 4.2). While knockdown of *fruCom* in hub cells with *upd-Gal4* did not yield a hub phenotype (data not shown), knocking down *fru* in the *dsx* heterozygous background with $dsx^{Gal4\Delta 2}$ (Robinett et al., 2010) recapitulated the hub elongation phenotype observed in $fru^{\Delta B}$ testes. In 8-day-old adult flies, 7.14% (Com1) and 12.2% (Com2) of *fruCom-RNAi* testes had hubs elongated along the A-P axis whereas control KD testes all had round hubs (Figure 4.3 A, B and G). Besides the hub elongation phenotype, we also noticed that 17.9% of *Com- RNAi* testes had hubs displaced (>20μm) from the testis apex (control, 0%, n=18; Com1, n=28; Com2, n=41) (Figure 4.3 C and G). The severity of hub defects was increased in older flies. In 12-day-old *Com1-RNAi* testes, 10.5% exhibited elongated hubs and 47.4% had displaced hubs (n=19). The percentage of *Com2-RNAi* testes with elongated hubs also increased to 31.6% at 12 days post eclosure, and these animals also exhibited the hub displacement phenotype (5.3%, n=19) (Figure 4.3 G).

To test whether hub elongation and displacement were two sequential steps of hub detaching the testis apex, we measured the distance between the hub and the testis tip. The average distant in *control-RNAi* testes was 2.1±1.4 μm at 8 days post eclosure and 5.3±2.6 μm at 12 days post eclosure. However, the hubs in *Com1-RNAi* testes were significantly

farther away from the testis tip (12.42±3.9 μm) than the control group at 8 days post eclosure, and the distance increased to 29.7±1.7 μm in 12-day-old *Com1-RNAi* testes. These results suggest that knockdown of *fru* causes the hub to detach from the testis tip and progressively migrate away from the testis tip.

Given that aged *control-RNAi* testes driven by $dsx^{Gal4\Delta 2}$ also showed hub defects (Figure 4 G), we performed knockdown of *fru* with *c587-Gal4*, which drives expression in the CySC lineage, to verify that hub defects were caused by *fru-RNAi* rather than $dsx^{Gal4\Delta 2}$. We observed hub elongation and displacement in 20% (n=49) of 14-day-old *Com1-RNAi* testes, and the penetrance increased to 33% (n=42) in 21-day-old testes (Figure 4.3 E, F, and H). In contrast, control RNAi testes showed a constant low frequency of hub defects (14 days, 4.9%, n=41; 21 days, 2%, n=45) (Figure 4.3 D and H). Taking these data together, we conclude that knocking down *fru* in the male GSC niche causes the hub to displace from the testis tip.

Figure 4.2: Efficient removal of Fru proteins by tissue-specific *fru RNAi*. (A) Wildtype testes with Fru expression in the hub and CySC lineage. (B) Removal of Fru protiens in the hub cells in *upd>fruCom1 RNAi* testes. (C) Removal of Fru proteins in the hub and the CySC lineage in *tj>fruCom1 RNAi* testes. (D) No Fru expression in the hub and the CySC lineage in $dsx^{Gal4\Delta 2}$*>fruCom2 RNAi* testes. Scale bar in (A) represents 20 μm and applies to all images.

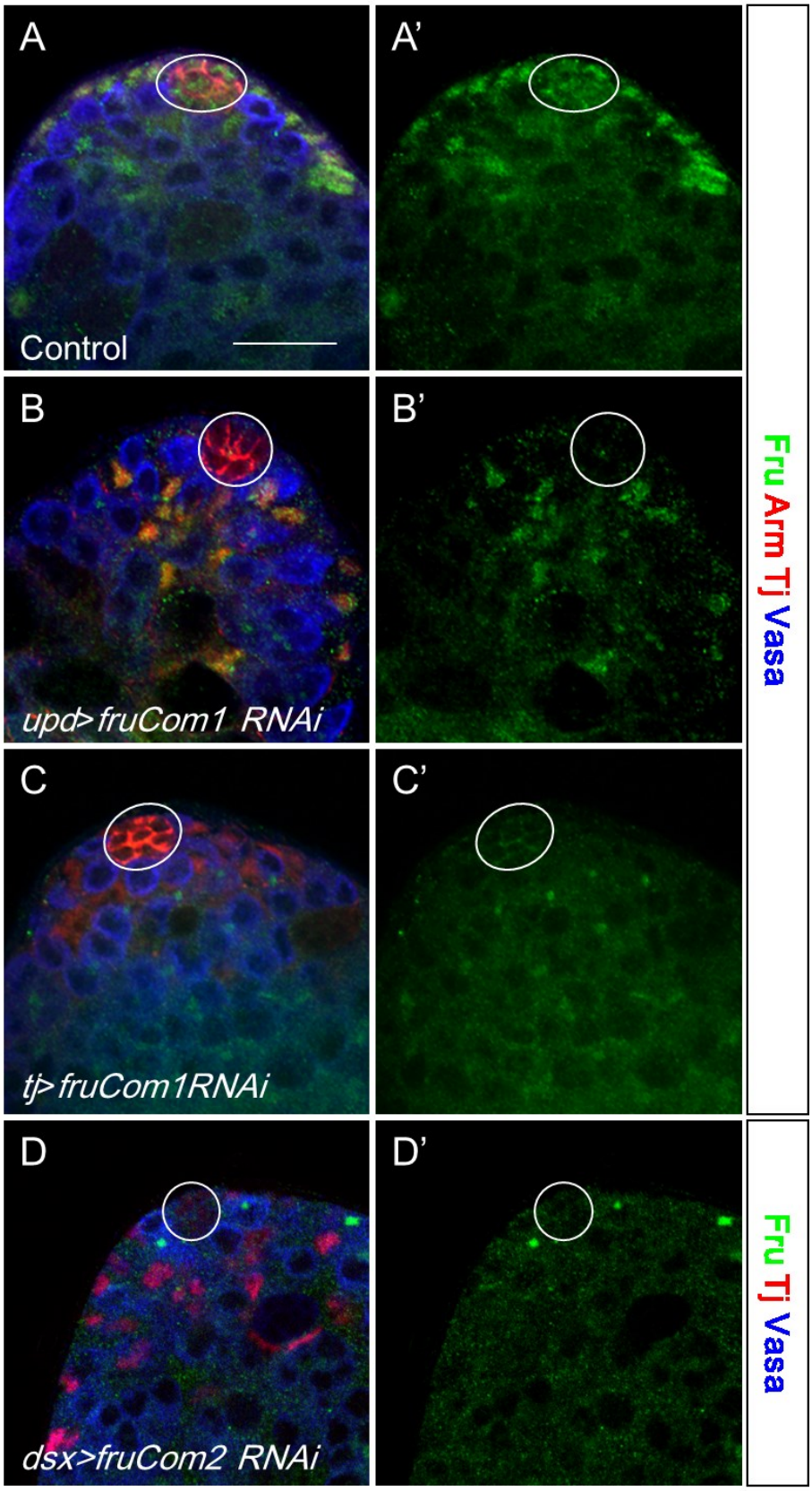
A
A'
Control
B
B'
upd> fruCom1 RNAi
C
C'
tj> fruCom1RNAi
D
D'
dsx>fruCom2 RNAi
Fru Arm Tj Vasa
Fru Tj Vasa

Figure 4.3: Knocking down *fru* with $dsx^{Gal4\Delta 2}$ and *c587-Gal4* caused hub elongation and displacement. (A-C) 8-day-old testes with *Control RNAi* (A) and *fruCom RNAi* (B and C) driven by $dsx^{Gal4\Delta 2}$. (D-F) 14-day-old testes with *Control RNAi* (A) and *fruCom1 RNAi* (E and F) driven by *c587-Gal4*. Representative images of normal hub (A and D), elongated hub (B and E) and displaced hub (C and F) are shown. (G) Summary of hub phenotypes in 8- and 12-day-old testes expressing *UAS-Control RNAi*, *UAS-fruCom1 RNAi* and *UAS-fruCom2 RNAi* with $dsx^{Gal4\Delta 2}$. (H) The percent of testes with elongated hub and displaced hub in *c587>control RNAi* and *c587> fruCom1 RNAi* testes.

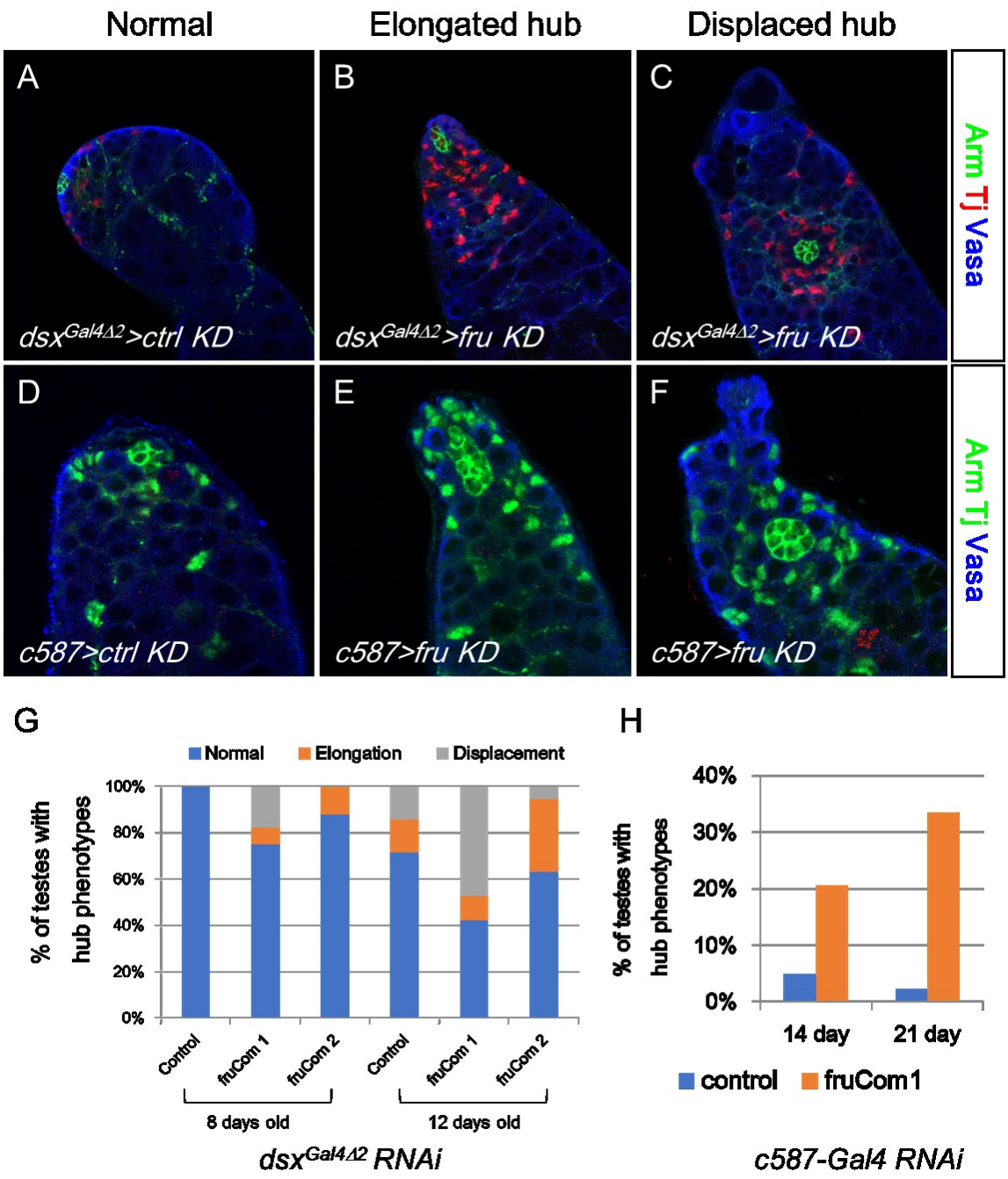
Normal
Elongated hub
Displaced hub
A
B
C
D
E
F
dsxGal4Δ2>ctrl KD
dsxGal4Δ2>fru KD
dsxGal4Δ2>fru KD
c587>ctrl KD
c587>fru KD
c587>fru KD
Arm Tj Vasa
Arm Tj Vasa
G
Normal
Elongation
Displacement
% of testes with hub phenotypes
100%
80%
60%
40%
20%
0%
Control
fruCom 1
fruCom 2
Control
fruCom 1
fruCom 2
8 days old
12 days old
dsxGal4Δ2 RNAi
H
% of testes with hub phenotypes
40%
30%
20%
10%
0%
14 day
21 day
control
fruCom1
c587-Gal4 RNAi

fru is cell-autonomously required in the CySCs and cyst cells

Next, we investigated the function of *fru* in the CySC lineage. In *fru* null and $fru^{\Delta B}$ mutant gonads, we noticed that *fru* null and $fru^{\Delta B}$ mutant gonads had slightly more Vasa-negative spermatogonial cysts than the control (Figure 4.1 B and 4.4 A), suggesting that these cysts were dying. Since germ cells undergo caspase-independent cell death, we utilized the LysoTracker dye which has been previously demonstrated to label dying germline cysts (Yacobi-Sharon et al., 2013). In both the control and *fru* null gonads of the white prepupal stage, Vasa-negative cysts were exclusively positive for LysoTracker (Figure 4.4 B and C). However, the presence of LysoTracker positive somatic cells next to Vasa-negative cysts was only observed in *fru* null gonads (control, 0%, n=8; *fru* null, 100%, n=9). These dying cyst cells were distinguished from dying germ cells by the smaller nuclei indicated by DAPI staining and the Arm staining that separated the somatic cell from the spermatogonia cyst (Figure 4.4 C' and C''). Since *fru* is only expressed in the somatic gonad, the germ cell death is likely a secondary effect of the cyst cell death.

Figure 4.4: *fru* mutant gonads display cyst cell death and germ cell death. (A) Quantification of Vasa-negative cysts between control and *fru* mutants. (B-C) WPP stage *fru* het and *fru* null gonads. LysoTracker positive spermatogonial cysts and cyst cell are outlined. Arrow: Arm-enriched cytoplasm separates LysoTracker-positive cyst cell from the LysoTracker-positive spermatogonial cyst.

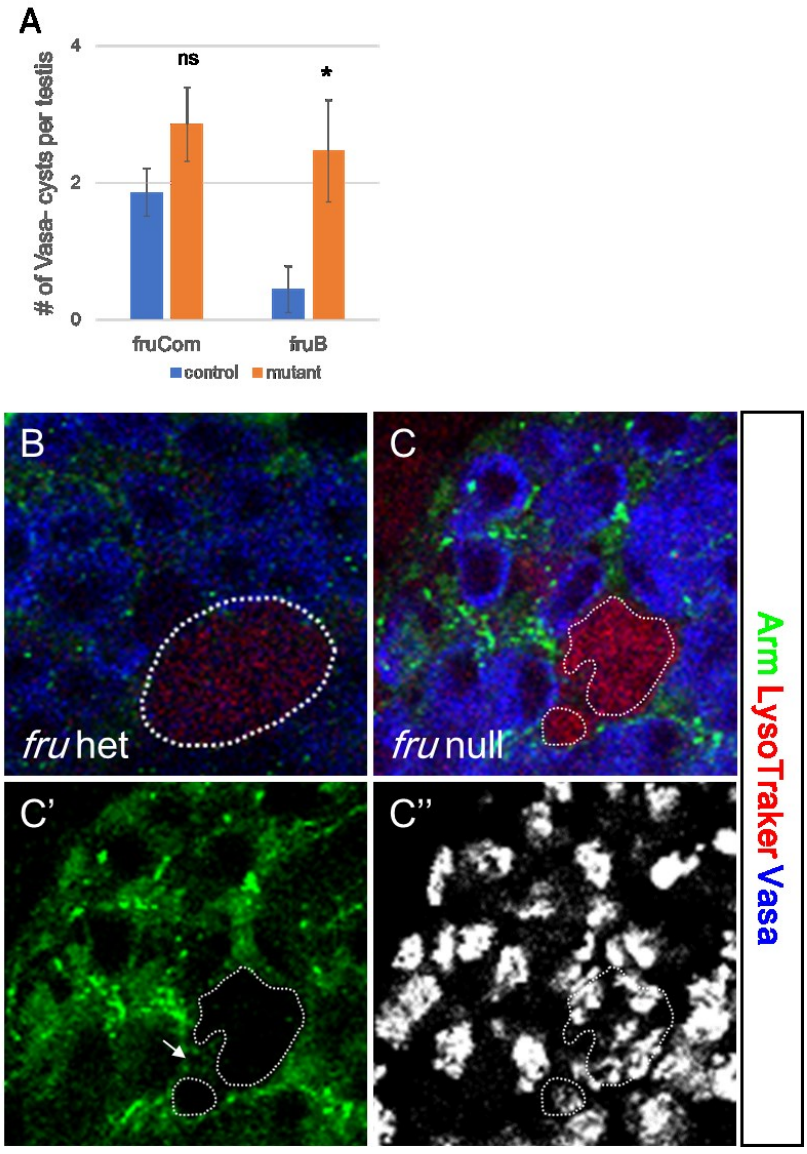

To further address *fru* function in the cyst lineage, we generated GFP-positive *fru* mutant CySC clones using the MARCM technique (Lee and Luo, 1999), and asked if clones could be generated and maintained. We located the hub by the expression of hub-specific markers, Arm or FasIII, or by the reduced Zfh-1/Tj expression in a cluster of cells surrounded by a rosette of Vasa-positive GSCs. CySCs were scored as Zfh-1-positive or Tj-positive cells within one cell diameter away from the hub and directly contacting the hub through the cytoplasmic extension as indicated by the membrane-bound GFP. Marked control (*FRT82B*) CySC clones were observed in 67% (n=61), 71% (n=65), 56% (n=129) and 43% (n=56) of the testes examined at 2, 4, 5, and 10 days post clone induction (pci), respectively (Figure 4.5 A, Table 4.1). Control CySC clones mutant for *ry* were generated and maintained at a similar rate (Table 4.1). In contrast, CySC clones homozygous mutant for fru^{Sat15} were observed less frequently at 2 days pci (26%, n=46), and were lost rapidly by 4-day pci (7%, n=72), and were completely absent by 10 days pci (0%, n=78). $fru^{\Delta B}$ mutant CySCs were also observed at a lower frequency than the control at 2 days pci (29%, n=55), and were lost at a similar rate as fru^{Sat15} clones (4 days pci: 7%, n=60; 5 days pci:4%, n=101; 10 days pci: 3% n=66). Interestingly, $fru^{\Delta C}$ mutant CySC clones were observed at a normal frequency at 2 days and 5 days pci (2 days pci: 57%, n=21; 5 days pci: 30%, n=24), whereas by 10 days pci only 5% of examined testes maintained the CySC clones (n=44). From these results, we conclude that both *fruB* and *fruC* are cell-autonomously required for the maintenance of CySC fate. But *fruB* plays a more important role than *fruC*.

Two possible explanations of CySC loss are precocious differentiation and cell death. At 2-4 days pci, we did not observe *fru* mutant CySC and cyst cell clones exhibiting precocious expression of the cyst cell differentiation marker Eya or reduced expression of

the stemness-marker Zfh-1 when compared with wildtype CySCs and daughters in the same testes or with control CySC clones (*FRT82B*, n=63; fru^{Sat15}, n=33; $fru^{\Delta B}$, n=21; $fru^{\Delta C}$, n=21) (Figure 4.5 B). These data suggest that *fru* mutant CySCs were not lost through precocious differentiation.

To test if *fru* mutant CySCs were lost through cell death, we performed the terminal deoxynucleotidyl transferase mediated dUTP nick end labeling (TUNEL) assay, which detects apoptotic cells that undergo extensive DNA degradation during the late stages of apoptosis. At 4 days pci, we did not find a control CySC clone or cyst cell clone positive for TUNEL (n=8). In age-matched testes containing $fru^{\Delta B}$ clones, TUNEL positive CySC clones were also not observed. However, 42% of examined testes with cyst cell clones had TUNEL-positive cyst cells surrounded by the membrane-bound mCD8:GFP (n=12) (Figure 4.5 C). To further confirm that dying cyst cells were GFP-marked *fru* mutant clones, we performed clonal analyses with a positive nuclear GFP marker. In 50% of testes carrying $fru^{\Delta B}$ cyst cell clones, the TUNEL signal overlapped with nuclear GFP signal (n=10) (Figure 4.5 D). Consistent with these results, we found that *fru* mutant cyst cell clones were lost at 10 days pci (Table 4.1). From these results, we conclude that *fru* mutant CySCs were not lost by apoptosis and that *fru* is autonomously required for cyst cells survival.

Earlier we proposed that the spermatogonial cyst death in *fru* null and $fru^{\Delta B}$ mutant gonad was caused by loss of *fru* in the encasing cyst cells. To test this hypothesis, we examined LysoTracker staining in testes 2-4 days pci containing control or *fru* mutant CySC and cyst cell clones. While both the control and the experimental group had Lysotracker-positive spermatogonial cysts, we observed GFP-marked cyst cells

surrounding Lysotracker-positive spermatogonial cysts in 14% of testes with fru^{Sat15} cyst cell clones (n=29) and 10% of testes with $fru^{\Delta B}$ cyst cell clones (n=29) but 0% of testes with control clones (n=63) (Figure 4.5 E and F). These results suggest that loss of *fru* in cyst cells induced cell death in the encased germ cells.

Figure 4.5: *fru* is cell-autonomously required for CySC maintenance and cyst cell survival. (A) The percentage of controls (82B and ry) and *fru* mutant CySC clones maintained at the niche post clone induction (pci). (B) A testis with $fru^{\Delta B}$ CySC clone and cyst cell clone 4 dpci. Zfh-1 level is indistinguishable between GFP+ and GFP- cells. Arrows: GFP+ clones; Arrowhead: a control differentiated cyst cell expressing Eya. (C-D) mCD8:GFP (C) and GFP.nls (D) marked cyst cells clones mutant for $fru^{\Delta B}$ are labeled by TUNEL and Tj. (E-F) $fru^{\Delta B}$ cyst cell clones ensheathing spermatogonia cysts are positive for LysoTracker. Arrows: the cell body of GFP+ cyst cell clones.

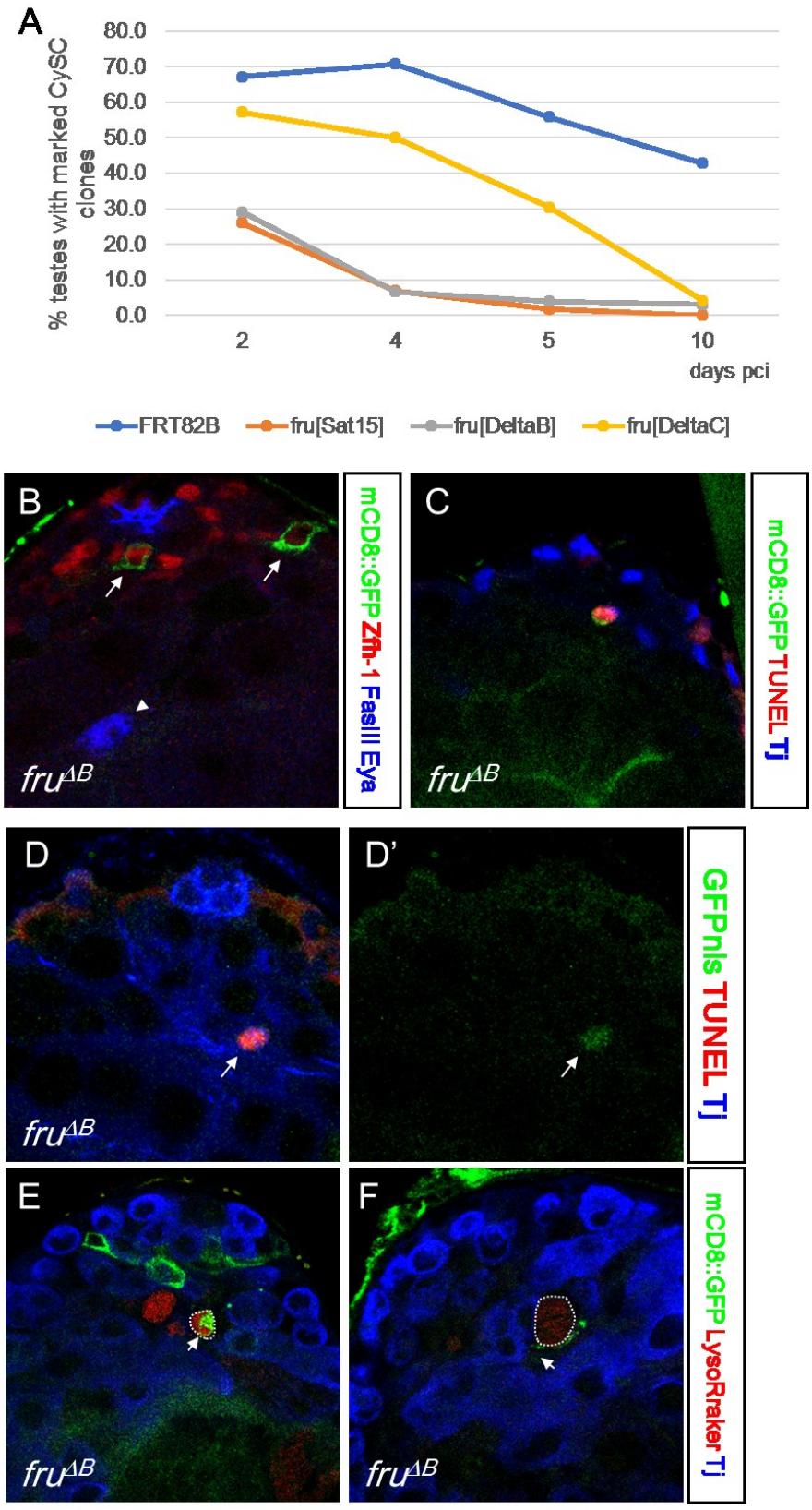
A
% testes with marked CySC clones
80.0
70.0
60.0
50.0
40.0
30.0
20.0
10.0
0.0
2
4
5
10
days pci
FRT82B
fru[Sat15]
fru[DeltaB]
fru[DeltaC]
B
mCD8::GFP Zfh-1 FasIII Eya
fruΔB
C
mCD8::GFP TUNEL Tj
fruΔB
D
fruΔB
D'
GFPnls TUNEL Tj
E
fruΔB
F
fruΔB
mCD8::GFP LysoRaker Tj

Table 4.1: Quantification of control and *fru* clones.

Genotype	Dpci	CySC clones (%)	Differentiated cyst cells (%)	GSC clones (%)	Testes scored
Control(*FRT82B*)	0	0.0	0.0	0.0	20
	2	67.2	75.4	18.0	61
	3	70.3	75.0	6.3	91
	4	70.8	86.2	6.2	65
	5	55.8	61.2	5.4	129
	10	42.9	48.2	8.9	56
Control(*ry*)	0	0.0	0.0	0.0	22
	2	50.0	64.0	0.0	50
	3	71.4	88.6	2.9	35
	4	60.5	48.1	21.0	81
	5	62.7	71.8	6.4	110
	10	41.2	49.0	0.0	51
fru^{Sat15}	2	26.1	50.0	2.2	46
	3	30.0	87.5	12.5	100
	4	6.9	65.3	0.0	72
	5	1.8	8.0	12.4	113
	10	0.0	0.0	2.6	78
$fru^{\Delta B}$	2	29.1	56.4	7.3	55
	3	25.4	55.2	13.8	59
	4	6.7	21.7	28.3	60
	5	4.0	10.9	15.8	101
	10	3.0	6.1	16.7	66
$fru^{\Delta C}$	2	57.1	85.7	14.3	21
	4	34.0	53.2	20.0	37
	5	29.2	31.8	34.8	24
	10	4.5	6.8	25.0	44

Knocking down fru causes delayed cyst cell and germline differentiation

We next asked whether *fru* plays a sex-specific role in the CySC lineage. The CySC sexual identity is actively maintained in adult testes. Loss of a closely related BTB-ZnF transcription factor, Chinmo (Chronologically inappropriate morphogenesis), results in cell fate conversion from the CySC to the follicle stem cell (Ma et al., 2014). However, knockdown of *fru* in the CySC lineage with *c587-Gal4* did not cause ectopic expression of FasIII outside the hub (data not shown). From this data, we conclude that *fru* is not required in the CySCs to maintain its sexual identity.

Nevertheless, we noticed that knockdown of *fru* caused a delay in cyst cell and germline differentiation. Nuclei of less differentiated germ cells (GSCs and mitotic spermatogonia cysts) stain more brightly with the DNA dye DAPI, leading to a characteristic "DAPI bright" region and the tip of the testis. While 7-day-old *control-RNAi* testes had 36.3±1.2 μm of DAPI-bright region, the DAPI-bright region in *Com1- RNAi* testes extended to 44.3±1.4 μm (*control-RNAi*, n=52; *Com1-RNAi*, n=39, $p<0.0001$, Student's t-test; Figure 4.6 A-C). The severity of the delayed differentiation phenotype increased with age. In 21-day-old testes, the length of DAPI-bright region was 47.1±1.8 μm in the control group and was increased to 61.7±3.7 μm in the experimental group (*control-RNAi*, n=45; *Com1-RNAi*, n=42, p=0.0001).

To determine if cyst cell differentiation was also affected, we examined the CySC marker, Zfh-1 and the undifferentiated cyst cell markers, Tj in control and *fru* knockdown testes. At 14 days after eclosure, we observed a significant increase in the number of Zfh-1 positive cells from 18.3±0.9 per control testis to 27.7±2.1 per *fru* knockdown testis (*control-RNAi*, n=19; *fru-RNAi*, n=18; p=0.0001, Student's t-test; Figure 4.6 D). Similarly,

the number of Tj+ cyst cells per testis was significantly increased when *fru* is knocked down in the CySC lineage (*Control-RNAi, 66.4*±1.7, n=28; *fru-RNAi, 101.1* ±3.5, n=28; $p<0.0001$, Student's t-test; Figure 4.6 E). From these results, we conclude that knockdown of *fru* in the CySC lineage delays cyst cell differentiation, which non-autonomously delays spermatogenesis.

Figure 4.6: *fru* knockdown delayed germline and cyst cell differentiation. (A-B) Representative 14-day-old testes with *c587>control* RNAi (A) and *c587>fru* RNAi (B) differ in the length of DAPI-bright zone. (C) Quantification of the length of DAPI-bright region in control and *fru* knock-down testes at 7-, 14- and 21-days after eclosure. Sample sizes are: 52, 39, 41, 49, 45, 42. Mean±SEM. (D-E) The number of Zfh-1- positive cells (D) and Tj-positive cells (E) in control and *fru* knock-down testes at 14 days poster eclosure. Bars represent Mean±SEM.

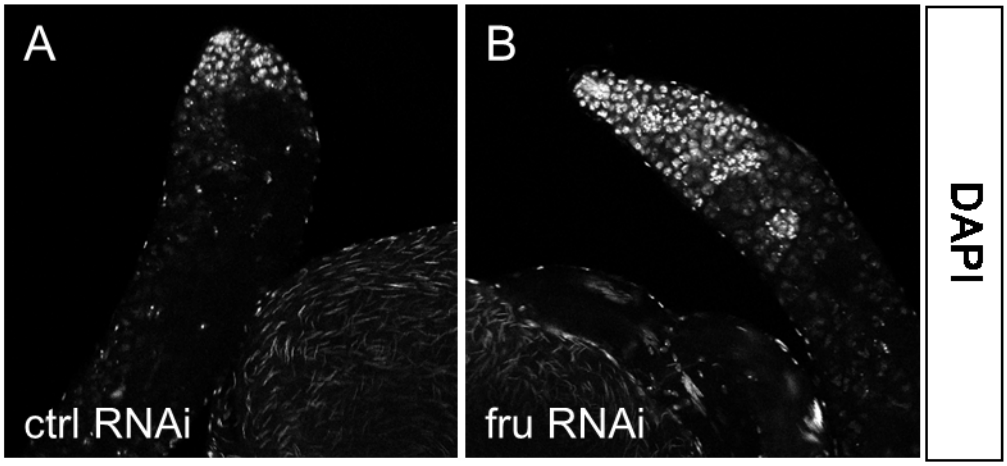
A
B
ctrl RNAi
fru RNAi
DAPI

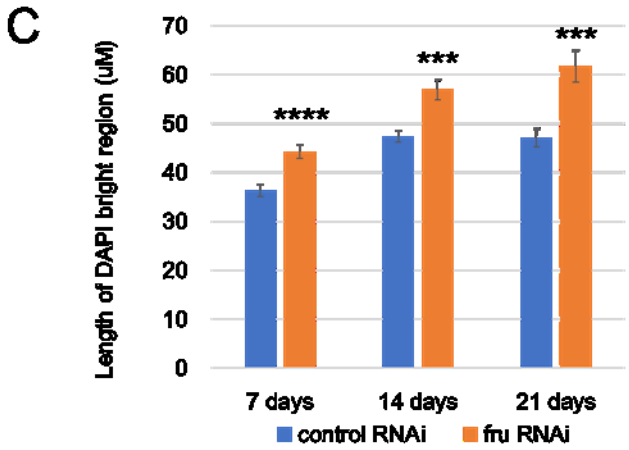
C
Length of DAPI bright region (uM)
70
60
50
40
30
20
10
0
****
***
***
7 days
14 days
21 days
control RNAi
fru RNAi

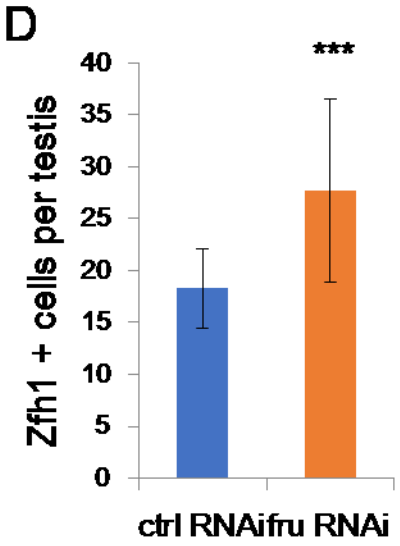
D
Zfh1 + cells per testis
40
35
30
25
20
15
10
5
0
***
ctrl RNAi
fru RNAi

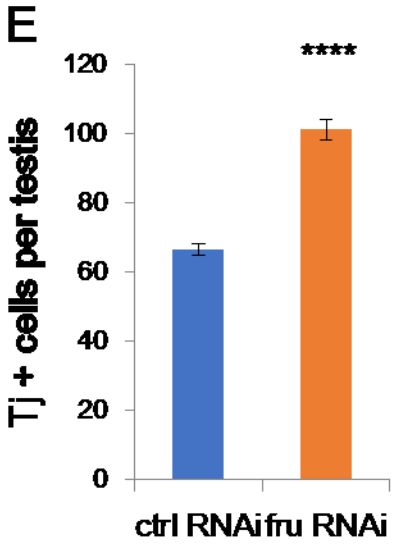
E
Tj + cells per testis
120
100
80
60
40
20
0
****
ctrl RNAi
fru RNAi

fru is important for maintenance of the hub fate during development

The onset of Fru expression in the L3 stage testes correlates with the time when niche plasticity is lost in the male gonad (Camara and Van Doren, submitted). Moreover, Fru is less likely to be expressed in *dsx* mutants that commit to the TF fate. Therefore, we next investigated whether *fru* plays a sex-specific role in the niche. While *fru* is not required for maintaining hub integrity, it may function as a masculinizing factor to prevent the hub from transdifferentiating into TFs. We reason that if *fru* promotes maleness of the niche, or prevents hub to TFs conversion, decreasing Fru dosage in *dsx* mutant gonads by removing one copy of *fru* will be sufficient to tip the balance and direct niche development towards the formation of TFs. Conversely, if Fru expression is only a consequence of male-specific cell fate, changing Fru expression level would not alter the chances of a *dsx* mutant gonad developing a hub or TFs.

To test this idea, we performed genetic interaction assays in *dsx* mutant backgrounds, where the niche stochastically commits to either the hub fate or the TF fate (Camara and Van Doren, submitted; Clough et al., 2014) (Figure 1.4 A-F and 4.7). The frequency of adult gonads with hubs and TFs can be used as a measurable read-out to reflect changes in male- and female-promoting signals (Clough et al., 2014). *dsx* mutant flies of 1-2 days old were scored for the presence of a hub, TFs or neither in the gonad. We defined the hub as Fas-III and N-Cad double positive somatic cells that forms a compact structure surrounded by a rosette of Vasa-expressing germ cells (Figure 4.7 B and D). The TFs were determined by the ladder-shaped N-Cad staining around stacks of disc-shaped nuclei indicated by DAPI stain (Figure 4.7 A and C).

Figure 4.7: *XX; dsx^{D}/+* gonads either have TFs or a hub in the adult. 2-day-old wildtype (A and B) and *XX; dsx^{D}/+* gonads. Staining as indicated. Representative *dsx* mutant gonads with a female niche (C) or a male niche(D) are shown. Arrows: TFs; circles: the hub.

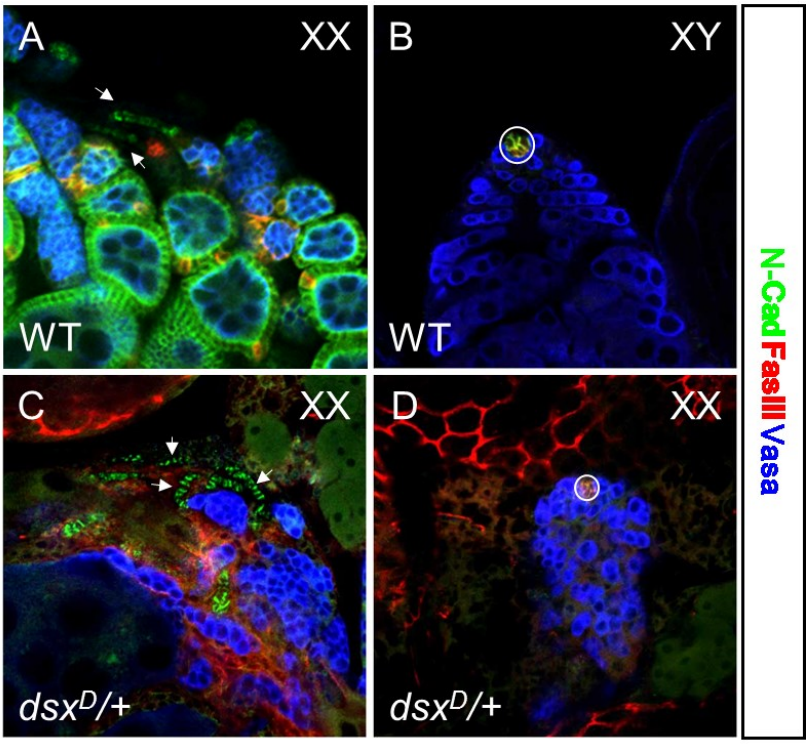

We first conducted genetic interaction between *fru* and *dsx* in the *dsx* null background. Consistent with previous observations (Camara and Van Doren, submitted), XY dsx^{3}/dsx^{1} mutants had 43.8 ± 0.8% of gonads with TFs and 40.6 ±15.0% of gonad with hubs (n=32). We predicted that placing a *fru* deficiency allele, fru^{Sat15}, in this genetic background would cause the ratios to shift to a higher frequency of the TF fate and a decreased frequency of the hub fate. We observed a statistically significant ($p<0.05$) drop of the hub fraction to 8 ± 3.6% (n=50), and an increase in the percentage of gonads with TFs (Figure 4.8). Since the variable Fru expression level in the *dsx* null gonad is independent of chromosomal sex, we predicted that the fractions of gonads committed to the hub fate versus the TF fate would be similar between XX and XY animals carrying a copy of fru^{Sat15}allele. Indeed, in XX animals with a fru^{Sat15}allele, we observed a low hub percentage (13.6 ±4.3%) and a high TF percentage (72.7 ±7.1%, n=44) (Figure 4.8). Considering that the FruB isoform is implicated to be the major isoform that functions in the gonad, we predicted that replace the wildtype *fru* allele with a $fru^{\Delta B}$ allele would similarly increase the chances of forming TFs. When the genetic interaction was performed with $fru^{\Delta B}$, we saw 16.2 ± 4.7% of examined *dsx* null gonads had a hub and 57.1 ± 9.3% had TFs (n=105). These results suggest that reducing the Fru level causes *dsx* mutant niches more likely to transdifferentiate from the hub to TFs.

Figure 4.8: *fru* genetically interacts with *dsx* in the *dsx* null background. Niche fate distribution in *dsx* null gonads. Genotype as indicated. Refer to **Table 4.2** for the sample size of each genetic background. Error bars represent SD. * denotes $p<0.05$, Student's t-test.

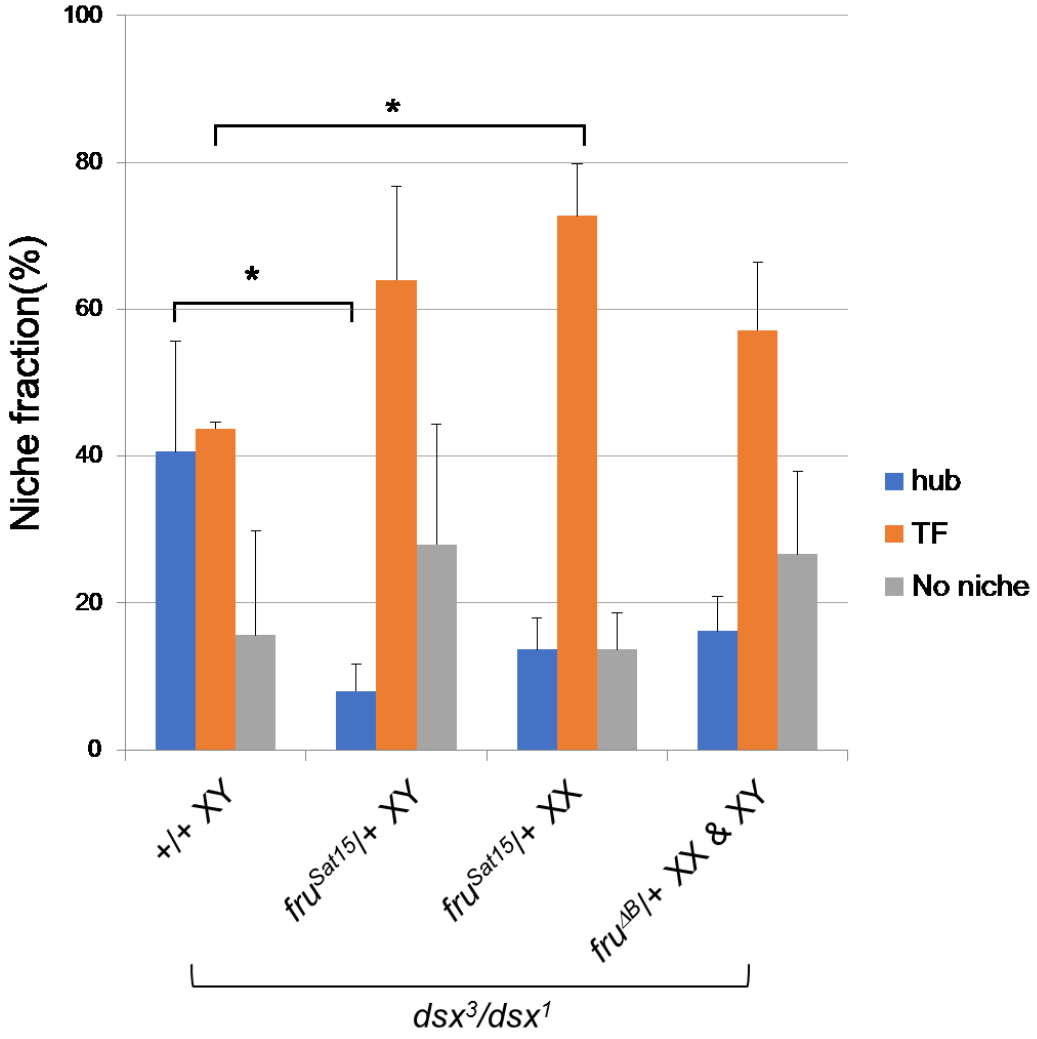

Table 4.2: Summary of genetic interaction in *dsx* null background.

Genotype	Sample size	Hub% (AVG±SD)	TF% (AVG±SD)	No niche% (AVG±SD)
dsx^{3}/dsx^{1} XY	32	40.63±14.95	43.75±0.81	15.63±14.14
$dsx^{3}, fru^{Sat15}/dsx^{1}$ XY	50	8.00±3.64	64.00±12.74	28.00±16.36
$dsx^{3}, fru^{Sat15}/dsx^{1}$ XX	44	13.64±4.31	72.73±7.07	13.64±4.99
$dsx^{1}, fru^{\Delta B}/dsx^{3}$ XX and XY	105	16.19±4.65	57.14±9.28	26.67±11.20

We also conducted similar experiments using the dsx^{D}/+ genetic background, where only XX individuals are mutant for *dsx* due to the simultaneous expression of DsxF and DsxM, which cancel each other out (Clough et al., 2014). In w^{1118} controls, we observed 62.7 ± 3.2% of *XX*; dsx^{D}/+ gonads formed TFs, 26.4 ± 3.9% retained the hub, and 10.9 ± 3.3% had no identifiable niche (n=110, Figure 4.9 A, Table 4.3). Similar ratios were observed in a second control (*CantonS*) background (Table 4.3). When one copy of *fru* was replaced with fru^{Sat15}, the fraction of gonads with a hub decreased to 4.7 ± 4.1% and the fraction of gonads with TFs increased to 87.5 ± 6.1% ($p<0.0001$, n=256). From this results, we conclude that *fru* maintains the hub fate and prevents the TF fate.

To further determine which C-terminal *fru* isoform promotes the hub fate, we performed genetic interaction assays with isoform-specific *fru* mutants. $fru^{\Delta A}$, $fru^{\Delta B}$, and $fru^{\Delta C}$ alleles, which have an early termination codon inserted before their respective C-terminal ZnF domain, were placed into the dsx^{D} background (Neville et al., 2014). In XX dsx^{D}/+ mutants heterozygous for *fruB* ($fru^{\Delta B651}$), 97.8 ± 2.3% of examined gonads specified TFs and only 1.7 ± 2.4% formed hubs (n=179) (Figure 4.9 A, Table 4.3). Genetic interaction with another *fruB* mutant stock, $fru^{\Delta B741}$, which had the same mutation but was independently isolated during mutagenesis, also resulted in 97.6 ± 1.9% of examined gonads formed TFs and 1.2 ± 1.5% formed hubs (n=83, Table 4.3), suggesting that the *fru* allele rather than background mutations caused the shift in niche frequencies. We saw a similar increase in TF frequency ($p<0.0001$) and a decrease in hub frequency ($p<0.0001$) in gonads carrying one copy of the $fru^{\Delta C}$ allele (n=163, Figure 4.9 A and Table 4.3), suggesting that FruC also plays a role in preventing the hub from transdifferentiating into TFs. On the other hand, $fru^{\Delta A}$ did not skew the chances towards the TF fate ($p>0.05$, Figure

4.9 A and Table 4.3). We observed 49.2 ± 12.1% and 36.5 ± 10.5% of examined gonads specified as TFs and the hub, respectively (n=63). From these results, we conclude that *fruB* and *fruC* but not *fruA* function in the male niche to promote the hub fate and to prevent TF formation.

Next, we asked whether increasing Fru dosage would be sufficient to prevent the hub from converting to TFs and increase the chance of gonads retaining the hub fate. We overexpressed FruB in the *XX; dsx^{D}/+* background by driving *UAS-fruMB* and *UAS-fruB* cDNA transgenes with *tj-Gal4*. Control *XX; dsx^{D}/+* adults with *tj*-Gal4 or *UAS-fru* cDNA alone exhibited a high frequency of TF fate similar to the wildtype (89.8% for *XX;tj-Gal4/+;dsx^{D}/+,* n=49; 81.5% for *XX; UAS-fruMB/+; dsx^{D}/+,* n=68; 70.4% for *XX; UAS-fruB/+;dsx^{D}/+,* n=27) (Figure 4.9 B). Strikingly, 0% of *XX; tj>fruB; dsx^{D}/+* gonads formed TFs (n=66), whereas 95.6% of gonads committed to the TF fate in *XX; tj>fruMB; dsx^{D}/+* flies (n=68). However, increasing FruB dosage did not result in more gonads committed to the hub fate. Only 1.5% of examined *tj>fruB* gonads had a hub (n=68). The rest of the gonads had increased N-cad and FasIII level throughout the gonad and lacked TFs (data not shown).

Taking together the above findings, we conclude that *fru* genetically interacts with *dsx* to specify niche fates. Decreasing Fru level leads to a higher frequency of niches converting to TFs, whereas increasing Fru expression level prevents the hub from converting to TFs.

Figure 4.9: *fru* genetically interacts with *dsx* in the *XX; dsx^{D}/+* background. (A) Distribution of niche fate in 2-day old *XX; dsx^{D}/+* gonads with control (*w^{1118}*) or *fru* mutant alleles. (B) Distribution of niche fate in 2-day old *XX; dsx^{D}/+* gonads with *tj-Gal4/UAS-fru cDNA* alone or *tj>fru cDNA*. Refer to **Table 4.3** for sample sizes. Error bars represent SD. *** denotes p<0.001; **** denotes p<0.0001; ns denotes p>0.05; Student's t-test.

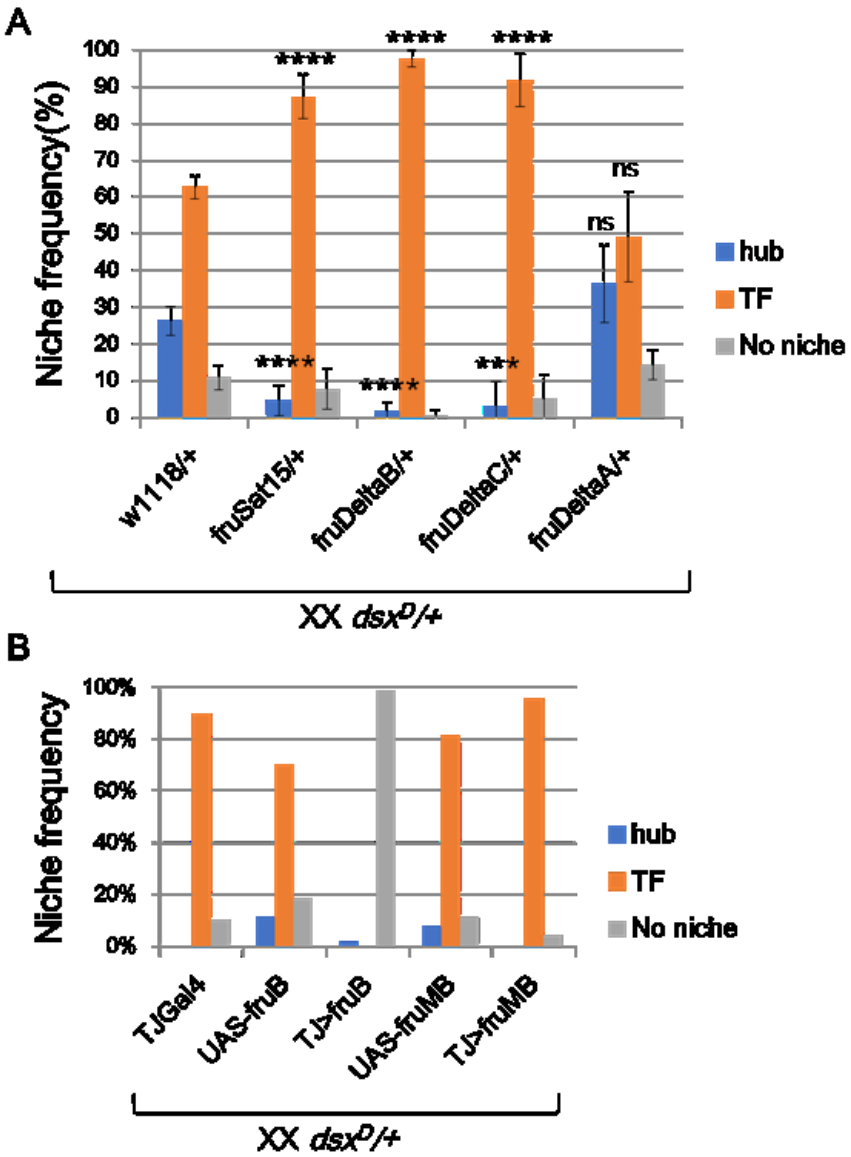

Table 4.3: Distribution of niche fates in *XX; dsx^{D}/+* gonads.

Genotype (*XX; dsx^{D}/+*)	Sample size	Hub% (AVG±SD)	TF% (AVG±SD)	No niche% (AVG±SD)
w^{1118}	110	26.4±3.9	62.7±3.2	10.9±3.3
CantonS	86	15.1±5.4	72.1±1.6	12.8±3.8
fru^{Sat15}/+	256	4.7±4.1	87.5±6.1	7.8±5.5
fru^{AB651}/+	179	1.7±2.4	97.8±2.3	0.6±1.5
fru^{AB741}/+	83	1.2±1.5	97.6±1.9	1.2±1.7
fru^{AC}/+	163	3.1±6.9	92.0±7.2	4.9±6.6
fru^{AA}/+	63	36.5±10.5	49.2±12.1	14.3±4.0

Genotype (*XX; dsx^{D}/+*)	Sample size	Hub%	TF%	No niche%
tj-Gal4/+	49	0.0	89.8	10.2
UAS-fruMB/+	27	7.4	81.5	11.1
UAS-fruB/+	27	11.1	70.4	18.5
tj-Gal4/UAS-fruB	66	1.5	0.0	98.5
tj-Gal4/UAS-fruMB	68	0.0	95.6	4.4

Ectopic expression of fru in female gonads inhibits terminal filament formation and partially masculinizes the gonad

We next asked whether ectopic *fru* expression in otherwise wildtype female gonads will inhibit TF formation and convert the niche into a hub. We drove the *UAS-fruB* cDNA transgene in *dsx*-expressing cells of the developing ovary with *dsx-Gal4* (Rideout et al., 2010; Song et al., 2002a). When white prepupae were examined, control ovaries lacking the *UAS* transgene all had 6-8 disc-shaped cells expressing the TF-specific marker Engrailed (En) and aligning at the base of the apical cap (n=7), whereas ovaries expressing FruB failed to robustly express En, which is required for TF cell specification (Bolivar et al., 2006) (Figure 4.10 A and B). Furthermore, none of the FruB expressing gonads had success intercalation of En-positive cells into a filament (n=25).

To determine if FruB-expressing XX gonads were masculinized, we examined the male-specific niche marker, *escargot* (*esg*), with an enhancer trap (esg^{M5-4}) that reports *esg* activity through the expression of LacZ (Le Bras and Van Doren, 2006). In wildtype gonads of the late L3 stage, esg-LacZ was expressed strongly in the hub and the early germ cells of the testis (n=6), whereas no lacZ was detected throughout the ovary (n=5) (Figure 4.10 C and D). When FruB was overexpressed, we observed robust expression of esg-LacZ only in somatic cells that locate anterior to the primordial germ cells (n=23), despite that *dsx-Gal4* drives expression in all the somatic cells of the ovary (Figure 4.10 E).

Figure 4.10: Ectopic expression of FruB represses TF formation and partially masculinizes the female gonad. (A-B) WPP stage XX gonads. Brackets: TFs; the outlined region in (B): apical cap from the top view. (C-E) WPP stage gonads. Circle: hub; brackets: TFs; the outlined region in (E): apical cap.

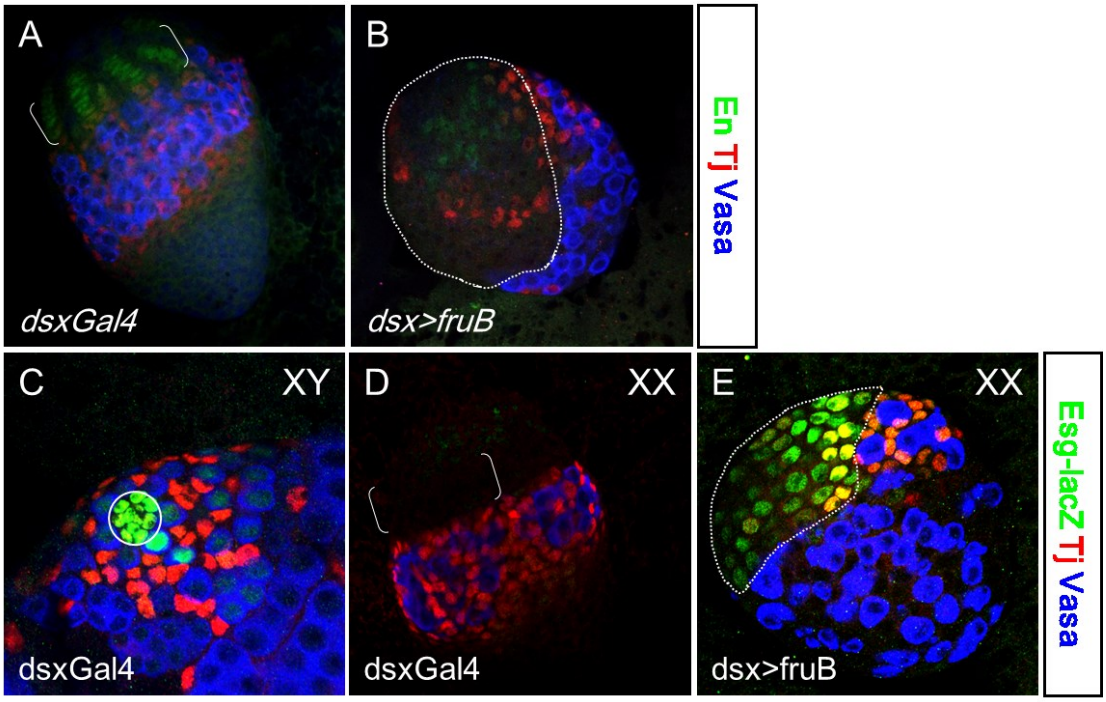

FruB overexpression driven by *dsx-Gal4* caused pupal lethality. To further test whether FruB expression is sufficient to induce hub formation, we restricted Fru overexpression to *tj*-expressing intermingle cells that give rise to cap cells via the *tj-Gal4* driver. Overexpression of FruB caused delayed TF formation in 50% of late L3 ovaries (n=20) and disorganized adult ovaries that resemble *dsx* mutant gonads (Figure 4.11 A-D and data not shown). On the other hand, overexpressing *UAS-fruM* isoforms in the intermingle cells did not affect ovary development. When the niche fate was examined, we found that 16.4% of the ovaries had neither TF or hub formed (n=61) (Figure 4.12 A). This result suggests that ectopic Fru expression in intermingle cells also represses TF formation.

More strikingly, in 9.8% of examined ovaries that had TFs, we observed a hub-like structure that was composed of a compact cluster of somatic cells and co-expressed the hub-specific marker FasIII and N-cad (Figure 4.12 C). However, we did not observe GSC attached to the "hub". These results indicate that the "hub" could not function as a male GSC niche. We also found that 37.5% (n=24) of ovaries with TFs failed to express the female-specific niche marker, Sox100B, in the TFs (Nanda et al., 2009) (Figure 4.12 B, D, and E). From these results, we conclude that the ectopic Fru expression in the intermingle cells masculinizes the niche and defeminizes the TFs.

Figure 4.11: Overexpressing *fruB* but not *fruMB* disrupts ovary development and TF formation. Wildtype late L3 ovary (A) and late L3 ovaries ectopically expressing FruB (B) and FruMB (C) in intermingle cells. (D) Percentage of late L3 ovaries with TFs when FruMB and FruB are overexpressed in intermingle cells.

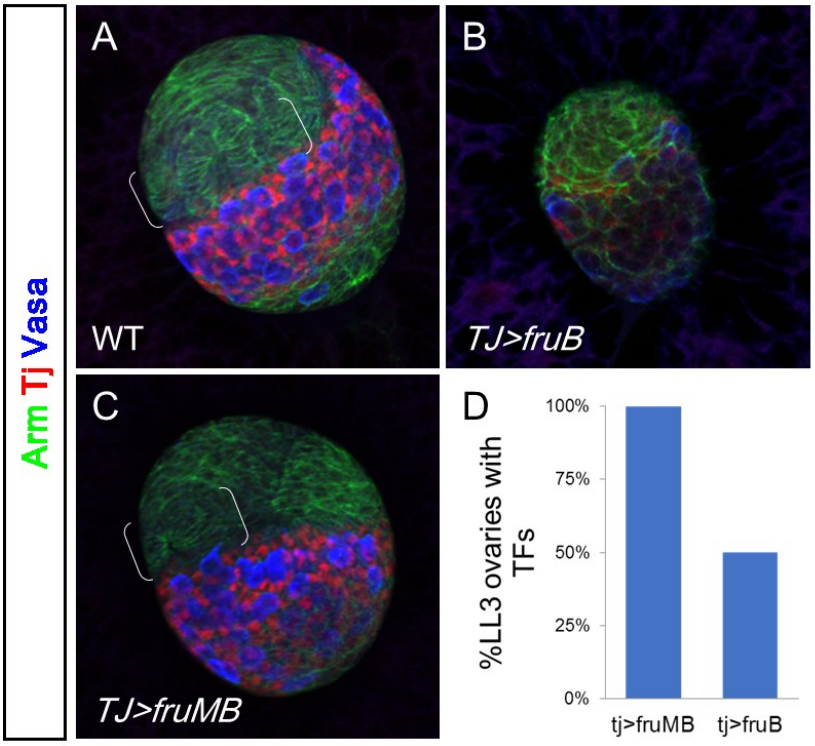

Figure 4.12: Adult ovaries with FruB ectopically expressed in intermingle cells partially reversed the niche fate. (A) Niche fate distribution in 2-day-old *tj>fruMB* and *tj>fruB* ovaries. (B) Sox100B expression in control adult ovaries and *tj>fruB* ovaries. (C) A representative 2-day-old *tj>fruB* ovary with both TFs (indicated by brackets) and a hub-like structure (indicated by a circle). (D-E) 2-day-old *tj>fruB* ovaries with normal Sox100B expression in TFs (D) and without Sox100B (E). Brackets: TFs.

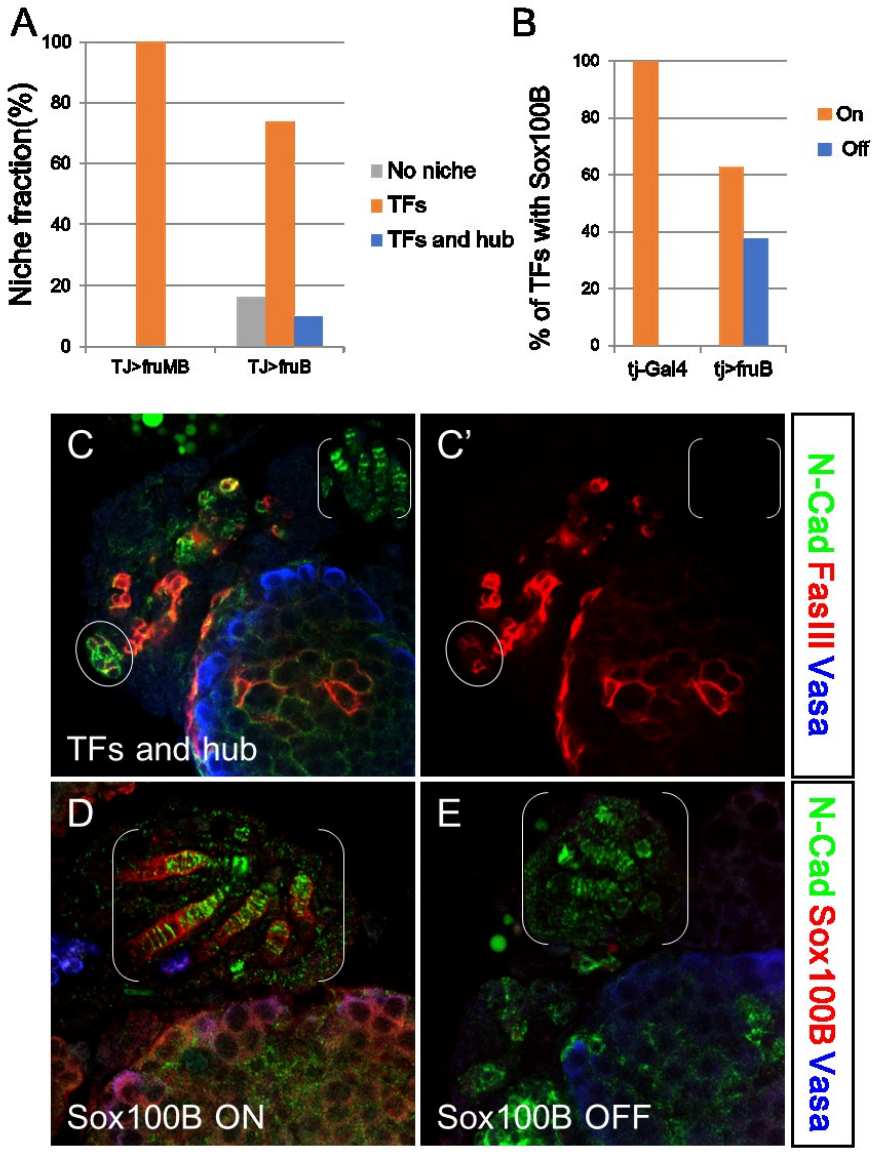

Next, we asked whether ectopic Fru expression would disrupt the maintenance of adult female GSC niche. We utilized the temperature-controlled *Gal4/Gal80^{ts}* system. Female flies were raised at the permissive temperature (18 ºC) till adulthood, then shifted to the non-permissive temperature (29ºC) to induce the expression of UAS-cDNA transgenes driven under *c587-Gal4* (Figure 4.13 A). While this system precisely controls expression with temperature in the desired cell types, as indicated by no GFP expression in ovaries raised in 18ºC and robust GFP expression in ovaries raised at 29ºC (Figure 4.13 B-C), we did not observe any oogenesis defect after overexpressing Fru for two weeks (Figure 4.13 D-E). This result suggests that Fru is not sufficient to interfere with the maintenance of the adult female GSC niche.

Figure 4.13: Overexpressing Fru in adult ovaries does not disrupt oogenesis. (A) Schematic of the temperature shifting experiment. (B-E) 14-day-old ovaries kept at 18ºC after eclosure (B and D) or shifted to 29ºC for two weeks (C and E). Genotype as indicated.

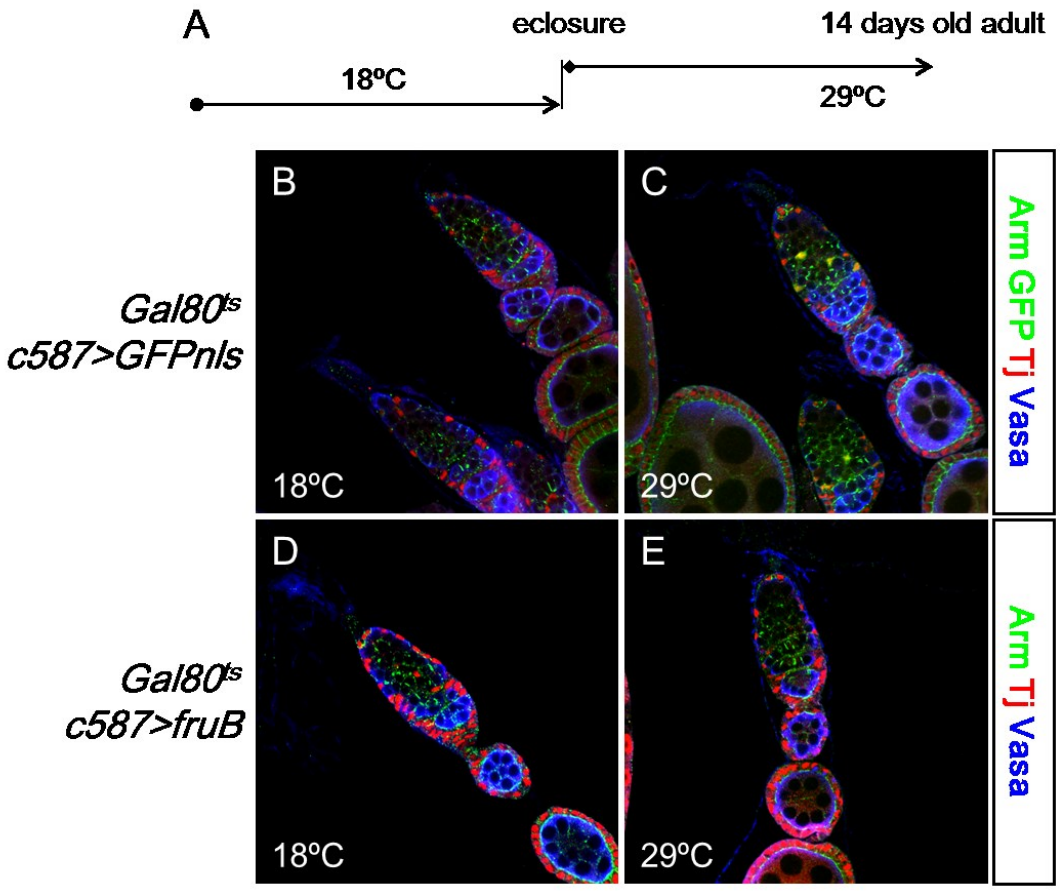

Conclusions and Discussion

Over the past decades, much effort has been focused on understanding *fruM* functions in regulating sex-specific courtship behaviors, yet it remains unclear whether *fru* is involved in the morphological branch of the sex determination pathway. In this chapter, we investigated *fru* function in the male GSC niche. We found that *fruCom* is required in adult testes to maintain the architecture and positioning of the hub. It is additionally required in the CySC lineage to maintain the CySC fate and to support cyst cell survival and proper differentiation. Loss of *fru* in cyst cells non-autonomously triggers germ cell death and delays germ cell differentiation. We also revealed a sex-specific role of *fruCom* downstream of *dsx* in promoting the hub fate and inhibiting TF formation during niche development. However, *fru* does not control the sexual identity of niche cells in adult flies.

fru is not the only masculinizing factor that prevents hub-to-TFs transdifferentiation

In the medaka fish, loss of *DMRT1* causes the gonads in XY individuals to initially develop into testes and later transdifferentiate into ovaries. This is similar to the sex reversal of *Drosophila* GSC niches in the absence of *dsx*. However, sex reversal occurs stochastically in *dsx* mutant gonads. Our results indicate that whether a *dsx* mutant gonad would undergo hub-to-TFs conversion depends on the expression level of Fru. Lowering the Fru expression level in *dsx* mutants resulted in a higher chance of the hub to transdifferentiate into TFs, whereas elevating the Fru expression level inhibited the hub from converting to TFs. Thus, *dsx* and *fru* function cooperatively to prevent niche sex reversal. On the other hand, our analyses showed that loss of *fru* is insufficient to convert hub cells into apical cap cells and TF cells. These results indicate that *fru* is not the only

gene that functions downstream of *dsx* to prevent hub cells from transdifferentiating into TF cells. Our working hypothesis is that *fru* is one of many masculinizing factors that function downstream of *dsx* to maintain the hub fate. Our finding that loss of either *dsx* or *fru* is insufficient to induce complete sex reversal reveals the robustness of the hub development program. Interestingly, it was recently found that loss of either *dsx* or *fru* is also insufficient to abolish male-specific courtship behaviors (Pan and Baker, 2014). It is likely that *dsx* and *fru* act in concert to ensure that sexual development is resistant to random mutants in the sex determination pathway.

Mechanism of fru preventing hub fate to TF fate conversion

How would *fru* prevent hub to TF transformation? One potential mechanism is to maintain *esg* expression in the hub. It has been shown that a high *esg* expression level is required to specify the hub from anterior somatic progenitors and to prevent hub cells from converting into CySCs (Le Bras and Van Doren, 2006; Voog et al., 2014). We have demonstrated through Fru gain-of-function studies in the ovary that *fru* is sufficient to activate *esg* expression in the anterior somatic progenitors of the larval ovary. *esg* has been identified as a putative target gene of FruM in the CNS (Neville et al., 2014). FruCom may also regulate *esg* expression to maintain the hub fate.

fru may also play an active role in preventing TF formation. This can be achieved either by repressing the expression of genes required for TF specification or by preventing the normal function of those genes. TF development is initiated by ecdysone signaling. Ecdysone-responsive genes are among the putative FruM targets (Neville et al., 2014). It has also been shown that the ecdysone receptor functions downstream of *fruM* to regulate

male-specific courtship behaviors (Dalton et al., 2009; Ganter et al., 2012). Similarly, FruCom may repress hub to TF conversion through blocking the male niche from responding to ecdysteroids. This hypothesis is supported by our finding that expressing Fru in intermingle cells delays the onset of TF formation. Known genes involved in TF formation, including *bab1*, *en*, *psq,* and *trl*, are also potentially regulated by FruM in the nervous system (Neville et al., 2014). Although FruM and FruCom differ in the N-terminal sex-specific domain, the shared C-terminal DNA binding domain may enable FruCom to regulate the same set of target genes as FruM. Our finding that Fru repressed the expression of En in the ovary supports this hypothesis. Lastly, FruCom may have a domain-negative role in inhibiting the function of female-specific BTB-ZnF transcription factors. *br*, *bab1*, *psq*, *btm,* and *trl* all belong to the *ttk* family of BTB-ZnF transcription factors and have been shown to regulate TF formation (Bartoletti et al., 2012; Couderc et al., 2002; Gancz et al., 2011). The BTB domains of *ttk* group interact with each other in yeast-two-hybrid assays (Bonchuk et al., 2011). Therefore, it is possible that Fru may form heterocomplex with female-specific BTB-ZnF proteins and inhibit their functions.

Fru functions in CySCs to regulate hub positioning

Genes required for hub formation manifest hub defects shortly after their loss of function (Tanentzapf et al., 2007; Voog et al., 2014). In contrast, we only observed mild hub defects in late pupal $fru^{\Delta B}$ testes and 1-week-old *fru* knockdown testes. These results suggest that *fru* does not play a key role in maintaining hub integrity. In Chapter 2, we found that Fru is not expressed when the hub forms during late embryonic stages. This result further suggests that *fru* is dispensable for hub formation.

The hub displacement phenotype caused by *fru* knockdown is similar to hub mispositioning phenotypes observed in testes with dysfunctional Integrin signaling (Lee et al., 2016; Schardt et al., 2015; Tanentzapf et al., 2007). However, loss of Integrin signaling components also causes a progressive reduction in hub cell number, which was not observed in *fru-RNAi* testes. While a hub shape abnormality was observed in *fru-RNAi* testes that were undergoing hub displacement, the displaced hubs retained normal hub morphology and had GSCs and CySCs properly attached. These results suggest that *fru* plays a role in the positioning of the hub rather than the maintenance of hub integrity. Indeed, we did not observe abnormal expression of adherens junction molecules such as FasIII and Arm in the hub (data not shown).

Furthermore, we found that hub displacement is caused by loss of *fru* in the CySCs. First, knockdown of *fru* in the hub failed to yield a hub phenotype. Second, knockdown of *fru* in the CySC lineage either with *c587-Gal4* or $dsx^{Gal4\Delta 2}$ caused hub elongation and displacement. How would *fru* function in CySCs to control hub positioning? It has been shown that loss of Lasp, a LIM and SH3 domain protein required for focal adhesion, in the CySC lineage causes similar displaced but functionally hubs (Lee et al., 2008). Knocking down βPS-integrin in CySC lineage also causes hub displacement (Lee et al., 2008). Therefore, *fru* may modulate integrin signaling and focal adhesion in CySCs to maintain proper positioning of the hub at the testis tip.

Cell-autonomous function of fru in CySC maintenance

We found that *fru* is required autonomously for CySC maintenance. At 2 days pci, testes with fru^{Sat15} and $fru^{\Delta B}$ CySC clones were observed at a much lower frequency than

control or $fru^{\Delta C}$ CySC clones. This data suggests that some *fru* mutant CySC clones were already lost by 2-day pci. It also indicates that *fruB* plays a more important role in the CySC than *fruC*. In Chapter 2 we found that loss of functional FruB causes a significant reduction in the total amount of Fru proteins. This may explain why $fru^{\Delta B}$ CySC clones were lost at a similar rate as fru^{Sat15} CySC clones. Interestingly, loss of FruMB affects almost all steps of courtship behaviors whereas FruMC is required for more specific steps of courtship behaviors (Neville et al., 2014; Nojima et al., 2014; von Philipsborn et al., 2014). Our finding reveals the similarity between the nervous system and the gonad in isoform-specific functions of Fru.

Our clonal analyses showed that *fru* mutant CySC clones were not lost through differentiation or apoptosis. The remaining possibility is that *fru* mutant CySC clones failed to adhere to the niche and were out-competed by other stem cells for niche occupancy. It has been shown that *fru* regulates the Slit-robo pathway and *robo1* is a direct target of FruMB in the CNS (Ito et al., 2016; Mellert et al., 2010). Interestingly, the Slit-Robo pathway also functions in the CySCs to modulate E-cadherin levels and control the ability of CySCs to compete for occupancy in the niche (Stine et al., 2014). The requirement of *fru* in CySCs for hub positioning also supports that *fru* modulates the adhesion between the CySCs and the hub. Rescuing *fru* mutant CySCs by increasing the E-cad level would be needed to test this hypothesis.

Fru function in cyst cell and germ cell survival

Several reports have demonstrated that *fruM* represses programmed cell death in the nervous system (Kimura et al., 2005; Rideout et al., 2007; Sanders and Arbeitman,

2008). It was further indicated that the cell death gene *reaper* is a putative target of FruM isoforms (Neville et al., 2014). Our finding that cyst cells mutant for *fru* undergo apoptosis suggests that *fruCom* is required for cyst cell survival likely through modulating programmed cell death. We further showed that *fru* is non-automonously required for the survival of trans-amplifying spermatogonia cysts. The mechanism by which loss of *fru* resulted in germ cell death may be similar to the nutrient-dependent elimination of trans-amplifying spermatogonia by encapsulated cyst cells (Chiang et al., 2017).

Fru function in cyst cell and germ cell differentiation

RNAi-mediated *fru* loss-of-function studies demonstrate that *fru* regulates cyst cell differentiation and indirectly controls germ cell differentiation rather than prevent CySC-to-follicle-stem-cell conversion. Analyses of cyst cell differentiation markers revealed that knockdown of *fru* impairs downregulation of Zfh-1 and Tj. Zfh-1functions downstream of the JAK/STAT pathway and is sufficient to maintain cyst cell and germ cell self-renewal outside the niche (Leatherman and Dinardo, 2008). Therefore, *fru* may modulate the JAK/STAT pathway to control proper differentiation of cyst cells and germ cells.

Apart from modulating signals that maintain the stemness, *fru* may also participate in signal pathways that promote differentiation. Egfr signaling is required in cyst cells for their proper differentiation and for the differentiation of the germline (Hudson et al., 2013; Tran et al., 2000). Egfr signaling components including *spitz*, *egfr*, *rho* and *stet* are putative Fru targets in the nervous system (Neville et al., 2014). FruCom may also modulate Egfr signaling in the cyst cell to promote cyst cell differentiation, and indirectly regulates spermatogenesis.

Conclusions

Through studying *fru* function in a non-neural setting, here we conclude that *fruCom* functions downstream of *dsx* to regulated the sexual development of the gonad stem cell niche and is required to maintain the homeostasis of the hub and the CySC lineage. We demonstrate that *fru* apart from its essential role in regulating sexual dimorphism of the nervous system, *fru* also play a role in the morphological branch of sexual dimorphism. Our findings indicate the similarity of Fru functions in the nervous system and in the gonad. This work will provide paradigm-shifting insight into the functions of *fru* in the sex determination hierarchy.

CHAPTER 5: CONCLUSIONS AND DISCUSSION

On the mechanism of Dsx regulation

How DsxF and DsxM regulate target gene expression is an important question that remains poorly addressed. Prior to our study, only few female-biased genes were identified as Dsx direct targets. It was therefore proposed that DsxF functions as a transcriptional activator and DsxM as a repressor. However, questions, such as whether DsxF could repress and DsxM could activate target gene expression and whether DsxF and DsxM always regulate gene expression in opposite directions, remained unaddressed. Our finding that DsxM activates *fru* expression and DsxF represses *fru* expression supports the existing model that DsxM and DsxF control gene expression in opposite directions. Our results that Dsx directly binds to the *fru* locus and that a canonical Dsx binding site is needed for robust transcription from the *fru* P4 promoter strongly suggest that *fru* is a direct target of Dsx. It further indicates that DsxM can activate gene expression in males and DsxF can repress gene expression in females. The mouse *dsx* orthology, DMRT1, has been shown to activate the expression of some genes and repress the expression of other genes (Murphy et al., 2010). Our study suggests that DsxF and DsxM also can positively and negatively regulate gene expression. The similarity between fly and mouse DMRTs as bifunctional transcriptional regulators demonstrates the evolutionary conservation of DMRTs. and implies that bifunctional transcriptional regulation may be a common feature of DMRTs.

While *dsx* is the most conserved component of the sex determination pathway, previous identified Dsx responsive elements are not highly conserved in other Drosophila species (Kopp et al., 2000; Luo and Baker, 2015), and the corresponding morphological traits are fast evolving in *Drosophila* species. Therefore, it remains unclear whether *dsx* controls conserved signaling pathways to create sexual dimorphism. Our identification of

the highly conserved Dsx responsive element upstream of *fru* P4 provides the first piece of evidence supporting the existence of conserved Dsx responsive elements and genes.

Discovery of a non-canonical sex determination pathway

Previously, it was assumed that Tra/Tra-2 mediated sex-specific alternative splicing is the only mechanism that generates sex-specific Fru expression, and that Fru proteins encoded by the nonP1 transcripts are expressed in both sexes. Here we demonstrate that a Dsx-dependent mechanism exists in *Drosophila* to control sex-specific transcription from the nonP1 promoters in both the CNS and the gonad (Figure 5.1). Notably, both the splicing and the transcriptional regulation mechanisms regulate male-specific Fru expression in the CNS. While *fruM* acts in parallel with *dsx* in the canonical sex determination pathway, *fruCom* is downstream of *dsx* in the non-canonical sex determination pathway.

Our discovery has important implications for studies of courtship behaviors controlled by *dsx* and *fru*. It has been known that while FruM is sufficient to induce courtship behaviors in female flies, loss of FruM fails to completely disrupt courtship behavior in male flies (Pan and Baker, 2014). Rather, *dsx* plays an important role in specifying a latent courtship circuitry that allows *fruM* mutant males to court (Pan and Baker, 2014; Rezaval et al., 2016). Our observation that FruCom is turned on by DsxM in the P1 neuron cluster of the XX CNS provides a potential explanation for how latent courtship behaviors is achieved in the absence of FruM. FruCom may function in a similar way as FruM in DsxM-expressing neurons to build the neural basis of courtship behaviors. Our work provides a direction for future studies of the mechanism whereby *dsx* promotes male-specific courtship behaviors.

Figure 5.1: The canonical and non-canonical sex determination pathways. The canonical sex determination pathway controls male-specific FruM expression in the CNS through sex-specific splicing of *fru* P1 transcripts. The non-canonical sex determination pathway controls male-specific Fru expression in the CNS and the gonad through transcriptional regulation by DsxM and DsxF. *fruP1* functions in parallel with *dsx* to control sexual dimorphism in courtship behavior. NonP1 *fru* functions downstream of *dsx* to regulate sexual dimorphism in courtship behavior and morphology.

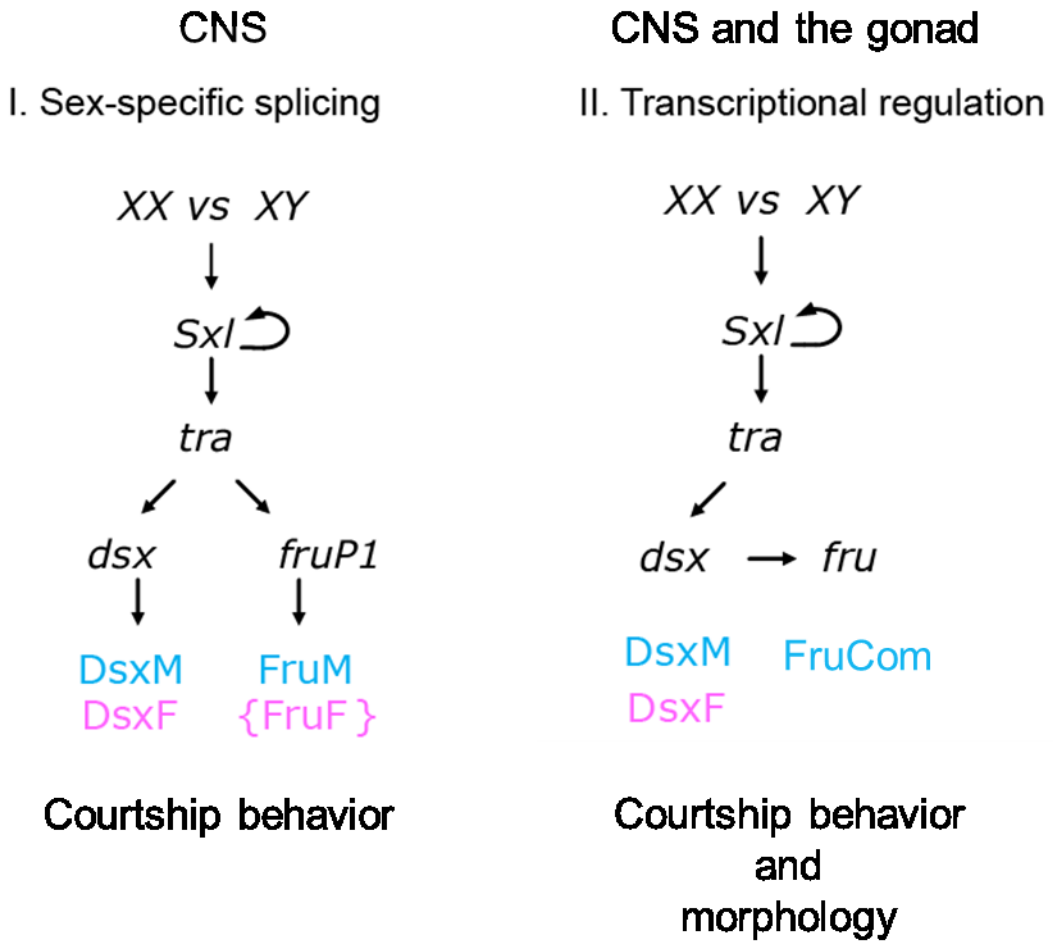

On the evolution of behavioral dimorphism

Proper gametogenesis and copulation are inseparable components of reproductive success. While sexual dimorphism of the gonad is controlled by DMRTs throughout the metazoan kingdom, it remains unclear whether courtship behaviors are controlled by an evolutionarily conserved mechanism. Despite that *fru* plays a central role in controlling courtship behaviors and is posited in parallel with *dsx* in the *Drosophila* sex determination pathway, *fru* homologs have not been identified outside of insect species. On the other hand, DMRTs control courtship behaviors in lower and higher species. In *C. elegans*, the *dsx* ortholog *mab-3* and the *dsx* homolog *dmd-3* control sex-specific responses to sex pheromones and male-specific copulation behaviors (Fagan et al., 2018; Serrano-Saiz et al., 2017). Mating behaviors in vertebrates are influenced by sex steroid hormone production from the gonad and are thus indirectly determined by *dsx* orthologs (Crews, 1984). Our finding that *fru* is downstream of *dsx* in the *Drosophila* sex determination pathway and the fact *dsx* acts as a fail-safe mechanism to maintain male-specific courtship behaviors imply that *dsx* plays an evolutionarily conserved role in regulating behavioral dimorphism in *Drosophila.*

We propose that the transcriptional regulation of *fru* by *dsx* represents the more ancient version of the sex determination pathway. When Tra-binding sites or similar elements were inserted at the P1 splicing site, the male-specific Fru expression became controlled directly by the upstream sex-determining gene and independent of *dsx*. This event would shift *fru* from a *dsx* target gene to a parallel actuator of the sex determination pathway. Studies of *fru* gene structures in distantly related Dipteran species and species of other orders indicate that this model might be what happened. In two Hawaiian picture-

winged group of subgenus *Drosophila*, the *fru* orthologues lack the P1 promoter (Davis et al., 2000a; Davis et al., 2000b). Furthermore, northern blot analysis on adult *D. heteroneura* revealed that nonP1 *fru* transcripts are expressed male-specifically (Davis et al., 2000a). In *Anopheles gambieae*, which separated from *D. melanogaster* ~250 Myr ago, 2 additional putative Tra/Tra-2 binding sites were identified near the regulated splice site of *AngfruF*, whereas the copy number of putative Tra/Tra-2 binding sites in the *Agdsx* gene decreased from 6 to 3 (Gailey et al., 2006; Hedley and Maniatis, 1991; Heinrichs et al., 1998). In the hymenopteran *Nasonia vitripensis*, sex-specific promoters (P0-P1), as well as non-sex-specific alternative promoters (P2-P6), are structured in a similar pattern as *D. melanogaster fru*. However, novel sequence repeats rather than Tra/Tra2 binding sites were found near the sex-specific splicing sites of *Nvitdsx and Nvitfru* (Bertossa et al., 2009). In orthopteran insects, including various grasshoppers, the desert locust *Schistocerca gregaria*, and the cockroach *Blatella germanica*, *fru* orthologues still have alternative transcription start sites, but only generate non-sex-specific mRNAs that resemble transcripts produced from P4 of *D. melanogaster* (Boerjan et al., 2012; Clynen et al., 2011; Ustinova and Mayer, 2006). Despite lacking sex-specific alternative splicing, *fru* orthologues play important roles in males to control courtship behaviors and copulation success (Boerjan et al., 2012; Clynen et al., 2011). This body of evidence suggests that sex-specific splicing of *fru* P1 is a newly evolved mechanism that controls male-specific Fru expression. It also suggests that the *fru* P4 promoters is highly conserved through evolution and may be responsible for courtship behaviors in insect species where *fru* is not alternatively spliced. The evolutionarily conserved Dsx binding site we identified upstream

of the P4 promoter further suggests that transcriptional regulation by *dsx* may serve as the ancient mechanism to generate sex-specific Fru expression.

It has been proposed that the upstream components of the sex determination hierarchy are less conserved than the downstream components. Changes in the *cis*-elements that control sex-specific alternative splicing of *fru* support that *fru* is more ancient than *tra* in the sex determination hierarchy. Moreover, the different rates of evolution between the sex-specific P1 promoter and nonP1 promoters suggest that *fruCom* is more conserved than *fruM* in the sex determination hierarchy. Our model of the *Drosophila* sex determination pathway highlights *dsx* as the core gene that controls behavioral dimorphism throughout the metazoan kingdom and shed light on how *fru* evolves into the specialized regulator of behavioral dimorphism in insect species.

Isoform-specific Fru functions

It has been implied that FruCom functions cannot be replaced by FruM during embryonic CNS development (Song et al., 2002a). Our finding that ectopic expression of FruCom but not FruM masculinizes the ovary further confirms the functional difference between these isoforms. It further suggests that the neural-specific peptide plays an important yet elusive role in modulating Fru function.

The functional difference between FruM and FruCom is reflected by the different evolutionary constraints on *fru* isoforms. Loss of *fruCom* causes defective imaginal disc development and pupal lethality, likely allowing *fruCom* promoters to be retained during evolution. In contrast, *fruM* seems to be dispensable. The Muscle of Lawrence, which is controlled specifically by *fruMC*, has been lost several times during the speciation of

Drosophila (Gailey et al., 1997). In Hawaiian *Drosophila* species, the absence of *fruM* and the emerging of male-male aggression behaviors, typical of *fruM* mutant phenotype in *D.* melanogaster, further suggest that aberrant courtship behaviors caused by loss of P1 can be the origin of new courtship behaviors. Further investigation into *fruCom* functions in non-neural tissues is needed to better assess the importance of *fru* in courtship behaviors versus morphogenesis.

BTB-ZnF transcription factors coordinating gonad and CNS development

The *ttk* family of BTB-C2H2 ZnF transcription factors comprises an important class of molecules that involves in development and carcinogenesis. However, they are often implicated in various functions and processes that seem unrelated. From investigating the functions and regulation of *fru*, we have revealed some striking similarities among BTB-ZnF transcription factors that may help understand the logic underlying the miscellaneous biological processes they regulate.

First, BTB-ZnF transcription factors are required for both the development of the nervous system and gonad. *chinmo*, *longitudinals lacking* (*lola*), and *fru* were initially discovered and named after their mutant phenotypes in the nervous system, and later found to play important roles in the male gonad. *chinmo* is a key effector of the JAK/STAT pathway that maintains the CySC fate (Flaherty et al., 2010). *lola* is required in the somatic gonadal precursors for the formation of embryonic gonad and for the maintenance of the CySC fate in adult testes (Davies et al., 2013; Weyers et al., 2011). Our study demonstrates that *fru* is also required for the maintenance of the CySC fate. Another member of this family, *ken*, is also highly expressed in the CNS and is required for maintenance of the

CySC fate (Issigonis and Matunis, 2012). On the other hand, a subgroup of this family, including *bab*, *psq*, *trl* and *broad,* has a female-biased expression in the gonad and are known to promote TF development besides their functions in the nervous system.

Second, BTB-ZnF transcription factors are implicated in signaling pathways that modulate cell self-renewal and differentiation. Notch and Egfr signaling pathways control a wide variety of cell fate decisions and are involved in the regulation of gonad stem cell niche development. Testis-specific BTB-ZnF proteins, including *fru*, *chinmo*, *ken*, *ab,* and *lola*, were identified as potential downstream targets of Notch and Egfr signaling (Djiane et al., 2013; Doggett et al., 2015). The hub displacement phenotype and delayed cyst cell differentiation phenotype caused by knockdown of *fru* in the testis is consistent with disrupted Notch and Egfr signaling.

Third, BTB-ZnF transcription factors are involved in the sex determination pathway. *bab1* has been previously characterized as a Dsx direct target and plays a female-specific role in the development of TFs. In this study, we demonstrate that *fru* is also a direct target of Dsx and is a masculinizing factor that helps to maintain the hub fate. It was recently shown that *chinmo* also plays a male-specific role in maintaining the CySC fate and preventing CySC-to-follicle-stem-cell transdifferentiation (Ma et al., 2014). *lola* also exhibits sexually-dimorphic expression patterns in the CNS (Neville et al., 2014). Our genomic analyses of *dsx* putative targets further indicate that members of the *ttk* family of BTB-ZnF transcription factors are among Dsx putative target genes.

Based on all the above observations, we propose that the conserved BTB-ZnF transcription factors function downstream of signal pathways crucial to gonad and CNS

development. By controlling the sex-specific expression of BTB-ZnF transcriptional factors, *dsx* fine-tunes developmental processes to create sexual dimorphism.

Conclusions

This work reveals a non-canonical sex determination pathway where *fru* functions downstream of *dsx* to regulate sexual dimorphism of the gonad stem cell niche. It highlights the interaction between the two effectors of the sex determination pathway in ensuring the robustness of developmental programs that create sexual dimorphism. This research will provide insight into how the sex determination pathway evolves to maintain the key characteristics while generating diversity at the same time.

REFERENCES

Ahmad, S.M., and Baker, B.S. (2002). Sex-specific deployment of FGF signaling in Drosophila recruits mesodermal cells into the male genital imaginal disc. Cell *109*, 651-661.

Anand, A., Villella, A., Ryner, L.C., Carlo, T., Goodwin, S.F., Song, H.J., Gailey, D.A., Morales, A., Hall, J.C., Baker, B.S.*, et al.* (2001). Molecular genetic dissection of the sex-specific and vital functions of the Drosophila melanogaster sex determination gene fruitless. Genetics *158*, 1569-1595.

Asaoka, M., and Lin, H. (2004). Germline stem cells in the Drosophila ovary descend from pole cells in the anterior region of the embryonic gonad. Development *131*, 5079-5089.

Bartoletti, M., Rubin, T., Chalvet, F., Netter, S., Dos Santos, N., Poisot, E., Paces-Fessy, M., Cumenal, D., Peronnet, F., Pret, A.M.*, et al.* (2012). Genetic basis for developmental homeostasis of germline stem cell niche number: a network of Tramtrack-Group nuclear BTB factors. PLoS One *7*, e49958.

Bertossa, R.C., van de Zande, L., and Beukeboom, L.W. (2009). The Fruitless gene in Nasonia displays complex sex-specific splicing and contains new zinc finger domains. Mol Biol Evol *26*, 1557-1569.

Billeter, J.C., and Goodwin, S.F. (2004). Characterization of Drosophila fruitless-gal4 transgenes reveals expression in male-specific fruitless neurons and innervation of male reproductive structures. J Comp Neurol *475*, 270-287.

Billeter, J.C., Villella, A., Allendorfer, J.B., Dornan, A.J., Richardson, M., Gailey, D.A., and Goodwin, S.F. (2006). Isoform-specific control of male neuronal differentiation and behavior in Drosophila by the fruitless gene. Curr Biol *16*, 1063-1076.

Boerjan, B., Tobback, J., Vandersmissen, H.P., Huybrechts, R., and Schoofs, L. (2012). Fruitless RNAi knockdown in the desert locust, Schistocerca gregaria, influences male fertility. J Insect Physiol *58*, 265-269.

Bolivar, J., Pearson, J., Lopez-Onieva, L., and Gonzalez-Reyes, A. (2006). Genetic dissection of a stem cell niche: the case of the Drosophila ovary. Dev Dyn *235*, 2969-2979.

Bonchuk, A., Denisov, S., Georgiev, P., and Maksimenko, O. (2011). Drosophila BTB/POZ domains of "ttk group" can form multimers and selectively interact with each other. J Mol Biol *412*, 423-436.

Borensztejn, A., Boissoneau, E., Fernandez, G., Agnes, F., and Pret, A.M. (2013). JAK/STAT autocontrol of ligand-producing cell number through apoptosis. Development *140*, 195-204.

Burtis, K.C., and Baker, B.S. (1989). Drosophila doublesex gene controls somatic sexual differentiation by producing alternatively spliced mRNAs encoding related sex-specific polypeptides. Cell *56*, 997-1010.

Burtis, K.C., Coschigano, K.T., Baker, B.S., and Wensink, P.C. (1991). The doublesex proteins of Drosophila melanogaster bind directly to a sex-specific yolk protein gene enhancer. EMBO J *10*, 2577-2582.

Camara, N., and Van Doren, M. (submitted). The creation of sexual dimorphism in Drosophila gonad stem cell niches.

Casper, A.L., and Van Doren, M. (2009). The establishment of sexual identity in the Drosophila germline. Development *136*, 3821-3830.
Chang, Y.C., Jang, A.C., Lin, C.H., and Montell, D.J. (2013). Castor is required for Hedgehog-dependent cell-fate specification and follicle stem cell maintenance in Drosophila oogenesis. Proc Natl Acad Sci U S A *110*, E1734-1742.
Chen, J., Godt, D., Gunsalus, K., Kiss, I., Goldberg, M., and Laski, F.A. (2001). Cofilin/ADF is required for cell motility during Drosophila ovary development and oogenesis. Nat Cell Biol *3*, 204-209.
Chiang, A.C., Yang, H., and Yamashita, Y.M. (2017). spict, a cyst cell-specific gene, regulates starvation-induced spermatogonial cell death in the Drosophila testis. Sci Rep *7*, 40245.
Chong, T., Collins, J.J., 3rd, Brubacher, J.L., Zarkower, D., and Newmark, P.A. (2013). A sex-specific transcription factor controls male identity in a simultaneous hermaphrodite. Nat Commun *4*, 1814.
Cline, T.W., and Meyer, B.J. (1996). Vive la difference: males vs females in flies vs worms. Annu Rev Genet *30*, 637-702.
Clough, E., Jimenez, E., Kim, Y.A., Whitworth, C., Neville, M.C., Hempel, L.U., Pavlou, H.J., Chen, Z.X., Sturgill, D., Dale, R.K., *et al.* (2014). Sex- and tissue-specific functions of Drosophila doublesex transcription factor target genes. Dev Cell *31*, 761-773.
Clynen, E., Ciudad, L., Belles, X., and Piulachs, M.D. (2011). Conservation of fruitless' role as master regulator of male courtship behaviour from cockroaches to flies. Dev Genes Evol *221*, 43-48.
Cohen, E.D., Mariol, M.C., Wallace, R.M., Weyers, J., Kamberov, Y.G., Pradel, J., and Wilder, E.L. (2002). DWnt4 regulates cell movement and focal adhesion kinase during Drosophila ovarian morphogenesis. Dev Cell *2*, 437-448.
Couderc, J.L., Godt, D., Zollman, S., Chen, J., Li, M., Tiong, S., Cramton, S.E., Sahut-Barnola, I., and Laski, F.A. (2002). The bric a brac locus consists of two paralogous genes encoding BTB/POZ domain proteins and acts as a homeotic and morphogenetic regulator of imaginal development in Drosophila. Development *129*, 2419-2433.
Crews, D. (1984). Gamete production, sex hormone secretion, and mating behavior uncoupled. Horm Behav *18*, 22-28.
Dalton, J.E., Fear, J.M., Knott, S., Baker, B.S., McIntyre, L.M., and Arbeitman, M.N. (2013). Male-specific Fruitless isoforms have different regulatory roles conferred by distinct zinc finger DNA binding domains. BMC Genomics *14*, 659.
Dalton, J.E., Lebo, M.S., Sanders, L.E., Sun, F., and Arbeitman, M.N. (2009). Ecdysone receptor acts in fruitless- expressing neurons to mediate drosophila courtship behaviors. Curr Biol *19*, 1447-1452.
Davies, E.L., Lim, J.G., Joo, W.J., Tam, C.H., and Fuller, M.T. (2013). The transcriptional regulator lola is required for stem cell maintenance and germ cell differentiation in the Drosophila testis. Dev Biol *373*, 310-321.
Davis, T., Kurihara, J., and Yamamoto, D. (2000a). Genomic organisation and characterisation of the neural sex-determination gene fruitless (fru) in the Hawaiian species Drosophila heteroneura. Gene *246*, 143-149.
Davis, T., Kurihara, J., Yoshino, E., and Yamamoto, D. (2000b). Genomic organisation of the neural sex determination gene fruitless (fru) in the Hawaiian species

Drosophila silvestris and the conservation of the fru BTB protein-protein-binding domain throughout evolution. Hereditas *132*, 67-78.
DeFalco, T., Camara, N., Le Bras, S., and Van Doren, M. (2008). Nonautonomous sex determination controls sexually dimorphic development of the Drosophila gonad. Dev Cell *14*, 275-286.
DeFalco, T.J., Verney, G., Jenkins, A.B., McCaffery, J.M., Russell, S., and Van Doren, M. (2003). Sex-specific apoptosis regulates sexual dimorphism in the Drosophila embryonic gonad. Dev Cell *5*, 205-216.
Demir, E., and Dickson, B.J. (2005). fruitless splicing specifies male courtship behavior in Drosophila. Cell *121*, 785-794.
Dinardo, S., Okegbe, T., Wingert, L., Freilich, S., and Terry, N. (2011). lines and bowl affect the specification of cyst stem cells and niche cells in the Drosophila testis. Development *138*, 1687-1696.
Djiane, A., Krejci, A., Bernard, F., Fexova, S., Millen, K., and Bray, S.J. (2013). Dissecting the mechanisms of Notch induced hyperplasia. EMBO J *32*, 60-71.
Doggett, K., Turkel, N., Willoughby, L.F., Ellul, J., Murray, M.J., Richardson, H.E., and Brumby, A.M. (2015). BTB-Zinc Finger Oncogenes Are Required for Ras and Notch-Driven Tumorigenesis in Drosophila. PLoS One *10*, e0132987.
Dornan, A.J., Gailey, D.A., and Goodwin, S.F. (2005). GAL4 enhancer trap targeting of the Drosophila sex determination gene fruitless. Genesis *42*, 236-246.
Erdman, S.E., and Burtis, K.C. (1993). The Drosophila doublesex proteins share a novel zinc finger related DNA binding domain. EMBO J *12*, 527-535.
Erdman, S.E., Chen, H.J., and Burtis, K.C. (1996). Functional and genetic characterization of the oligomerization and DNA binding properties of the Drosophila doublesex proteins. Genetics *144*, 1639-1652.
Erickson, J.W., and Quintero, J.J. (2007). Indirect effects of ploidy suggest X chromosome dose, not the X:A ratio, signals sex in Drosophila. PLoS Biol *5*, e332.
Evans, C.J., Olson, J.M., Ngo, K.T., Kim, E., Lee, N.E., Kuoy, E., Patananan, A.N., Sitz, D., Tran, P., Do, M.T.*, et al.* (2009). G-TRACE: rapid Gal4-based cell lineage analysis in Drosophila. Nat Methods *6*, 603-605.
Fagan, K.A., Luo, J., Lagoy, R.C., Schroeder, F.C., Albrecht, D.R., and Portman, D.S. (2018). A Single-Neuron Chemosensory Switch Determines the Valence of a Sexually Dimorphic Sensory Behavior. Curr Biol *28*, 902-914 e905.
Flaherty, M.S., Salis, P., Evans, C.J., Ekas, L.A., Marouf, A., Zavadil, J., Banerjee, U., and Bach, E.A. (2010). chinmo is a functional effector of the JAK/STAT pathway that regulates eye development, tumor formation, and stem cell self-renewal in Drosophila. Dev Cell *18*, 556-568.
Foronda, D., Martin, P., and Sanchez-Herrero, E. (2012). Drosophila Hox and sex-determination genes control segment elimination through EGFR and extramacrochetae activity. PLoS Genet *8*, e1002874.
Fuller, M.T., and Spradling, A.C. (2007). Male and female Drosophila germline stem cells: two versions of immortality. Science *316*, 402-404.
Gailey, D.A., Billeter, J.C., Liu, J.H., Bauzon, F., Allendorfer, J.B., and Goodwin, S.F. (2006). Functional conservation of the fruitless male sex-determination gene across 250 Myr of insect evolution. Mol Biol Evol *23*, 633-643.

Gailey, D.A., and Hall, J.C. (1989). Behavior and cytogenetics of fruitless in Drosophila melanogaster: different courtship defects caused by separate, closely linked lesions. Genetics *121*, 773-785.
Gailey, D.A., Ohshima, S., Santiago, S.J., Montez, J.M., Arellano, A.R., Robillo, J., Villarimo, C.A., Roberts, L., Fine, E., Villella, A.*, et al.* (1997). The muscle of lawrence in Drosophila: a case of repeated evolutionary loss. Proc Natl Acad Sci U S A *94*, 4543-4547.
Gailey, D.A., Taylor, B.J., and Hall, J.C. (1991). Elements of the fruitless locus regulate development of the muscle of Lawrence, a male-specific structure in the abdomen of Drosophila melanogaster adults. Development *113*, 879-890.
Gancz, D., Lengil, T., and Gilboa, L. (2011). Coordinated regulation of niche and stem cell precursors by hormonal signaling. PLoS Biol *9*, e1001202.
Ganter, G.K., Desilets, J.B., Davis-Knowlton, J.A., Panaitiu, A.E., Sweezy, M., Sungail, J., Tan, L.C., Adams, A.M., Fisher, E.A., O'Brien, J.R.*, et al.* (2012). Drosophila female precopulatory behavior is modulated by ecdysteroids. J Insect Physiol *58*, 413-419.
Garner, S.R.C., Castellanos, M.C., Baillie, K.E., Lian, T., and Allan, D.W. (2018). Drosophila female-specific Ilp7 motoneurons are generated by Fruitless-dependent cell death in males and by a double-assurance survival role for Transformer in females. Development *145*.
Garrett-Engele, C.M., Siegal, M.L., Manoli, D.S., Williams, B.C., Li, H., and Baker, B.S. (2002). intersex, a gene required for female sexual development in Drosophila, is expressed in both sexes and functions together with doublesex to regulate terminal differentiation. Development *129*, 4661-4675.
Gilboa, L., and Lehmann, R. (2004). Repression of primordial germ cell differentiation parallels germ line stem cell maintenance. Curr Biol *14*, 981-986.
Godt, D., and Laski, F.A. (1995). Mechanisms of cell rearrangement and cell recruitment in Drosophila ovary morphogenesis and the requirement of bric a brac. Development *121*, 173-187.
Gonczy, P., Matunis, E., and DiNardo, S. (1997). bag-of-marbles and benign gonial cell neoplasm act in the germline to restrict proliferation during Drosophila spermatogenesis. Development *124*, 4361-4371.
Gonczy, P., Viswanathan, S., and DiNardo, S. (1992). Probing spermatogenesis in Drosophila with P-element enhancer detectors. Development *114*, 89-98.
Hedley, M.L., and Maniatis, T. (1991). Sex-specific splicing and polyadenylation of dsx pre-mRNA requires a sequence that binds specifically to tra-2 protein in vitro. Cell *65*, 579-586.
Heinrichs, V., Ryner, L.C., and Baker, B.S. (1998). Regulation of sex-specific selection of fruitless 5' splice sites by transformer and transformer-2. Mol Cell Biol *18*, 450-458.
Hempel, L.U., and Oliver, B. (2007). Sex-specific DoublesexM expression in subsets of Drosophila somatic gonad cells. BMC Dev Biol *7*, 113.
Hodin, J., and Riddiford, L.M. (1998). The ecdysone receptor and ultraspiracle regulate the timing and progression of ovarian morphogenesis during Drosophila metamorphosis. Dev Genes Evol *208*, 304-317.

Hsu, H.J., and Drummond-Barbosa, D. (2009). Insulin levels control female germline stem cell maintenance via the niche in Drosophila. Proc Natl Acad Sci U S A *106*, 1117-1121.
Hsu, H.J., and Drummond-Barbosa, D. (2011). Insulin signals control the competence of the Drosophila female germline stem cell niche to respond to Notch ligands. Dev Biol *350*, 290-300.
Hudry, B., Khadayate, S., and Miguel-Aliaga, I. (2016). The sexual identity of adult intestinal stem cells controls organ size and plasticity. Nature *530*, 344-348.
Hudson, A.G., Parrott, B.B., Qian, Y., and Schulz, C. (2013). A temporal signature of epidermal growth factor signaling regulates the differentiation of germline cells in testes of Drosophila melanogaster. PLoS One *8*, e70678.
Issigonis, M., and Matunis, E. (2012). The Drosophila BCL6 homolog Ken and Barbie promotes somatic stem cell self-renewal in the testis niche. Dev Biol *368*, 181-192.
Ito, H., Fujitani, K., Usui, K., Shimizu-Nishikawa, K., Tanaka, S., and Yamamoto, D. (1996). Sexual orientation in Drosophila is altered by the satori mutation in the sex-determination gene fruitless that encodes a zinc finger protein with a BTB domain. Proc Natl Acad Sci U S A *93*, 9687-9692.
Ito, H., Sato, K., Koganezawa, M., Ote, M., Matsumoto, K., Hama, C., and Yamamoto, D. (2012). Fruitless recruits two antagonistic chromatin factors to establish single-neuron sexual dimorphism. Cell *149*, 1327-1338.
Ito, H., Sato, K., Kondo, S., Ueda, R., and Yamamoto, D. (2016). Fruitless Represses robo1 Transcription to Shape Male-Specific Neural Morphology and Behavior in Drosophila. Curr Biol *26*, 1532-1542.
Kato, Y., Perez, C.A.G., Mohamad Ishak, N.S., Nong, Q.D., Sudo, Y., Matsuura, T., Wada, T., and Watanabe, H. (2018). A 5' UTR-Overlapping LncRNA Activates the Male-Determining Gene doublesex1 in the Crustacean Daphnia magna. Curr Biol *28*, 1811-1817 e1814.
Kawase, E., Wong, M.D., Ding, B.C., and Xie, T. (2004). Gbb/Bmp signaling is essential for maintaining germline stem cells and for repressing bam transcription in the Drosophila testis. Development *131*, 1365-1375.
Kiger, A.A., Jones, D.L., Schulz, C., Rogers, M.B., and Fuller, M.T. (2001). Stem cell self-renewal specified by JAK-STAT activation in response to a support cell cue. Science *294*, 2542-2545.
Kimura, K., Ote, M., Tazawa, T., and Yamamoto, D. (2005). Fruitless specifies sexually dimorphic neural circuitry in the Drosophila brain. Nature *438*, 229-233.
King, R.C. (1970). Ovarian development in Drosophila melanogaster (New York,: Academic Press).
Kitadate, Y., and Kobayashi, S. (2010). Notch and Egfr signaling act antagonistically to regulate germ-line stem cell niche formation in Drosophila male embryonic gonads. Proc Natl Acad Sci U S A *107*, 14241-14246.
Kitadate, Y., Shigenobu, S., Arita, K., and Kobayashi, S. (2007). Boss/Sev signaling from germline to soma restricts germline-stem-cell-niche formation in the anterior region of Drosophila male gonads. Dev Cell *13*, 151-159.
Kiuchi, T., Koga, H., Kawamoto, M., Shoji, K., Sakai, H., Arai, Y., Ishihara, G., Kawaoka, S., Sugano, S., Shimada, T.*, et al.* (2014). A single female-specific piRNA is the primary determiner of sex in the silkworm. Nature *509*, 633-636.

Koganezawa, M., Kimura, K., and Yamamoto, D. (2016). The Neural Circuitry that Functions as a Switch for Courtship versus Aggression in Drosophila Males. Curr Biol *26*, 1395-1403.
Kopp, A., Duncan, I., Godt, D., and Carroll, S.B. (2000). Genetic control and evolution of sexually dimorphic characters in Drosophila. Nature *408*, 553-559.
Lai, C.M., Lin, K.Y., Kao, S.H., Chen, Y.N., Huang, F., and Hsu, H.J. (2017). Hedgehog signaling establishes precursors for germline stem cell niches by regulating cell adhesion. J Cell Biol *216*, 1439-1453.
Lambeth, L.S., Raymond, C.S., Roeszler, K.N., Kuroiwa, A., Nakata, T., Zarkower, D., and Smith, C.A. (2014). Over-expression of DMRT1 induces the male pathway in embryonic chicken gonads. Dev Biol *389*, 160-172.
Le Bras, S., and Van Doren, M. (2006). Development of the male germline stem cell niche in Drosophila. Dev Biol *294*, 92-103.
Leatherman, J.L., and Dinardo, S. (2008). Zfh-1 controls somatic stem cell self-renewal in the Drosophila testis and nonautonomously influences germline stem cell self-renewal. Cell Stem Cell *3*, 44-54.
Lee, G., Foss, M., Goodwin, S.F., Carlo, T., Taylor, B.J., and Hall, J.C. (2000). Spatial, temporal, and sexually dimorphic expression patterns of the fruitless gene in the Drosophila central nervous system. J Neurobiol *43*, 404-426.
Lee, G., Hall, J.C., and Park, J.H. (2002). Doublesex gene expression in the central nervous system of Drosophila melanogaster. J Neurogenet *16*, 229-248.
Lee, J.Y., Chen, J.Y., Shaw, J.L., and Chang, K.T. (2016). Maintenance of Stem Cell Niche Integrity by a Novel Activator of Integrin Signaling. PLoS Genet *12*, e1006043.
Lee, S., Zhou, L., Kim, J., Kalbfleisch, S., and Schock, F. (2008). Lasp anchors the Drosophila male stem cell niche and mediates spermatid individualization. Mech Dev *125*, 768-776.
Lee, T., and Luo, L. (1999). Mosaic analysis with a repressible cell marker for studies of gene function in neuronal morphogenesis. Neuron *22*, 451-461.
Lei, N., Karpova, T., Hornbaker, K.I., Rice, D.A., and Heckert, L.L. (2009). Distinct transcriptional mechanisms direct expression of the rat Dmrt1 promoter in sertoli cells and germ cells of transgenic mice. Biol Reprod *81*, 118-125.
Lindeman, R.E., Gearhart, M.D., Minkina, A., Krentz, A.D., Bardwell, V.J., and Zarkower, D. (2015). Sexual cell-fate reprogramming in the ovary by DMRT1. Curr Biol *25*, 764-771.
Luo, S.D., and Baker, B.S. (2015). Constraints on the evolution of a doublesex target gene arising from doublesex's pleiotropic deployment. Proc Natl Acad Sci U S A *112*, E852-861.
Luo, S.D., Shi, G.W., and Baker, B.S. (2011). Direct targets of the D. melanogaster DSXF protein and the evolution of sexual development. Development *138*, 2761-2771.
Ma, Q., Wawersik, M., and Matunis, E.L. (2014). The Jak-STAT target Chinmo prevents sex transformation of adult stem cells in the Drosophila testis niche. Dev Cell *31*, 474-486.
Mathews, K.W., Cavegn, M., and Zwicky, M. (2017). Sexual Dimorphism of Body Size Is Controlled by Dosage of the X-Chromosomal Gene Myc and by the Sex-Determining Gene tra in Drosophila. Genetics *205*, 1215-1228.

Matsuda, M., Nagahama, Y., Shinomiya, A., Sato, T., Matsuda, C., Kobayashi, T., Morrey, C.E., Shibata, N., Asakawa, S., Shimizu, N.*, et al.* (2002). DMY is a Y-specific DM-domain gene required for male development in the medaka fish. Nature *417*, 559-563.
McKeown, M., Belote, J.M., and Baker, B.S. (1987). A molecular analysis of transformer, a gene in Drosophila melanogaster that controls female sexual differentiation. Cell *48*, 489-499.
McKeown, M., Belote, J.M., and Boggs, R.T. (1988). Ectopic expression of the female transformer gene product leads to female differentiation of chromosomally male Drosophila. Cell *53*, 887-895.
Mellert, D.J., Knapp, J.M., Manoli, D.S., Meissner, G.W., and Baker, B.S. (2010). Midline crossing by gustatory receptor neuron axons is regulated by fruitless, doublesex and the Roundabout receptors. Development *137*, 323-332.
Morris, L.X., and Spradling, A.C. (2011). Long-term live imaging provides new insight into stem cell regulation and germline-soma coordination in the Drosophila ovary. Development *138*, 2207-2215.
Murphy, M.W., Sarver, A.L., Rice, D., Hatzi, K., Ye, K., Melnick, A., Heckert, L.L., Zarkower, D., and Bardwell, V.J. (2010). Genome-wide analysis of DNA binding and transcriptional regulation by the mammalian Doublesex homolog DMRT1 in the juvenile testis. Proc Natl Acad Sci U S A *107*, 13360-13365.
Murphy, M.W., Zarkower, D., and Bardwell, V.J. (2007). Vertebrate DM domain proteins bind similar DNA sequences and can heterodimerize on DNA. BMC Mol Biol *8*, 58.
Nagoshi, R.N., and Baker, B.S. (1990). Regulation of sex-specific RNA splicing at the Drosophila doublesex gene: cis-acting mutations in exon sequences alter sex-specific RNA splicing patterns. Genes Dev *4*, 89-97.
Nanda, S., DeFalco, T.J., Loh, S.H., Phochanukul, N., Camara, N., Van Doren, M., and Russell, S. (2009). Sox100B, a Drosophila group E Sox-domain gene, is required for somatic testis differentiation. Sex Dev *3*, 26-37.
Neville, M.C., Nojima, T., Ashley, E., Parker, D.J., Walker, J., Southall, T., Van de Sande, B., Marques, A.C., Fischer, B., Brand, A.H.*, et al.* (2014). Male-specific fruitless isoforms target neurodevelopmental genes to specify a sexually dimorphic nervous system. Curr Biol *24*, 229-241.
Nojima, T., Neville, M.C., and Goodwin, S.F. (2014). Fruitless isoforms and target genes specify the sexually dimorphic nervous system underlying Drosophila reproductive behavior. Fly (Austin) *8*, 95-100.
Ottolenghi, C., and McElreavey, K. (2000). Deletions of 9p and the quest for a conserved mechanism of sex determination. Mol Genet Metab *71*, 397-404.
Pan, Y., and Baker, B.S. (2014). Genetic identification and separation of innate and experience-dependent courtship behaviors in Drosophila. Cell *156*, 236-248.
Pan, Y., Meissner, G.W., and Baker, B.S. (2012). Joint control of Drosophila male courtship behavior by motion cues and activation of male-specific P1 neurons. Proc Natl Acad Sci U S A *109*, 10065-10070.
Panchal, T., Chen, X., Alchits, E., Oh, Y., Poon, J., Kouptsova, J., Laski, F.A., and Godt, D. (2017). Specification and spatial arrangement of cells in the germline stem cell niche

of the Drosophila ovary depend on the Maf transcription factor Traffic jam. PLoS Genet *13*, e1006790.
Pfeiffer, B.D., Jenett, A., Hammonds, A.S., Ngo, T.T., Misra, S., Murphy, C., Scully, A., Carlson, J.W., Wan, K.H., Laverty, T.R., *et al.* (2008). Tools for neuroanatomy and neurogenetics in Drosophila. Proc Natl Acad Sci U S A *105*, 9715-9720.
Raymond, C.S., Kettlewell, J.R., Hirsch, B., Bardwell, V.J., and Zarkower, D. (1999). Expression of Dmrt1 in the genital ridge of mouse and chicken embryos suggests a role in vertebrate sexual development. Dev Biol *215*, 208-220.
Reilein, A., Melamed, D., Park, K.S., Berg, A., Cimetta, E., Tandon, N., Vunjak-Novakovic, G., Finkelstein, S., and Kalderon, D. (2017). Alternative direct stem cell derivatives defined by stem cell location and graded Wnt signalling. Nat Cell Biol *19*, 433-444.
Rezaval, C., Pattnaik, S., Pavlou, H.J., Nojima, T., Bruggemeier, B., D'Souza, L.A.D., Dweck, H.K.M., and Goodwin, S.F. (2016). Activation of Latent Courtship Circuitry in the Brain of Drosophila Females Induces Male-like Behaviors. Curr Biol *26*, 2508-2515.
Rideout, E.J., Billeter, J.C., and Goodwin, S.F. (2007). The sex-determination genes fruitless and doublesex specify a neural substrate required for courtship song. Curr Biol *17*, 1473-1478.
Rideout, E.J., Dornan, A.J., Neville, M.C., Eadie, S., and Goodwin, S.F. (2010). Control of sexual differentiation and behavior by the doublesex gene in Drosophila melanogaster. Nat Neurosci *13*, 458-466.
Rideout, E.J., Narsaiya, M.S., and Grewal, S.S. (2015). The Sex Determination Gene transformer Regulates Male-Female Differences in Drosophila Body Size. PLoS Genet *11*, e1005683.
Robinett, C.C., Vaughan, A.G., Knapp, J.M., and Baker, B.S. (2010). Sex and the single cell. II. There is a time and place for sex. PLoS Biol *8*, e1000365.
Ryner, L.C., Goodwin, S.F., Castrillon, D.H., Anand, A., Villella, A., Baker, B.S., Hall, J.C., Taylor, B.J., and Wasserman, S.A. (1996). Control of male sexual behavior and sexual orientation in Drosophila by the fruitless gene. Cell *87*, 1079-1089.
Sahai-Hernandez, P., and Nystul, T.G. (2013). A dynamic population of stromal cells contributes to the follicle stem cell niche in the Drosophila ovary. Development *140*, 4490-4498.
Sahut-Barnola, I., Godt, D., Laski, F.A., and Couderc, J.L. (1995). Drosophila ovary morphogenesis: analysis of terminal filament formation and identification of a gene required for this process. Dev Biol *170*, 127-135.
Salz, H.K., and Erickson, J.W. (2010). Sex determination in Drosophila: The view from the top. Fly (Austin) *4*, 60-70.
Sanders, L.E., and Arbeitman, M.N. (2008). Doublesex establishes sexual dimorphism in the Drosophila central nervous system in an isoform-dependent manner by directing cell number. Dev Biol *320*, 378-390.
Sarikaya, D.P., Belay, A.A., Ahuja, A., Dorta, A., Green, D.A., 2nd, and Extavour, C.G. (2012). The roles of cell size and cell number in determining ovariole number in Drosophila. Dev Biol *363*, 279-289.
Schafer, A.J., and Goodfellow, P.N. (1996). Sex determination in humans. Bioessays *18*, 955-963.

Schardt, L., Ander, J.J., Lohmann, I., and Papagiannouli, F. (2015). Stage-specific control of niche positioning and integrity in the Drosophila testis. Mech Dev *138 Pt 3*, 336-348.
Serrano-Saiz, E., Oren-Suissa, M., Bayer, E.A., and Hobert, O. (2017). Sexually Dimorphic Differentiation of a C. elegans Hub Neuron Is Cell Autonomously Controlled by a Conserved Transcription Factor. Curr Biol *27*, 199-209.
Shen, M.M., and Hodgkin, J. (1988). mab-3, a gene required for sex-specific yolk protein expression and a male-specific lineage in C. elegans. Cell *54*, 1019-1031.
Sheng, X.R., Posenau, T., Gumulak-Smith, J.J., Matunis, E., Van Doren, M., and Wawersik, M. (2009). Jak-STAT regulation of male germline stem cell establishment during Drosophila embryogenesis. Dev Biol *334*, 335-344.
Shirangi, T.R., Dufour, H.D., Williams, T.M., and Carroll, S.B. (2009). Rapid evolution of sex pheromone-producing enzyme expression in Drosophila. PLoS Biol *7*, e1000168.
Siegal, M.L., and Baker, B.S. (2005). Functional conservation and divergence of intersex, a gene required for female differentiation in Drosophila melanogaster. Dev Genes Evol *215*, 1-12.
Song, H.J., Billeter, J.C., Reynaud, E., Carlo, T., Spana, E.P., Perrimon, N., Goodwin, S.F., Baker, B.S., and Taylor, B.J. (2002a). The fruitless gene is required for the proper formation of axonal tracts in the embryonic central nervous system of Drosophila. Genetics *162*, 1703-1724.
Song, X., Zhu, C.H., Doan, C., and Xie, T. (2002b). Germline stem cells anchored by adherens junctions in the Drosophila ovary niches. Science *296*, 1855-1857.
Stine, R.R., Greenspan, L.J., Ramachandran, K.V., and Matunis, E.L. (2014). Coordinate regulation of stem cell competition by Slit-Robo and JAK-STAT signaling in the Drosophila testis. PLoS Genet *10*, e1004713.
Stockinger, P., Kvitsiani, D., Rotkopf, S., Tirian, L., and Dickson, B.J. (2005). Neural circuitry that governs Drosophila male courtship behavior. Cell *121*, 795-807.
Tanentzapf, G., Devenport, D., Godt, D., and Brown, N.H. (2007). Integrin-dependent anchoring of a stem-cell niche. Nat Cell Biol *9*, 1413-1418.
Taylor, B.J. (1992). Differentiation of a male-specific muscle in Drosophila melanogaster does not require the sex-determining genes doublesex or intersex. Genetics *132*, 179-191.
Taylor, B.J., Villella, A., Ryner, L.C., Baker, B.S., and Hall, J.C. (1994). Behavioral and neurobiological implications of sex-determining factors in Drosophila. Dev Genet *15*, 275-296.
Tran, J., Brenner, T.J., and DiNardo, S. (2000). Somatic control over the germline stem cell lineage during Drosophila spermatogenesis. Nature *407*, 754-757.
Ustinova, J., and Mayer, F. (2006). Alternative starts of transcription, several paralogues, and almost-fixed interspecific differences of the gene fruitless in a hemimetabolous insect. J Mol Evol *63*, 788-800.
Vied, C., Reilein, A., Field, N.S., and Kalderon, D. (2012). Regulation of stem cells by intersecting gradients of long-range niche signals. Dev Cell *23*, 836-848.
Villella, A., and Hall, J.C. (1996). Courtship anomalies caused by doublesex mutations in Drosophila melanogaster. Genetics *143*, 331-344.

von Philipsborn, A.C., Jorchel, S., Tirian, L., Demir, E., Morita, T., Stern, D.L., and Dickson, B.J. (2014). Cellular and behavioral functions of fruitless isoforms in Drosophila courtship. Curr Biol *24*, 242-251.
Voog, J., D'Alterio, C., and Jones, D.L. (2008). Multipotent somatic stem cells contribute to the stem cell niche in the Drosophila testis. Nature *454*, 1132-1136.
Voog, J., Sandall, S.L., Hime, G.R., Resende, L.P., Loza-Coll, M., Aslanian, A., Yates, J.R., 3rd, Hunter, T., Fuller, M.T., and Jones, D.L. (2014). Escargot restricts niche cell to stem cell conversion in the Drosophila testis. Cell Rep *7*, 722-734.
Wagamitsu, S., Takase, D., Aoki, F., and Suzuki, M.G. (2017). Identification of the Doublesex protein binding sites that activate expression of lozenge in the female genital disc in Drosophila melanogaster. Mech Dev *143*, 26-31.
Wawersik, M., Milutinovich, A., Casper, A.L., Matunis, E., Williams, B., and Van Doren, M. (2005). Somatic control of germline sexual development is mediated by the JAK/STAT pathway. Nature *436*, 563-567.
Weyers, J.J., Milutinovich, A.B., Takeda, Y., Jemc, J.C., and Van Doren, M. (2011). A genetic screen for mutations affecting gonad formation in Drosophila reveals a role for the slit/robo pathway. Dev Biol *353*, 217-228.
Williams, T.M., Selegue, J.E., Werner, T., Gompel, N., Kopp, A., and Carroll, S.B. (2008). The regulation and evolution of a genetic switch controlling sexually dimorphic traits in Drosophila. Cell *134*, 610-623.
Wingert, L., and DiNardo, S. (2015). Traffic jam functions in a branched pathway from Notch activation to niche cell fate. Development *142*, 2268-2277.
Xie, T., and Spradling, A.C. (2000). A niche maintaining germ line stem cells in the Drosophila ovary. Science *290*, 328-330.
Xu, J., Zhan, S., Chen, S., Zeng, B., Li, Z., James, A.A., Tan, A., and Huang, Y. (2017). Sexually dimorphic traits in the silkworm, Bombyx mori, are regulated by doublesex. Insect Biochem Mol Biol *80*, 42-51.
Yacobi-Sharon, K., Namdar, Y., and Arama, E. (2013). Alternative germ cell death pathway in Drosophila involves HtrA2/Omi, lysosomes, and a caspase-9 counterpart. Dev Cell *25*, 29-42.
Yi, W., and Zarkower, D. (1999). Similarity of DNA binding and transcriptional regulation by Caenorhabditis elegans MAB-3 and Drosophila melanogaster DSX suggests conservation of sex determining mechanisms. Development *126*, 873-881.
Yoshimoto, S., Ikeda, N., Izutsu, Y., Shiba, T., Takamatsu, N., and Ito, M. (2010). Opposite roles of DMRT1 and its W-linked paralogue, DM-W, in sexual dimorphism of Xenopus laevis: implications of a ZZ/ZW-type sex-determining system. Development *137*, 2519-2526.
Zhang, Y., and Kalderon, D. (2001). Hedgehog acts as a somatic stem cell factor in the Drosophila ovary. Nature *410*, 599-604.
Zhu, C.H., and Xie, T. (2003). Clonal expansion of ovarian germline stem cells during niche formation in Drosophila. Development *130*, 2579-2588.
Zhu, L., Wilken, J., Phillips, N.B., Narendra, U., Chan, G., Stratton, S.M., Kent, S.B., and Weiss, M.A. (2000). Sexual dimorphism in diverse metazoans is regulated by a novel class of intertwined zinc fingers. Genes Dev *14*, 1750-1764.

CURRICULUM VITAE

Hong Zhou
Johns Hopkins University • Department of Biology • 3400 North Charles Street •
Baltimore, MD 21218
Phone: (410) 516-4830 • E-mail: hzhou16@jhu.edu

EDUCATION

Ph.D. in Cell, Molecular, Developmental Biology
October 2018
Johns Hopkins University
Baltimore, Maryland

Bachelor of Science in Biotechnology
June 2011
Peking University
Beijing, China

GRADUATE RESEARCH

Johns Hopkins University, Department of Biology
2006-2012
Principle Investigator: Mark Van Doren
Thesis: "Male-specific development of the germline stem cell niche regulated by *doublesex* and *fruitless*"

- Characterized the sex-specific expression pattern of Fruitless in the gonad stem cell niche
- Determined that the sex-specific Fruitless expression pattern is under the direct transcriptional regulation of Doublesex
- Discovered sex-specific functions of Fruitless in the development and maintenance of the male germline stem cell niche

UNDERGRADUATE RESEARCH EXPERIENCE

Peking University, School of Life Sciences
2007-2009
Principle Investigator: Chuanmao Zhang

- Characterized Aurora-A kinase subcellular localization during different stages of the cell cycle in HeLa and 293T cell lines
- Performed immunoprecipitation and pull-down assays to test protein interaction between Aurora-A and Lamin-A
- Constructed a GFP-tagged Lamin-A reporter with a kinase dead mutation in the putative Aurora-A phosphorylation site, and characterized the mutation effect on nuclear membrane dessembly during mitosis

PUBLICATIONS

Zhou H, Whitworth C, Pozmanter C, Van Doren M., *fruitless* functions downstream of *doublesex* to promote sexual dimorphism of the gonad stem cell niche. (In preparation)

PRESENTATIONS

Talk

Zhou H, Whitworth C, Pozmanter C, Van Doren M.*, Sex-specific development of the germline stem cell niche is regulated by a novel doublesex - fruitless regulatory interaction.* 58th Annual Drosophila Research Conference. San Diego, CA, 2017.

Posters

Zhou, H. and Van Doren, M., *Male-specific development of Drosophila melanogaster gonad stem cell niche regulated by doublesex and fruitless*. Society of Developmental Biology Mid-Atlantic Regional Meeting, 2017.

Zhou, H. and Van Doren, M., *Sex-specific development of the germline stem cell niche is regulated by a novel doublesex - fruitless regulatory interaction.* 57st Annual Drosophila Research Conference, 2016.

Zhou, H. and Van Doren, M., *Sex-specific development of the germline stem cell niche is regulated by a novel doublesex - fruitless regulatory interaction.* 56st Annual Drosophila Research Conference, 2015.

Zhou, H. and Van Doren, M., *Sexual differentiation of the Drosophila germline stem cell niche regulated by doublesex and fruitless*. Society of Developmental Biology Mid-Atlantic Regional Meeting, 2015.

Zhou, H. and Van Doren, M., *Sexual differentiation of the Drosophila gonad germline stem cell niche regulated by doublesex and the masculinizing gene fruitless*. Society of Developmental Biology Mid-Atlantic Regional Meeting, 2014.

TEACHING EXPERIENCE

Graduate Teaching Assistant, Developmental Biology Lecture	2014-2018
Graduate Teaching Assistant, Biochemistry Lecture	Fall 2016
Graduate Teaching Assistant, Gene Regulation during Development and Diseases Lecture	Fall 2015
Mentor of Graduate Rotation Research Project	2014-2015
Tutor, Undergraduate Cell Biology	Spring 2014
Laboratory Teaching Assistant, Developmental Biology lab	Spring 2014
Laboratory Teaching Assistant, Biochemistry Lab	Fall 2013